"Stability Analysis of Fly Ash-Bottom Ash Mix Embankment"

A DISSERTATION

SUBMITTED IN PARTIAL FULFILLMENT

FOR REQUIREMENT OF THE DEGREE OF

MASTER OF TECHNOLOGY

IN

CIVIL ENGINEERING
(Geotechnical Engineering)

Submitted by

PRAVESH RAWAT

(2K20/GTE/14)

Under the supervision of

Prof. KONGAN ARYAN

DEPARTMENT OF CIVIL ENGINEERING

DELHI TECHNOLOGICAL UNIVERSITY

Bawana road, Delhi – 110042

May - 2022

CANDIDATE'S DECLARATION

I, **Pravesh Rawat, 2K20/GTE/14**, student of M. Tech (Civil Engineering), hereby declare that the project dissertation titled **"Stability Analysis of Fly Ash-Bottom Ash Mix Embankment"** is submitted to the Department of Civil Engineering, Delhi Technological University, Delhi, by me in partial fulfillment of requirement for the award of degree of **Master of Technology (Geotechnical Engineering)**. This thesis is original work done by me and not obtained from any source without proper citation. This project work has not previously formed the basis for award of any degree, diploma, fellowship or other similar title or recognition.

Place: Delhi

PRAVESH RAWAT

(2K20/GTE/14)

Date: 31/05/2022

DEPARTMENT OF CIVIL ENGINEERING

DELHI TECHNOLOGICAL UNIVERSITY

Bawana road, Delhi – 110042

CERTIFICATE

I hereby certify that project dissertation titled **"Stability Analysis of Fly Ash-Bottom Ash Mix Embankment"** submitted by **Pravesh Rawat, 2K20/GTE/14,** Department of Civil Engineering, Delhi Technological University, Delhi, in partial fulfillment for the award of degree of Master of Technology, is a project work carried out by the student under my supervision. To the best of my knowledge, this work has not been submitted in part or full for any degree or diploma to this university or elsewhere.

Supervisor

Prof. KONGAN ARYAN

DEPARTMENT OF CIVIL ENGINEERING

Delhi Technological University,

Delhi-110042

ABSTRACT

Coal-fired thermal power stations are India's primary source of electricity generation. The majority of electricity is generated by coal-fired thermal power plants, which account for 51.1% of total electricity generation (Ministry of Power). Today's coal-based thermal power industries are growing at a rapid pace due to the need for higher electricity production. In comparison to imported coal, which has a low ash level of 10-15%, the coal available in India is low-grade coal with an ash content of 30-45%. This leads to the generation of ash in high volumes causing disposal and environmental problems. In most cases, these plants create two forms of ash: fly ash and bottom ash.

In the present study, a complete experimental analysis of the strength and other geotechnical parameters of different mixes of fly ash and bottom ash was carried out. The study's major goal was to analyse the engineering behaviour of fly ash-bottom ash mixes obtained from NTPC Dadri Plant and their feasibility for use as an embankment material. Fly ash (FA) and bottom ash (BA) were mixed in different percentages such as FA:BA=100:0, FA:BA=75:25 (i.e., FA=75% and Bottom ash=25%), FA:BA=50:50, FA:BA=25:75 and FA:BA=0:100 by dry weight. The geotechnical properties of different fly ash-bottom ash mixes were determined in the laboratory by conducting several experiments such as particle size distribution, specific gravity, light weight compaction test, Core Cutter Test, and Direct shear test.

The test results data obtained from the above tests were used in the analysis of the embankment in GeoStudio SLOPE/W 2018 software which is based on the limit equilibrium method. The embankments made of different mixes of fly ash and bottom ash were analysed under the effect of their self-weight, surcharge loading, presence of water table and pseudo-static loading, and their variation in Factor of Safety (FOS) was determined.

Keywords: Fly ash, Bottom ash, Limit equilibrium method, GeoStudio SLOPE/W, Factor of Safety.

ACKNOWLEDGEMENTS

I express my deep gratitude and indebtedness to **Prof. Kongan Aryan**, Department of Civil Engineering, DTU, Delhi, for his guidance, and valuable feedback throughout this project work. His able knowledge and supervision with unswerving patience fathered my project work at every stage, for without his encouragement, the fulfilment of task would have been impossible and difficult.

I express my sincere thanks to **Prof. Anil Kumar Sahu**, Department of Civil Engineering, DTU, Delhi, for his cooperation, support and persistent efforts in guiding at each stage of the project work. I wish to express my gratitude towards our Head of Department, **Prof. V. K. Minocha**, Department of Civil Engineering, DTU, Delhi, for showing interest and providing help throughout the period of my project work.

I am genuinely appreciative to all my friends for their support and suggestions during my work. Lastly, I would like to thank the Almighty GOD and my parents, whose committed and untiring efforts towards me have brought me at this stage of my life.

PRAVESH RAWAT
(2K20/GTE/14)
Date: 31/05/2022

CONTENTS

LIST OF TABLES

LIST OF FIGURES

LIST OF GRAPHS

CHAPTER 1 - INTRODUCTION

1.1 Impact of excavation on soil

Soil excavation for the aim of exploiting top soil for road construction, earth dam construction, and backfill material is a severe problem since natural top soil takes thousands of years to generate. Soil excavation causes deforestation, which has a negative impact on biodiversity. Coal ash, a type of industrial waste, may be used as a soil substitute.

1.2 Production, Hazard and Disposal of coal ash

The electricity demand has grown dramatically as a result of industrialization and rapid economic growth. A number of coal-fired thermal power facilities have been built to accommodate this need. In India, thermal power plants produced 232.56 million tonnes fly ash out of which 214.91 million tonnes fly ash was utilised for various purposes (CEA, 2020-21). However, the focus should be on the 100% utilization of fly ash. When pulverised coal is placed in the boiler's combustion chamber, it instantly ignites, generating molten mineral residue. The molten residue cools, solidifies, and ash forms once the heat from the boiler is extracted. The coarser ash particles, called bottom ash, settle in the combustion chamber's bottom, while the finer ash particles, known as fly ash (which accounts for about 80% of total ash), stay suspended in the flue gas and are collected by particulate emission control devices like electrostatic precipitators (ESPs).

Coal ash pollutes the environment, poses health risks, and necessitates the disposal of huge tracts of valuable land. The disposal of ash generated at thermal power plants has become an essential and difficult problem as environmental concerns and understanding of the negative consequences of pollution have grown. Fly ash may be used in a number of ways, as evidenced by substantial research and development as well as field demonstration. However, bulk utilization of coal ash is feasible in civil engineering field, such as the construction of embankments.

Since the properties of coal ash vary from one location to other, their variability has to be checked before utilization. As a result, it’s critical to investigate the characteristics of fly ash from diverse sources before using it as a construction material. Bottom ash and Fly ash were procured from the NTPC Dadri plant for this investigation.

1.3 Classification of fly ash

ASTM C618 divides fly ash into three types: Class N fly ash, Class F fly ash and Class C fly ash.

Class F fly ash is produced from the burning of anthracite or bituminous coals. This class of fly ash has pozzolanic properties with little or no cementing value.

Class C fly ash is derived from the burning of lignite or subbituminous coals. This class of fly ash has some cementing properties along with pozzolanic properties.

Table 1.1: Modes of Fly ash utilization in year 2020-21 *(Source: CEA annual report 2020-2021)*

S.NO.	**Mode of utilization**	**Utilization (Million tonnes)**	**% Utilization**
1	Cement.	60.0229	25.81
2	Low-Lying Area Reclamation	36.2463	15.59
3	Roads and Flyovers	34.9851	15.04
4	Bricks and Tiles	30.1832	12.98
5	Ash Dyke Raising	18.4722	7.94
6	Mine Filling	14.4187	6.20
7	Concrete	1.9189	0.83
8	Agriculture.	0.0773	0.03
9	Hydro Power Sector	0.0611	0.03
10	Others.	18.5267	7.97
11	Unutilized Fly Ash	17.6469	7.59
	Total	**232.5595**	**100.00**

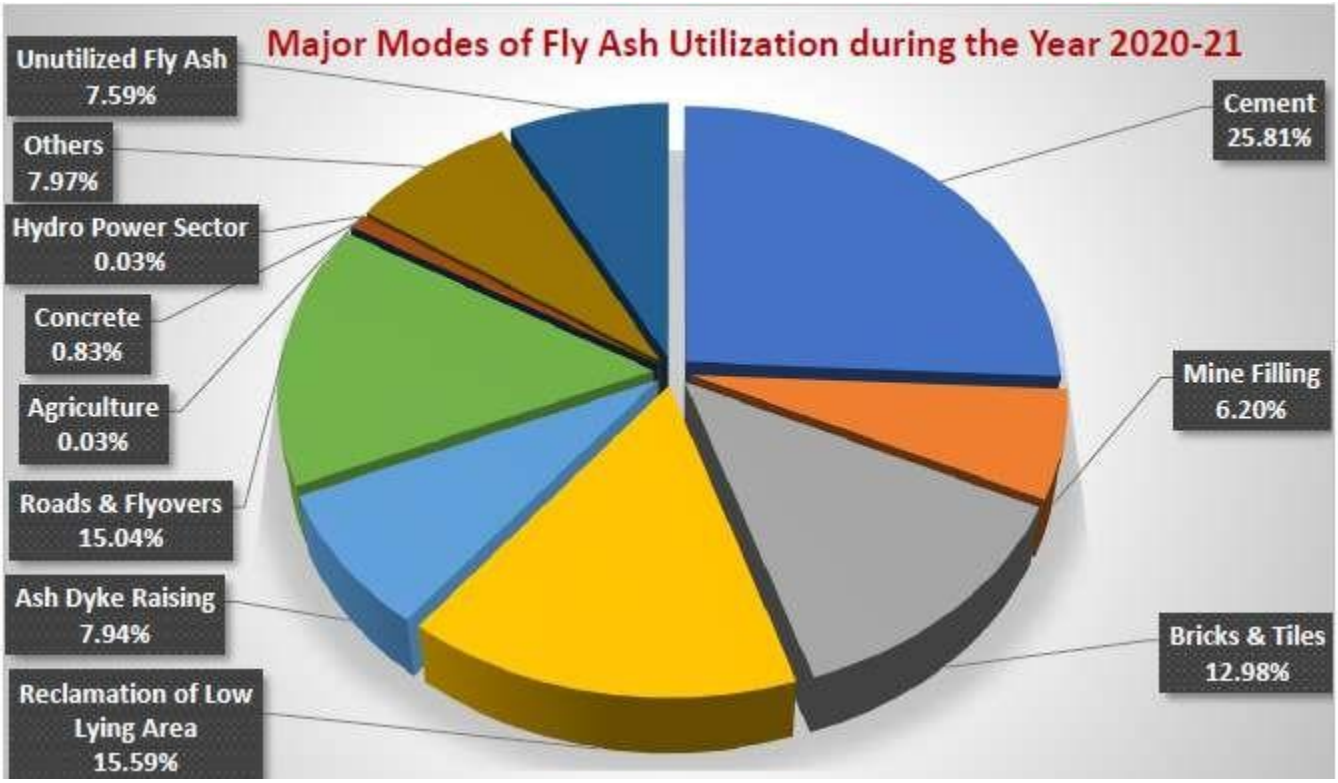

Figure 1.1: Major Modes of Fly ash utilization in year 2020-21 *(Source: CEA annual report 2020-2021)*

1.4 Fly ash-Bottom ash mix embankments

This study focuses on use of fly ash and bottom ash mixes in various percentages as embankment materials. The embankment is analyzed employing GeoStudio slope/w under a variety of situations, including surcharge loading, water table influence, and pseudo static loading. The stability analysis of embankment is then carried out in terms of its safety factor (FOS) in this research.

Pseudo static method, Newmark's Sliding Block method and Numerical techniques employing rigorous dynamic analysis are three methodologies to analysing the performance of a soil slope during an earthquake. In pseudo-static analysis, the effect of earthquake is represented by horizontal (k_h) and vertical acceleration coefficients (k_v) and the FOS is calculated using limit equilibrium or the finite element method.

1.5 GeoStudio SLOPE/W: Overview

The limit equilibrium approach is employed in SLOPE/W to assess the stability of a particular geometry. In limit equilibrium method, a sliding mass is sliced into no. of vertical slices by a trial slip surface. The factor through which shear strength of all the slices should be lowered in such a manner that sliding mass

is almost at the position of static equilibrium is calculated using an iterative approach (before failure occurs). The safety factor is the term for this reduction factor. Moment or force equilibrium can be used to measure equilibrium. As a result, SLOPE/W calculates two safety factors: one is for overall moment equilibrium and another for horizontal force equilibrium. In the current study, Morgenstern-price approach is employed using the interslice force function as a half sine function.

1.6 Morgenstern-Price method

The Morgenstern-price approach is one of the limit equilibrium methods present for analysis in SLOPE/W 2018. This approach takes into account various interslice force functions. Morgenstern & Price (1965) proposed an equation in the Generalized Limit Equilibrium (GLE) approach that considers interslice shear forces, which is expressed as:

$$X = E\,\lambda\,f(x)$$

where,

X = Inter slice shear force

E = Inter slice normal force

$f(x)$ = Inter slice force function

λ = % of the function used (in decimal)

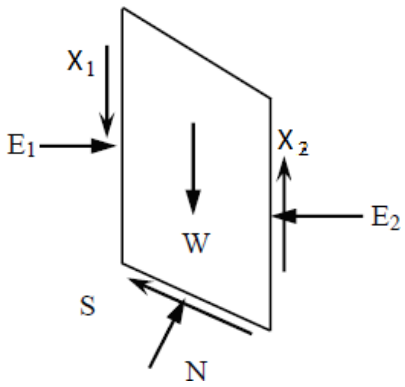

Figure 1.2: Free Body Diagram of a slice

In SLOPE/W, the GLE method may accept a broad range of interslice force functions, including constant, trapezoidal, clipped-sine, half-sine and fully specified functions. In the current investigation, the half-sine function is employed among the many interslice force functions in SLOPE/W. For a given lambda (λ) value, the GLE method calculates the moment FOS and the force FOS. A plot similar to Figure 1.2 can be

produced using these computed data. The FOS is calculated using the Morgenstern-Price technique at the point where the two curves intersect.

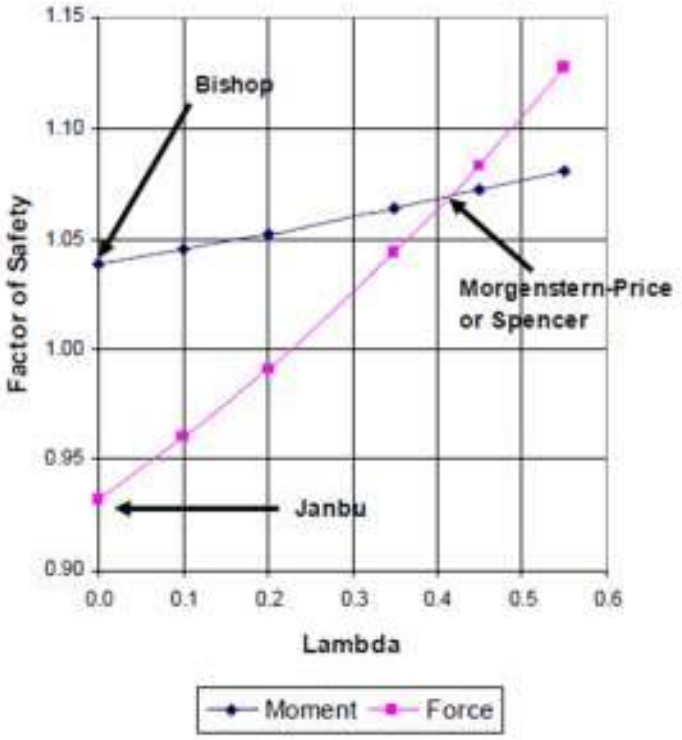

Figure 1.3: FOS versus lambda (λ) plot (Source: GeoStudio manual)

1.7 Constitutive Model

Strength characteristics of geomaterials can be represented by different constitutive model exhibiting varying stress-strain characteristics of soils, namely Mohr-Coulomb, Undrained soil, Impenetrable Bedrock, Bilinear soil, Anisotropic strength, and even Spatial Mohr-Coulomb. The shear strength for all the fly ash-bottom ash mixtures and soil is given in the current study using Mohr-failure Coulomb's criteria, which is described as:

$$r = \sigma_n \, tan \, \phi$$

where,

r = Shear strength

σ_n = Normal stress on shear plane

ϕ = Angle of internal friction

The numerical model for the embankment made of different fly ash-bottom ash mixes under surcharge loading, hydraulic loading and pseudo static loading can be made using the above background.

1.8 OBJECTIVES OF CURRENT STUDY

The following are the objectives of the study:

1. To utilize fly ash-bottom ash mix as a soil replacement in embankment construction.
2. To evaluate the geotechnical properties of various Fly ash-Bottom ash mixes by experimental studies.
3. To calculate the FOS of various embankments made of different mixes of Fly ash and Bottom ash under the effect of self-weight, presence of water table, surcharge load and Pseudo Static load using Limit equilibrium method (Morgenstern-Price Method).
4. To find out the optimum proportion of FA-BA mix to be used in embankment construction.

CHAPTER 2 – REVIEW OF LITERATURE

LITERATURE REVIEW

- **Sharma and Singh, (2020)** mixed bottom ash and fly ash in different proportions in soil. The geotechnical parameters of different samples were tested using Proctor test, Atterberg's limits and CBR tests. The optimum percentage of bottom ash and fly ash mixture to maximise the bearing capacity of soil was reported to be 12 % and 18 % respectively.
- **Bhatt et al., (2019)** reviewed the physical, chemical, and geotechnical properties of coal fly ash. From their study, they concluded that fly ash more often is poorly graded than well-graded. Optimum moisture content (OMC) values for fly ashes vary from 11 to 53%, and maximum dry density values range from 1.01 to 1.78 g/cm^3. Fly ash tends to be non-plastic, meaning it will not swell if used as a foundation material for structures. Fly ash shrinkage limits range from 38 to 65. Permeability of fly ash generally varies from 10^{-4} to 10^{-7} cm/s, and angle of friction varies from 25° to 40°.
- **Reddy et al., (2018)** examined the physical, chemical as well as geotechnical characterisation of municipal solid waste, bottom ash and fly ash from Telangana, India. Fly ash, bottom ash and municipal waste were found to have specific gravity values of 1.86, 1.77, and 2.2, respectively. Bottom ash, fly ash, and municipal waste had peak friction angles of 33.77°, 37.02°, and 35.23° respectively. Bottom ash, fly ash and municipal solid waste have permeabilities of 2.01×10^{-4} cm/s, 1.01×10^{-4} cm/s, and 1.16×10^{-4} cm/s respectively. Based on the findings of the testing, they discovered that fly ash, bottom ash, and municipal waste from Telangana are feasible materials to be used as backfill material, filter, and embankment construction.
- **Gimhan et al., (2018)** performed experiments on fly ash, bottom ash and their mixes procured from Lak Vijaya power plant in Sri Lanka to check their suitability as an embankment material. The experimental results showed that coal ash grains were mostly of silt size having some sand size grains. Coal ash had a lesser MDD and a higher OMC than traditional granular soils utilised in embankments. Furthermore, compared to other forms of construction fills, this fly ash had larger value of friction angle. As a result, both FA and BA can be employed in civil engineering projects as a low weight back fill material or embankment.
- **Saravanan et al., (2017)** performed experiments to determine the impact of addition of bottom ash in soil. 8%, 12% and 16% bottom ash were added in soil. The results indicated that the MDD and

UCS values of the treated sample were increasing, but the CBR decreased by adding bottom ash. The MDD calculated for treated soil sample was 22 kN/ m^3 obtained at 12% bottom ash addition.

- **Dungca and Jao (2017)** investigated the permeability and strength of road foundation materials with fly ash and bottom ash. Representative samples of bottom ash and class C fly ash, as well as standard road foundation materials, were collected. Bottom ash substitutes were changed at various mixing ratios varying from 0% to 100% of fine aggregates, whereas fly ashes were added to behave as fines. The results revealed that a 100 percent bottom ash blend produces the best strength. The inclusion of bottom ash to fine aggregates from 0% to nearly 50% increased hydraulic conductivity because they operate similarly to natural sands, allowing water to flow freely.
- **Dey et al., (2016)** analyzed the stability of ash dykes in static, pseudo static and seismic conditions using limit equilibrium and finite element methods. Slope/w, Sigma/w, Seep/w, and Quake/w were employed for the above analysis. Quake/w was used to carry out for the dynamic analysis. The ash dyke's stability had been determined using safety factor obtained from the analysis.
- **Yao et al., (2015)** conducted a complete investigation for use of fly ash. They discussed the worldwide generation, physicochemical qualities, and risks of coal fly ash before focusing on its current and future applications, such as soil improvement, building, ceramics, catalysis, depth separation, zeolite synthesis, etc. in their study.
- **Singh et al., (2015)** found out the viability of using fly ash as an embankment material. The fly ash was procured from a power plant in Ropar. They concluded that fly ash compaction is less affected by water content and that it may be utilised as an embankment material even when wet. In comparison to natural soils, fly ash has a high angle of shearing resistance, which allows for improved slope stability.
- **Saikia et al., (2015)** performed pseudo static analysis of slopes having various slope angles and other parameters considering Zone V as per IS code using Slope/w software and their FOS was computed. The failed slopes were then stabilised using only soil nails, only retaining wall or combination of both. According to the findings, the most efficient combination was observed when both soil nails and retaining wall was provided.
- **Latifi et al., (2015)** studied the strength and physico-chemical characteristics of fly ash and bottom ash mixes taken from a power plant in Malaysia. The researchers came to the conclusion that fly ash particles are tiny rounded particles having smooth surface, whereas particles of bottom ash are irregular and have a rough surface. The elasticity modulus fell as the bottom ash amount increased

from 30 to 70%, according to the findings. Increasing the BA concentration from 30% to 70%, on the other hand, had no effect on the FA–BA mix's shear strength.

- **Shivamanth et al., (2015)** performed limit equilibrium and finite element analysis for stability of dyke. Limit equilibrium analysis was done with Slope/w software, while finite element analysis was performed using Plaxis 2D. On both the upstream and downstream sides, a 14 m high dyke with crest of 6 m and a slope of 1V:2H was simulated. Based on the findings, the sudden drawdown situation was the most crucial of all the conditions, followed by constant seepage, which was critical for the dyke's downstream slope.
- **Kumar et al., (2014)** examined the geotechnical parameters of different quantities of bottom ash and fly ash mixes. Various tests were performed on various ratios of bottom ash and fly ash. It was seen that MDD decreased as the bottom ash content was increased. Reduction in permeability was seen as the fly ash content increased. For both soaked as well as unsoaked samples, the CBR value fell as the fly ash concentration increased.
- **Hasan et al., (2014)** evaluated the morphological and geotechnical behaviour of Dadri fly ash. Most of fly ash grains were seen to be spherical. Fly ash was classed as a low-cohesion class F fly ash. Dadri fly ash was found to have a specific gravity of 2.19, and it was classified as ML soil with a C_u of 5.60 and a C_c of 0.72. The MDD, OMC and shear strength parameters showed that it may be utilised as a soil substitute.
- **Deb and Pal (2014)** studied impact of fly ash on geotechnical parameters of soil-fly ash mixed samples. Fly ash was collected from Kolaghat Power Plant in West Bengal. 10-30% of fly ash was added with local silty-clay soil taken from a river bank near NIT, Agartala by its dry weight. Increased fly ash percentage in soil samples dropped specific gravity, plasticity, shrinkage, degree of saturation, MDD, UCS, and increased OMC, according to test results. In geotechnical engineering projects, soil containing up to 30% fly ash can be utilised as a liner, while soil having more than 30% fly ash is suitable for landfills and embankments.
- **Rai et al., (2010)** investigated use of fly ash in highway embankments and backfill material. They described the properties of fly ash to be used in highway embankments as well as design considerations. They further concluded that fly ash has the advantages of its lesser unit weight and higher shear strength. The disadvantages include that it is easily eroded by wind or water because to its fine grained non-cohesive nature.
- **Prakash and Sridharan (2009)** examined the geotechnical characteristics of coal ash obtained from various sources. They concluded that coal ash has low compressibility, low specific gravity,

higher consolidation rate, high CBR, water insensitivity to compaction etc. Its application in geotechnical engineering field can significantly reduce the problem of its effective disposal in bulk.

- **Yoon et al., (2009)** carried out construction of a test embankment of length, width and height as 100 m, 60 m and 7.6 m respectively made with an ash mix of 60:40 by weight of fly ash-bottom ash on State Road 641, Terre Haute, Indiana. According to USCS, the ash mix was sandy silt. The ash mixture's MDD and OMC were found to be 15 kN/m^3 and 19% respectively. The test embankment was monitored for a year after construction began. After eight months of work, the highest settlement was found to be 80 mm. The embankment's settlement stabilised around 5 months after construction was completed. At the embankment's top, the differential settlement was around 5 mm. According to the findings, the ash mixture may be utilised as an embankment material.
- **Kim et al., (2005)** explored the geotechnical characteristics of fly ash-bottom ash mixtures for highway embankments. For laboratory testing, three mixes of fly ash and bottom ash were created with varying mixing ratios (50, 75, and 100%) of the fly ash by weight. Wabash River Plant and A. B. Brown Plant ash mixes were collected. Compaction, permeability, shear strength, and consolidation properties were all measured. With an increase in bottom ash of up to 50%, the gradation became more evenly graded. The soil permeability reduces as fly ash concentrations increases. When fly ash quantity surpassed 50%, there was a reduction in MDD and increase in OMC. With increase in bottom ash, compressibility of soil increased slightly. It was also observed that at a relative compaction of 95%, fly ash-bottom ash mixture behaved like dense sand and at relative density of 90%, the mixture behaved like loose sand.
- **Pandian (2004)** studied the characterisation of fly ash for geotechnical applications. He determined that fly ash had a lot of potential for geotechnical applications based on extensive studies done both internationally and at the IISC. Because of its lower specific gravity, easily draining behavior, ease in compaction, insensitivity to water content, and strong frictional qualities, it may be used to build embankments, highways, fill behind retaining structures, low lying land reclamation, and more. Fly ash, according to the research, is a free draining material having internal friction angle more than 30°. Unit weights are reduced due to lower specific gravity, resulting in lesser earth pressures.
- **Benson et al., (2004)** conducted case study on stabilizing sandy-clay soil subgrade using Class C fly ash. After curing for 7 days, the stabilised soil had CBRs ranging from 46 to 150, whereas the soil's CBR in its natural moist condition was nearly zero. The stabilised soil's UCS varied from 276 to 607 kN/m^2 at 7 days curing and from 304 to 683 kN/m^2 after 28 days, whereas UCS of unstabilised soil was less than 200 kN/m^2.

CHAPTER 3 – MATERIALS

In this study, various mixes of fly ash and bottom ash obtained from NTPC, Dadri plant were tested for the determining their engineering properties.

3.1 FLY ASH

The term "fly ash" refers to the fine portion of coal combustion products (CCPs). The size of fly ash ranges between fine silt to fine sand. About 80% of the coal ash produced is of very fine nature. This component is taken away with the flue gases and is collected using electrostatic or cyclone precipitator. Fly ash used in this study was procured from NTPC Dadri. The fly ash obtained from Dadri is Class F type (Bhatt et al., 2019). The results of grain size distribution of fly ash represented that most of the particles lie in the range of silt.

Figure 3.1: Fly ash sample

Table 3.1: Properties of Class F fly ash (NTPC Dadri)

Properties	**Values**
Specific Gravity	2.072
Plasticity Limit	Non-plastic
Liquid Limit	24%, (Hasan et al., 2014)
Plasticity Index	24 %
MDD	11.32 kN/m^3

OMC	23 %
Cohesion	0.863 kPa
Internal Friction Angle	29.94˚
Uniformity Coefficient (C_u)	5.423
Curvature Coefficient (C_c)	0.762

Table 3.2: Chemical Composition of Dadri Fly Ash (Hasan et al., 2014)

S.No.	**Chemical Constituents**	**% Composition**
1.	Silicon dioxide (SiO_2)	59.00
2.	Alumina (Al_2O_3)	29.00
3.	Iron oxide (Fe_2O_3)	6.50
4.	Calcium oxide (CaO)	1.80
5.	Magnesium oxide (MgO)	1.44
6.	Sodium oxide (Na_2O)	0.80
7.	Sulphur trioxide (SO_3)	0.28
8.	Potassium oxide (K_2O)	0.10

3.2 BOTTOM ASH

Bottom ash is another byproduct of coal combustion. These are coarser particles collected from the bottom of furnace. Bottom ash used for this study is also collected from NTPC Dadri plant. The grain size distribution revealed that the majority of bottom ash particles are in the fine sand category.

Figure 3.2: Bottom ash sample

Table 3.3: Properties of Bottom ash (NTPC Dadri)

Properties	**Values**
Specific Gravity	2.182
Plasticity Limit	Non plastic
MDD	12.23 kN/m^3
OMC	17.6 %
Cohesion	0.775 kN/m^2
Internal Friction Angle	28.30˚
Uniformity Coefficient (C_u)	3.433
Curvature Coefficient (C_c)	1.106

CHAPTER 4 – METHODOLOGY

4.1 EXPERIMENTAL PROGRAM

The studies and experiments carried out to identify the engineering behaviour of various Fly ash and Bottom ash mixtures are detailed in this chapter. The primary purpose of these studies is to assess the geotechnical properties of different fly ash-bottom ash mixes derived from Dadri plant. Fly ash generated from NTPC Dadri plant is Class F type Fly ash.

The various mixes used in this study are:

FA:BA=100:0

FA:BA=75:25 (i.e., FA=75% and BA=25%)

FA:BA=50:50

FA:BA=25:75

FA:BA=0:100

Where FA refers to Fly Ash.

and BA refers to Bottom ash

The fly ash and bottom ash are subjected to a number of characterisation tests, including grain size distribution analysis (sieve analysis and hydrometer analysis) and specific gravity test for material characterization. The geotechnical investigation of the fly ash-bottom ash mixtures is then assessed using laboratory tests, including the Light weight compaction test and the Direct shear test. Along with fly ash and bottom ash, the soil taken from DTU campus is also tested for above laboratory experiments.

4.1.1 PARTICLE SIZE DISTRIBUTION ANALYSIS

Particle size analysis is used to determine the different sizes of particles present in a particular sample of soil, which aids in establishing the type of soil according to IS:2720 (Part 4)-1985. The grain size analysis of Bottom ash and Fly ash was performed. The bottom ash particles are coarser in nature than that of fly ash. Wet sieving was performed for coarser particles larger than 75 μ while hydrometer analysis was performed for smaller particles less than 75 μ. For the particle size analysis of both Bottom ash and Fly ash, first the sample was passed through a set of sieves i.e., 4.75 mm, 2 mm, 1.18 mm, 600 μ, 425 μ, 300 μ, 150 μ and 75 μ sieves. The hydrometer analysis was then conducted for the particles passing through 75 μ sieve. For the hydrometer analysis, 50 grams sample passing 75 μ was first soaked into the water sample containing sodium hexametaphosphate as dispersing agent.

Figure 4.1: Sets of sieves for particle size distribution

4.1.2 SPECIFIC GRAVITY DETERMINATION

Specific gravity is the dimensionless quantity which is expressed as the ratio of density of soil solids to the density of water at specified temperature.

As per IS: 2720 (Part 3/Sec 2) -1980, the specific gravity of bottom ash and fly ash was calculated by the pycnometer method. 200-400 gm oven dried sample passing is taken in this test.

Calculate and note the empty weight of pycnometer, M_1. Fill this pycnometer with 200-400 g of oven dried sample and weight it as M_2. Using distilled water, fill the pycnometer halfway to three-quarters full. Allow 10 minutes for the sample to soak. Connect the pycnometer to a vacuum pump for roughly 10 min to release the trapped air. Stop the vacuum, wipe the exterior of the pycnometer with a dry cloth, and pour it to the mark with distilled water, and weigh it as M_3. Empty, clean, and refill the pycnometer using water to the mark. This should be weighed as M4. The specific gravity is then determined by using the relation:

$$G = \frac{M_2 - M_1}{(M_4 - M_1) - (M_3 - M_2)}$$

Figure 4.2: Specific gravity determination through Pycnometer

4.1.3 COMPACTION TEST

Compaction is the process of using mechanical compactive effort to reduce voids between soil particles. Compaction is associated with reducing the volume of voids by removing the pore air. The compaction test determines the relation between dry density and soil moisture content. It also determines the MDD and OMC of the soil. In this study, Light compaction test is performed as per IS:2720 (Part 7)-1980 in order to determine the MDD and OMC of different Fly ash-bottom ash mixes and DTU soil. In a light compaction test, a 5 kg material passing through a 20 mm IS sieve is compacted in a 1000 cc mould. The material would then be filled in the mould in 3 stages, each getting 25 no. of blows from a hammer of 2.6 kg with a free fall of height 310 mm drop height. With the sample, the technique is repeated, this time altering the water content to determine the dry density corresponding to various water content and calculating the OMC as well as MDD.

Figure 4.3: Light compaction test mould

4.1.4 IN-SITU DENSITY OF SOIL USING CORE CUTTER

The in-situ density of DTU soil was found by conducting core cutter test as per IS:2720 (Part 29)-1975 and its natural moisture content was determined using oven drying method. The internal height and diameter of core cutter was determined so as to calculate its volume (V). The mass of empty core cutter was measured as M_1. The core cutter was then pressed into the soil mass to be tested and then the weight of core cutter with soil was measured as M_2. A representative sample of soil was taken for determining its moisture content (w).

In-situ density of soil (Υ_b) = $(M_2-M_1)/V$

Dry density (Υ_d) = $\Upsilon_b/(1+w)$

4.1.5 DIRECT SHEAR TEST (DST)

The Cohesion (c) and internal friction angle (φ) of different fly ash-bottom ash mixtures, as well as undisturbed and compacted samples of DTU soil, were found out using the DST. According to IS:2720 (Part 13)-1986, the shear parameters of fly ash-bottom ash mixtures as well as compacted DTU samples were calculated at their respective MDD and OMC. the shear parameters of undisturbed DTU soil were

determined at its field density and natural moisture content.

The samples were obtained by inserting a 60mmX60mmX25mm sampling device into samples collected in the sampler. Prior to testing, the specimens were trimmed and straightened. All samples were sheared at a rate of 0.25 mm/min in direct shear machine. At normal stress values of 0.5 kg/cm^2, 1 kg/cm^2, and 1.5 kg/cm^2, the maximum shear stress values were measured. A graph was then plotted between normal stress and maximum shear stress keeping normal stress as abscissa and shear stress as ordinate. The intercept of the line at Y-axis represents Cohesion (c) and the slope of the line represents angle of internal friction(φ).

The shear parameters of the fly ash-bottom ash mixes as well as compacted DTU samples at their corresponding MDD and OMC were determined as per IS: 2720 (Part 13)-1986.

Figure 4.4: Failed specimen in Direct Shear Test

4.2 NUMERICAL MODELLING

4.2.1 Problem Statement

The numerical modelling in this work is carried out using the GeoStudio SLOPE/W 2018 software. Slope/w analyzes the given slope based on various limit equilibrium methods. In this study, Morgenstern Price Method considering half sine function as interslice force function was used to find critical slip surface and corresponding FOS for all the models under consideration. The various mixes of Bottom ash and fly ash were used as embankment material under different conditions including the effect of water

table, surcharge load and Pseudo static load. Total 20 models were analyzed in the Slope/w software for this study.

The top width of the embankment was kept as 15 m, height of embankment was kept as 6 m and a side slope of 1V:2H was considered. The sides and top of the embankment were covered with DTU soil compacted to its MDD at OMC as per IRC: SP:58-1999. The intermediate layers of compacted soil were also provided as per IRC: SP:58-1999 requirements. The undisturbed DTU soil was considered as the subgrade. For modelling in slope/w, half the model was made for the analysis (due to symmetricity). The ground water table is considered at a height of 3 m from toe of the embankment. The surcharge load of 24 kN/m^2 is applied up to a distance of 6 m from the center. For seismic analysis, pseudo static forces are applied. The pseudo static load is applied on embankment considering it to lie in Zone 4. The Peak Ground Acceleration (PGA) is 0.24 g. The K_h value was considered as 0.5 PGA/g i.e., 0.12 (IRC:75-2015) and K_v as 0.25 PGA/g i.e., 0.06.

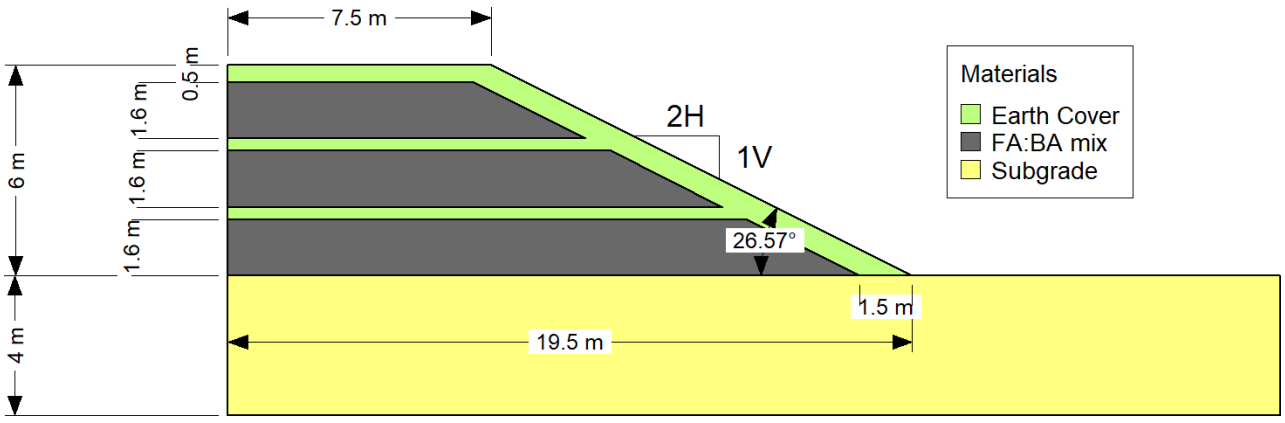

Figure 4.5: Geometry of the embankment

The models analyzed in this study are as follows:

Model 1: Stability Analysis of FA:BA=100:0 mix embankment under the effect of its self-weight.

Model 2: Stability Analysis of FA:BA=100:0 mix embankment under the effect of its self-weight and surcharge load.

Model 3: Stability Analysis of FA:BA=100:0 mix embankment under the effect of its self-weight, water table and surcharge load.

Model 4: Stability Analysis of FA:BA=100:0 mix embankment under the effect of its self-weight, water table, surcharge load and pseudo static load.

Model 5: Stability Analysis of FA:BA=75:25 mix embankment under the effect of its self-weight.

Model 6: Stability Analysis of FA:BA=75:25 mix embankment under the effect of its self-weight and surcharge load.

Model 7: Stability Analysis of FA:BA=75:25 mix embankment under the effect of its self-weight, water table and surcharge load.

Model 8: Stability Analysis of FA:BA=75:25 mix embankment under the effect of its self-weight, water table, surcharge load and pseudo static load.

Model 9: Stability Analysis of FA:BA=50:50 mix embankment under the effect of its self-weight.

Model 10: Stability Analysis of FA:BA=50:50 mix embankment under the effect of its self-weight and surcharge load.

Model 11: Stability Analysis of FA:BA=50:50 mix embankment under the effect of its self-weight, water table and surcharge load.

Model 12: Stability Analysis of FA:BA=50:50 mix embankment under the effect of its self-weight, water table, surcharge load and pseudo static load.

Model 13: Stability Analysis of FA:BA=25:75 mix embankment under the effect of its self-weight.

Model 14: Stability Analysis of FA:BA=25:75 mix embankment under the effect of its self-weight and surcharge load.

Model 15: Stability Analysis of FA:BA=25:75 mix embankment under the effect of its self-weight, water table and surcharge load.

Model 16: Stability Analysis of FA:BA=25:75 mix embankment under the effect of its self-weight, water table, surcharge load and pseudo static load.

Model 17: Stability Analysis of FA:BA=0:100 mix embankment under the effect of its self-weight.

Model 18: Stability Analysis of FA:BA=0:100 mix embankment under the effect of its self-weight and surcharge load.

Model 19: Stability Analysis of FA:BA=0:100 mix embankment under the effect of its self-weight, water table and surcharge load.

Model 20: Stability Analysis of FA:BA=0:100 mix embankment under the effect of its self-weight, water table, surcharge load and pseudo static load.

Table 4.1: Properties of Subgrade soil

Model	Mohr-Coulomb
Unit Weight, Υ_b	16.4 kN/m^3
Cohesion, c	18.678 kN/m^2
Internal friction angle, φ	25.63°

Table 4.2: Properties of Earth cover

Model	Mohr-Coulomb
Unit Weight, Υ_b	19.31 kN/m^3
Cohesion, c	25.005 kN/m^2
Internal friction angle, φ	30.56°

CHAPTER 5 – RESULTS AND DISCUSSION

5.1 EXPERIMENTAL RESULTS

5.1.1 PARTICLE SIZE DISTRIBUTION

5.1.1.1 FLY ASH

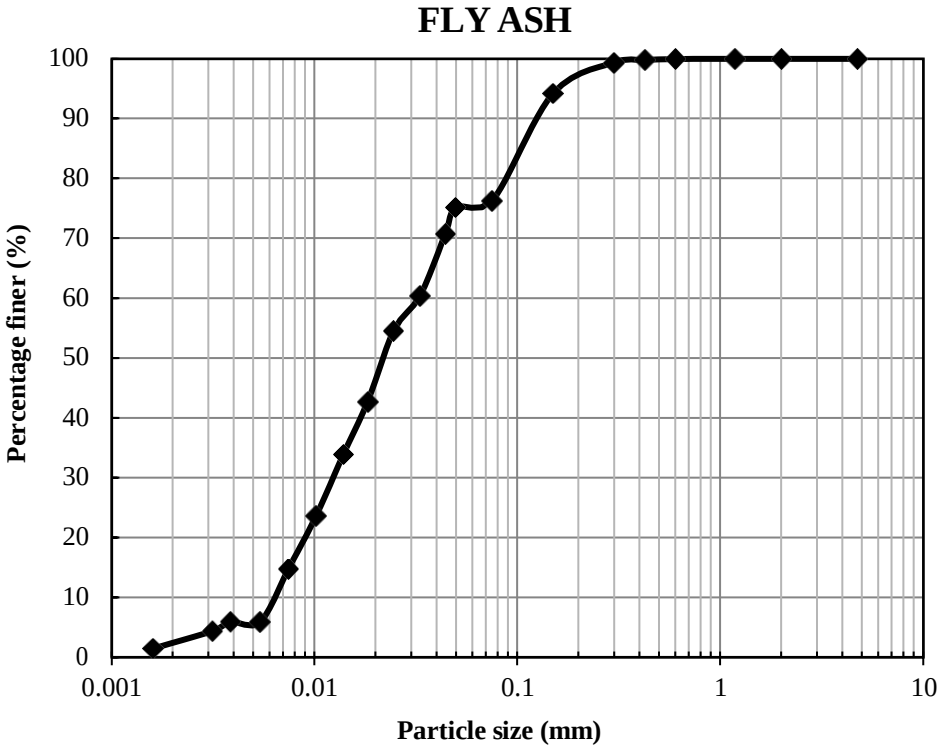

Graph 5.1: Particle size distribution curve for Fly ash

Table 5.1: Uniformity Coefficient and Curvature Coefficient of Fly Ash

Parameters	Values
D_{10} (mm)	0.0059
D_{30} (mm)	0.012
D_{60} (mm)	0.032
Uniformity Coefficient $C_u = D_{60}/ D_{10}$	**5.423**
Curvature Coefficient $C_c = D_{30}^2/ (D_{10}. D_{60})$	**0.762**

5.1.1.2 BOTTOM ASH

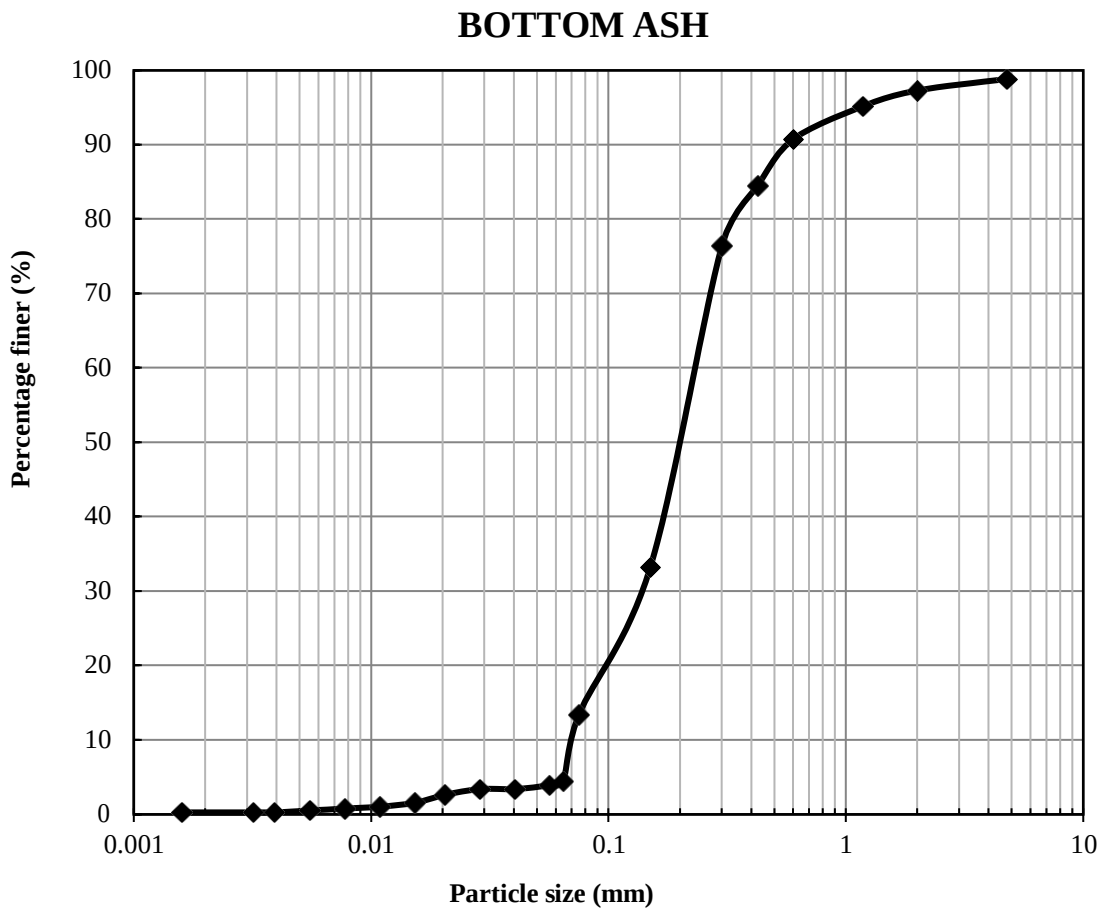

Graph 5.2: Particle size distribution curve for Bottom ash

Table 5.2: Uniformity Coefficient and Curvature Coefficient of Bottom Ash

Parameters	**Values**
D_{10} (mm)	0.0708
D_{30} (mm)	0.138
D_{60} (mm)	0.243
Uniformity Coefficient $C_u = D_{60}/ D_{10}$	**3.433**
Curvature Coefficient $C_c = D_{30}^2/ (D_{10}. D_{60})$	**1.106**

5.1.2 SPECIFIC GRAVITY TEST

The specific gravity of coal ash is less as that of inorganic soil which lies in the range of 2.6-2.8. For this study, the bottom ash and fly ash were obtained from NTPC Dadri and their specific gravity was determined according to IS: 2720 (Part 3/Sec 2) -1980.

Table 5.3: Specific Gravity of Fly Ash

		SAMPLE 1	**SAMPLE 2**	**SAMPLE 3**
Mass of empty Pycnometer	**M_1 (gm)**	685.5	685.5	685.5
Empty Pycnometer+Dry Fly ash	**M_2 (gm)**	894.5	902	899.5
Empty Pycnometer+Dry Fly ash +Water	**M_3 (gm)**	1670.5	1675	1673
Empty Pycnometer+Water	**M_4 (gm)**	1562.5	1562.5	1562.5
Specific Gravity	**G**	2.069	2.081	2.0647

Average value of specific gravity of Fly ash= (2.069+2.081+2.0647)/3=**2.072**

Table 5.4: Specific Gravity of Bottom Ash

		SAMPLE 1	**SAMPLE 2**	**SAMPLE 3**
Mass of empty Pycnometer	**M_1 (gm)**	703.5	703.5	703.5
Empty Pycnometer+Dry Bottom ash	**M_2 (gm)**	902.5	900	905

Empty Pycnometer+Dry Bottom ash+Water	**M_3 (gm)**	1680	1679.5	1683
Empty Pycnometer+Water	**M_4 (gm)**	1573	1573	1573
Specific Gravity	**G**	2.163	2.183	2.202

Average value of specific gravity of Bottom ash= (2.163+2.183+2.202)/3=**2.182**

Table 5.5: Specific Gravity of DTU soil

		SAMPLE 1	**SAMPLE 2**	**SAMPLE 3**
Mass of empty Pycnometer	**M_1 (gm)**	685.50	685.50	685.50
Empty Pycnometer+Dry Fly ash	**M_2 (gm)**	895	910	905
Empty Pycnometer+Dry soil+Water	**M_3 (gm)**	1692	1699.5	1697
Empty Pycnometer+Water	**M_4 (gm)**	1562.50	1562.50	1562.50
Specific Gravity	**G**	2.619	2.565	2.582

Average value of specific gravity of DTU soil= (2.619+2.565+2.582)/3=**2.588**

5.1.3 COMPACTION TEST

The compaction test of various fly ash-bottom mixes and DTU soil was carried out by Light compaction test according to IS:2720 (Part 7)-1980.

5.1.3.1 FA:BA=100:0 mix

Table 5.6: Water content and Dry density relation for FA:BA=100:0 mix

S. NO.	DRY DENSITY, Υ_d (g/cm^3)	WATER CONTENT, w (%)
1	1.021	16.31
2	1.04	18.96
3	1.089	21.11
4	1.154	23.02
5	1.087	25.21

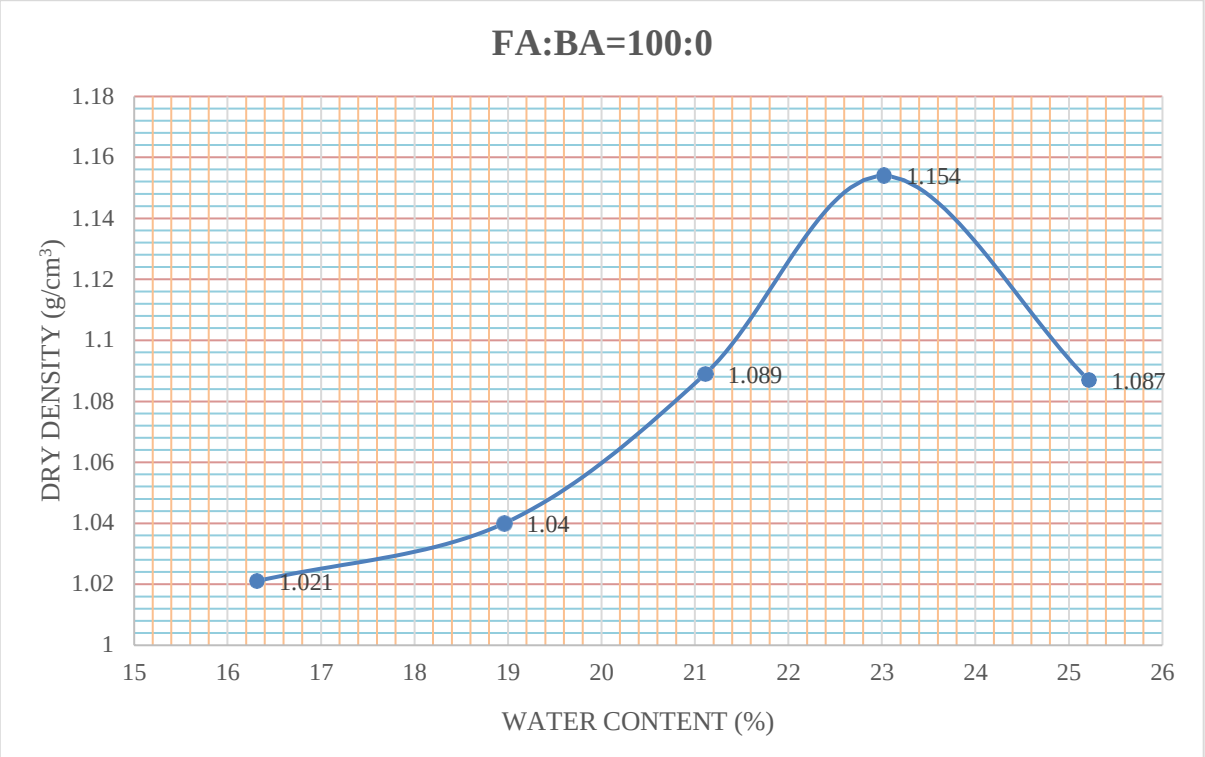

Graph 5.3: Compaction curve for FA:BA=100:0 mix

OMC= 23 %

MDD= 1.154 g/cm^3

5.1.3.2 FA:BA=75:25 mix

Table 5.7: Water content and Dry density relation for FA:BA=75:25 mix

S. NO.	DRY DENSITY, Υ_d (g/cm^3)	WATER CONTENT, w (%)
1	1.07	14.76
2	1.104	16.61
3	1.143	19.31
4	1.188	22.2
5	1.166	24.86
6	1.15	26

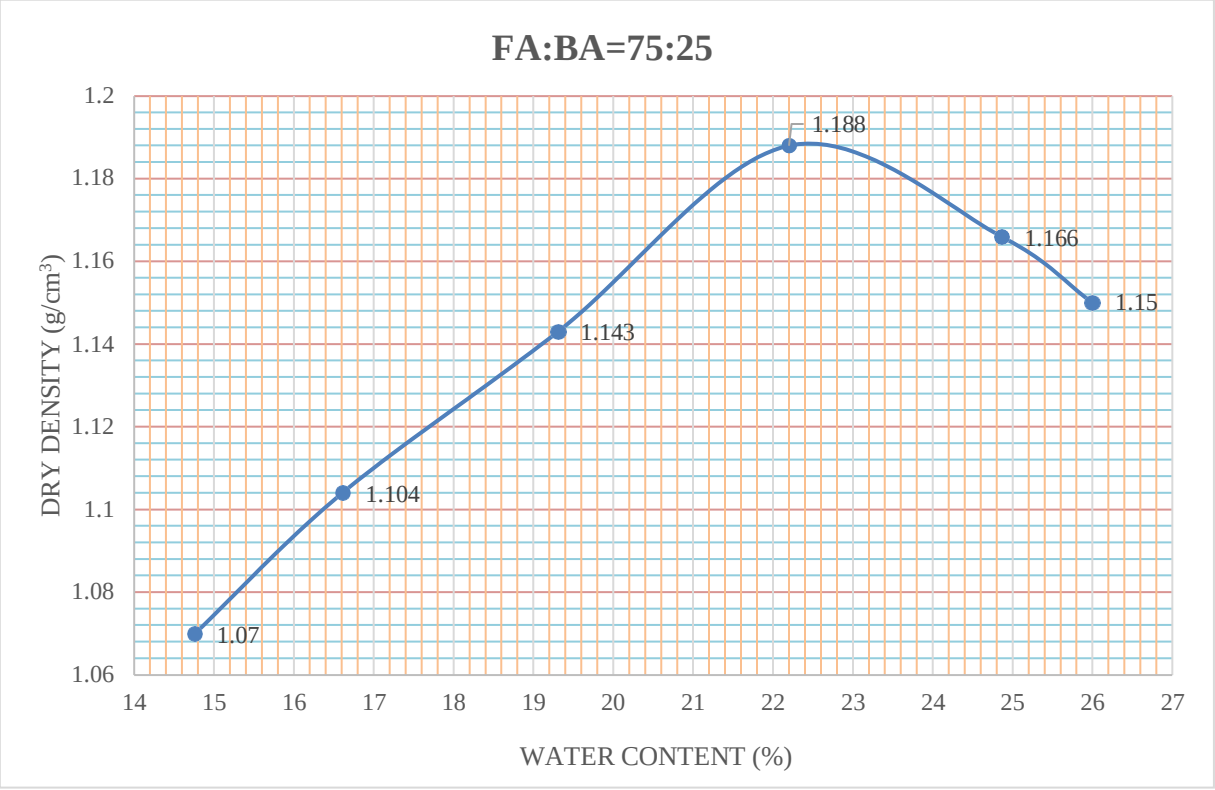

Graph 5.4: Compaction curve for FA:BA=75:25 mix

OMC= 22.2 %

MDD= 1.188 g/cm^3

5.1.3.3 FA:BA=50:50 mix

Table 5.8: Water content and Dry density relation for FA:BA=50:50 mix

S. NO.	DRY DENSITY, Υ_d (g/cm^3)	WATER CONTENT, w (%)
1	1.12	16.279
2	1.147	18.04
3	1.189	19.71
4	1.231	21.32
5	1.215	24.22
6	1.205	26.23

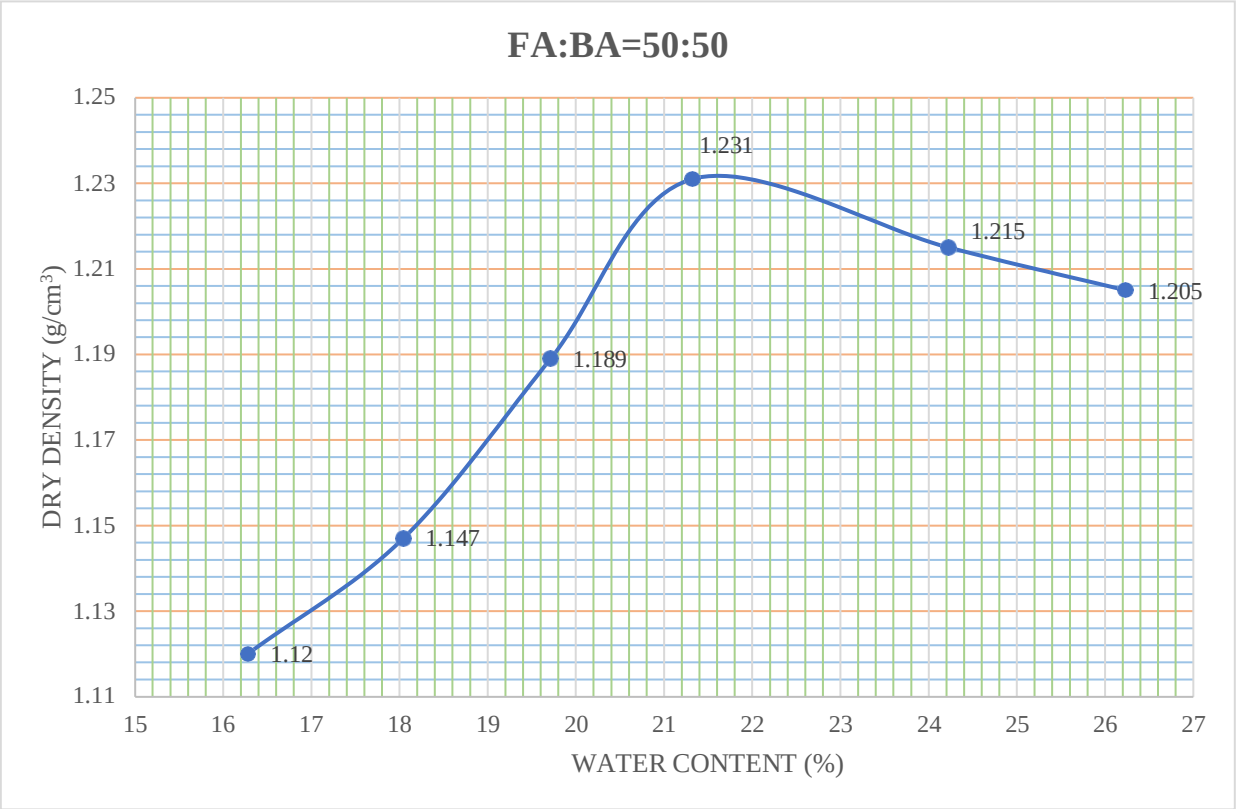

Graph 5.5: Compaction curve for FA:BA=50:50 mix

OMC= 21.6 %

MDD= 1.232 g/cm^3

5.1.3.4 FA:BA=25:75 mix

Table 5.9: Water content and Dry density relation for FA:BA=25:75 mix

S. NO.	DRY DENSITY, Υ_d (g/cm^3)	WATER CONTENT, w (%)
1	1.168	9.55
2	1.178	14.34
3	1.225	17.19
4	1.26	19.26
5	1.218	22.33

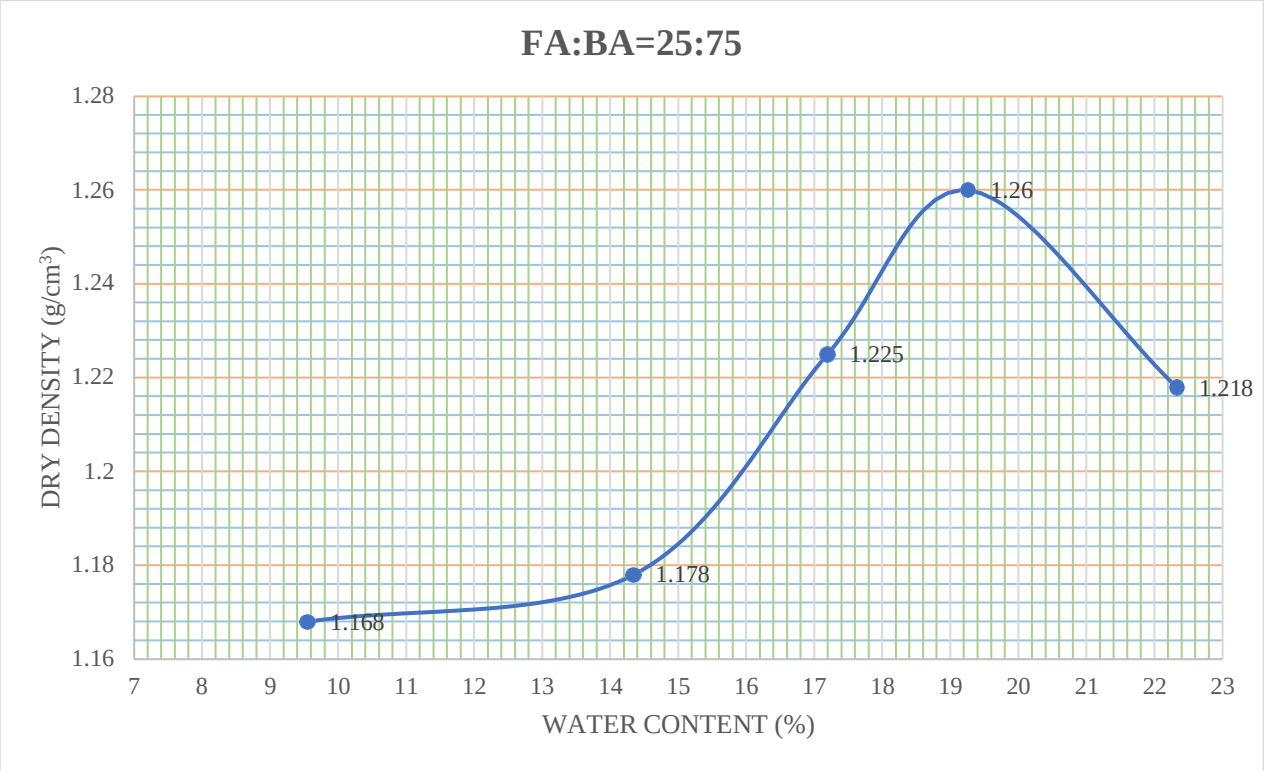

Graph 5.6: Compaction curve for FA:BA=25:75 mix

OMC= 19.2 %

MDD= 1.26 g/cm^3

5.1.3.5 FA:BA=0:100 mix

Table 5.10: Water content and Dry density relation for FA:BA=0:100 mix

S. NO.	DRY DENSITY, Υ_d (g/cm^3)	WATER CONTENT, w (%)
1	1.178	13.69
2	1.225	15.42
3	1.247	17.6
4	1.218	21.18
5	1.2	22.58

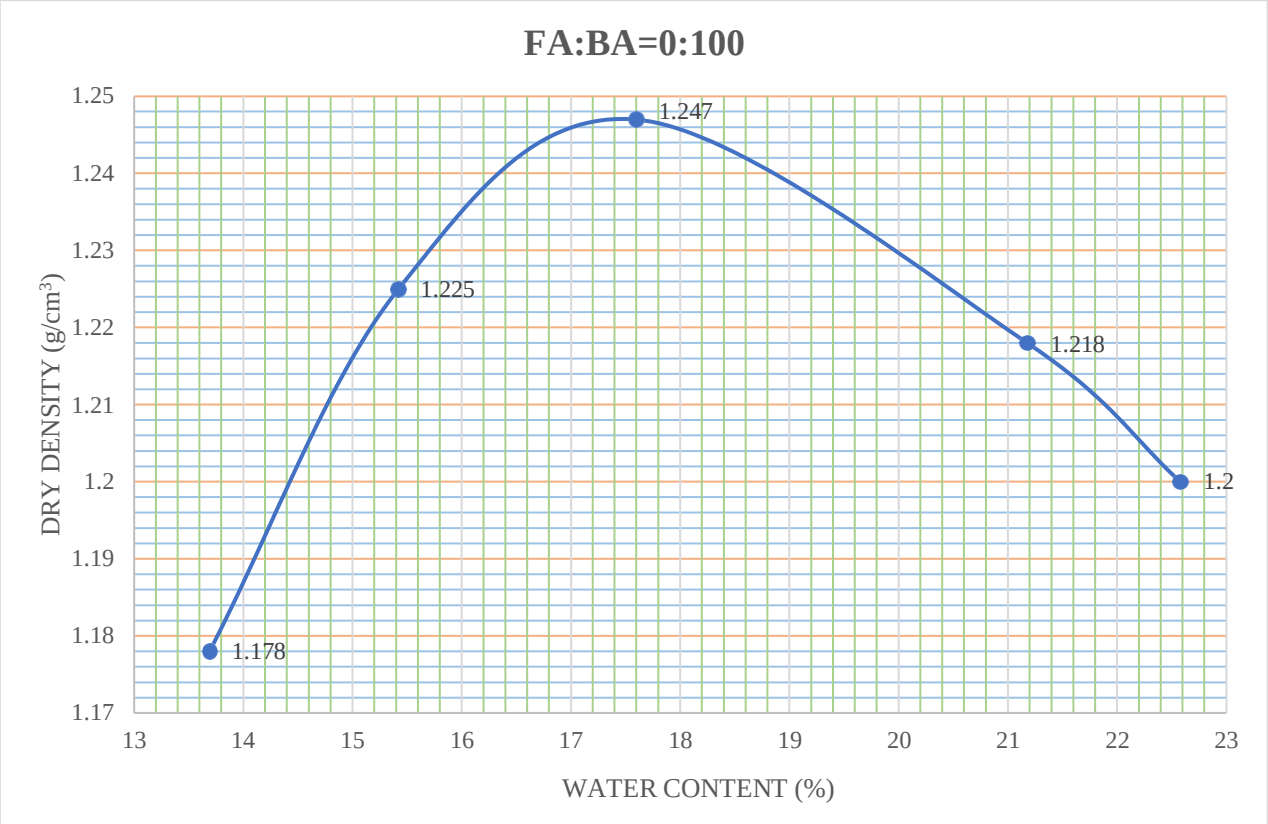

Graph 5.7: Compaction curve for FA:BA=0:100 mix

OMC= 17.6 %

MDD= 1.247 g/cm^3

5.1.3.6 DTU SOIL

Table 5.11: Water content and Dry density relation for DTU soil

S. NO.	DRY DENSITY, Υ_d (g/cm^3)	WATER CONTENT, w (%)
1	1.698	12.22
2	1.733	12.86
3	1.74	13.24
4	1.722	14.35
5	1.686	15.03
6	1.67	15.22

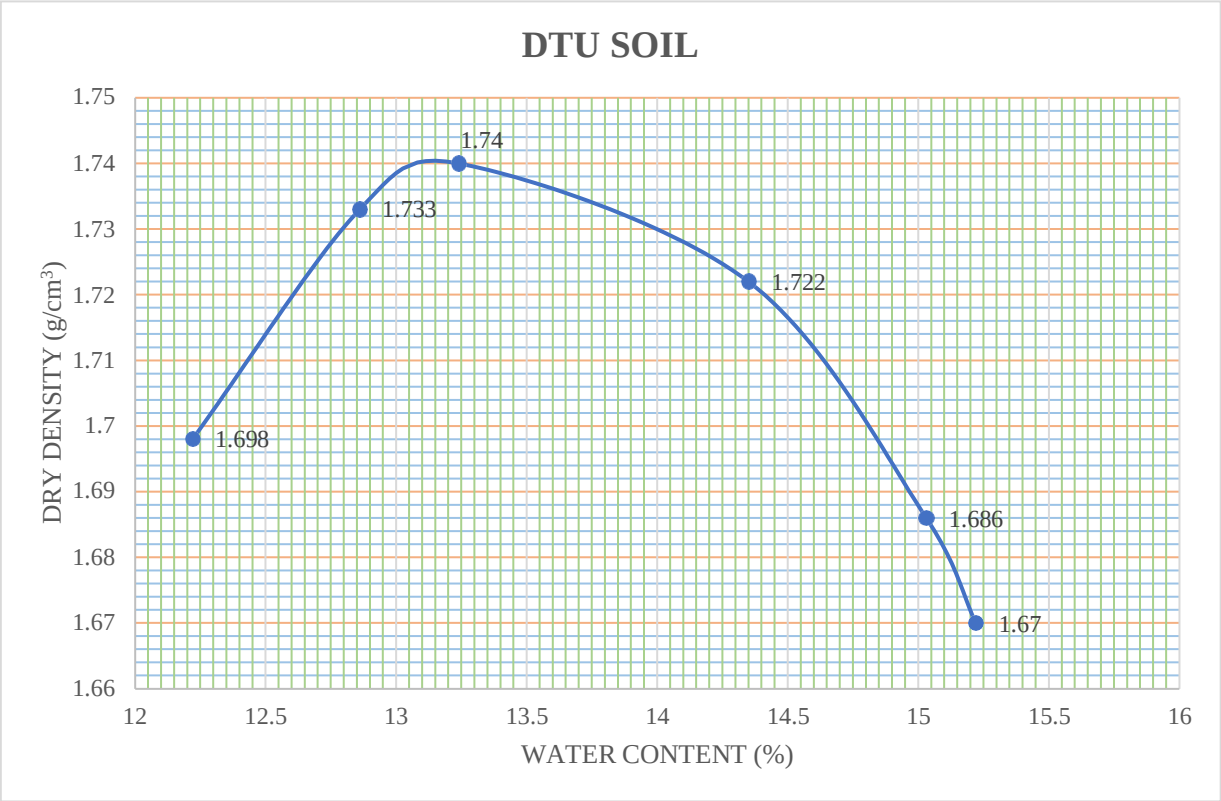

Graph 5.8: Compaction curve for DTU soil

OMC= 13.1 %

MDD= 1.741 g/cm^3

Table 5.12: Results of Compaction test for all the tested samples

SAMPLE	**OMC (%)**	**MDD, Υ_{dmax}**		**Corresponding Bulk density, Υ_b**	
		(g/cm^3)	**($kN/m^{3)}$**	**(g/cm^3)**	**($kN/m^{3)}$**
FA:BA=100:0	23	1.154	11.32	1.419	13.92
FA:BA=75:25	22.2	1.188	11.65	1.451	14.23
FA:BA=50:50	21.6	1.232	12.08	1.498	14.69
FA:BA=25:75	19.2	1.26	12.36	1.501	14.72
FA:BA=0:100	17.6	1.247	12.23	1.466	14.38
DTU SOIL (COMPACTED)	13.1	1.741	17.07	1.969	19.31

5.1.4 IN-SITU DENSITY BY CORE CUTTER

The in-situ density of DTU campus soil was determined by conducting core cutter test as per IS:2720 (Part 29)-1975. The results obtained are as follows:

Table 5.13: Results of In-situ density of DTU soil

		SAMPLE 1	SAMPLE 2	SAMPLE 3
Internal Diameter	**D (cm)**	10	10	10
Internal height	**H (cm)**	13	13	13
Mass of empty core cutter	**M_1 (gm)**	968	968	968
Mass of core cutter with soil	**M_2 (gm)**	2676	2680	2671
Mass of wet soil	**M (gm)= (M_2 -M_1)**	1708	1712	1703
Volume of core cutter	**V (cm^3)**	1021.01	1021.01	1021.01
In-situ density	**Υ_b (g/cm^3)**	1.672	1.676	1.668
Water content	**w (%)**	14.6	14.75	14.7
Dry density	**Υ_d (g/cm^3)**	1.459	1.461	1.454

Average value of In-situ density of soil, Υ_b= 1.672 g/cm^3

Average value of field dry density of soil, Υ_d= 1.458 g/cm^3

5.1.5 DIRECT SHEAR TEST

The shear parameters C and φ and were calculated using a DST on different mixtures of Bottom ash and Fly ash, as well as DTU soil (Undisturbed and Compacted) as per IS:2720 (Part 13)-1986.

5.1.5.1 FA:BA=100:0 mix

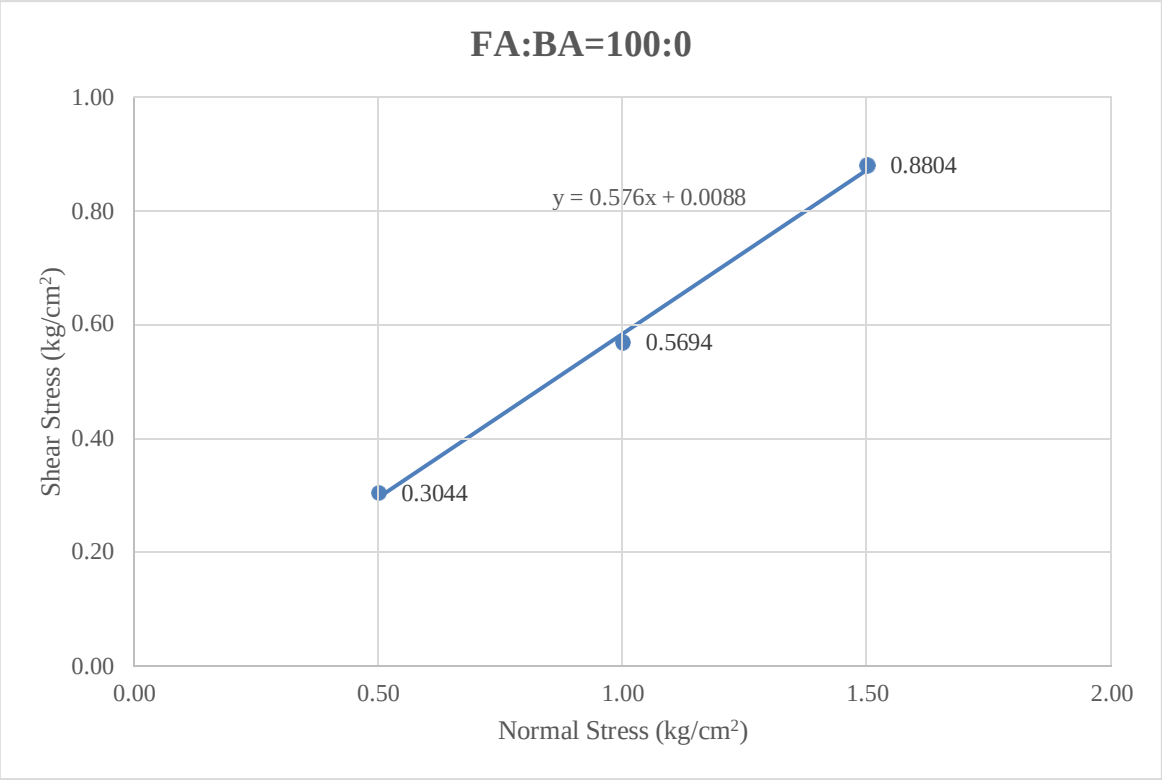

Graph 5.9: Mohr failure envelope for FA:BA=100:0 mix

Cohesion (kg/cm²)	0.0088
Internal Friction Angle (˚)	29.94

5.1.5.2 FA:BA=75:25 mix

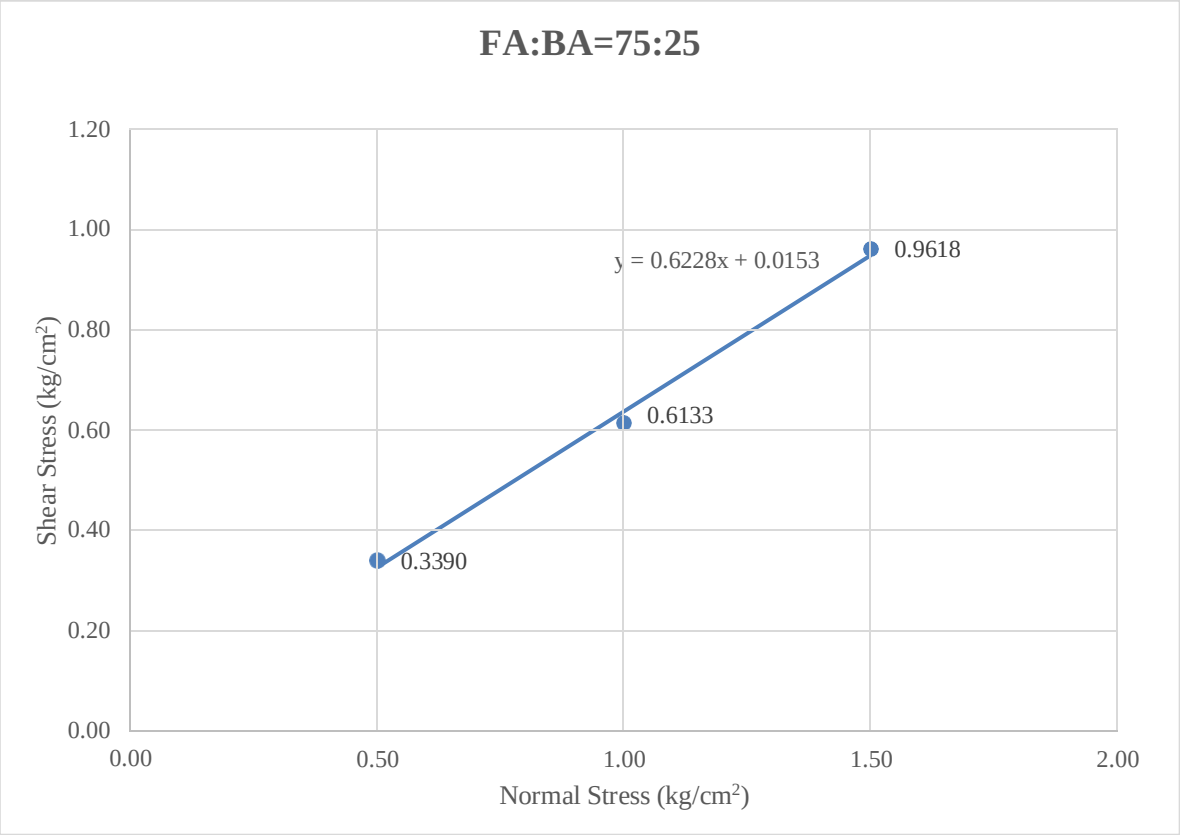

Graph 5.10: Mohr failure envelope for FA:BA=75:25 mix

Cohesion (kg/cm²)	0.0153
Internal Friction Angle (˚)	31.91

5.1.5.3 FA:BA=50: 50 mix

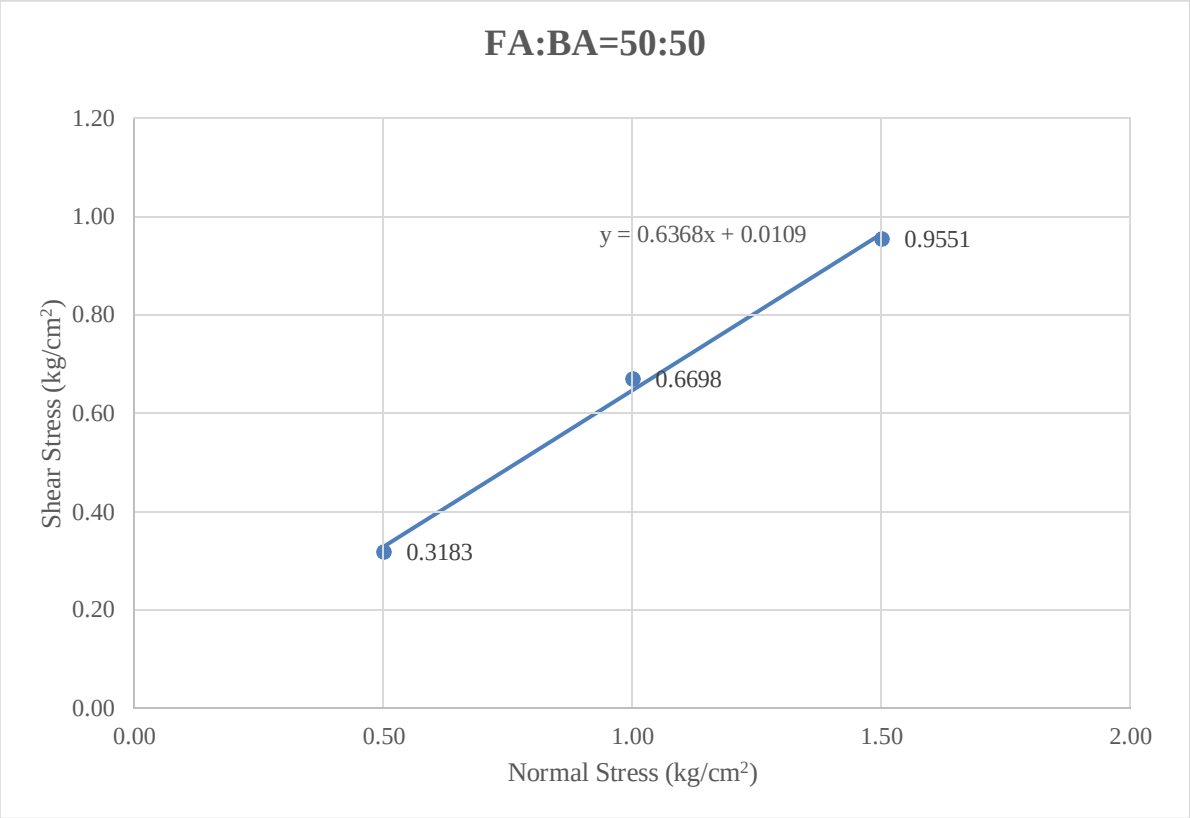

Graph 5.11: Mohr failure envelope for FA:BA=50:50 mix

Cohesion (kg/cm²)	0.0109
Internal Friction Angle (˚)	32.48

5.1.5.4 FA:BA=25: 75 mix

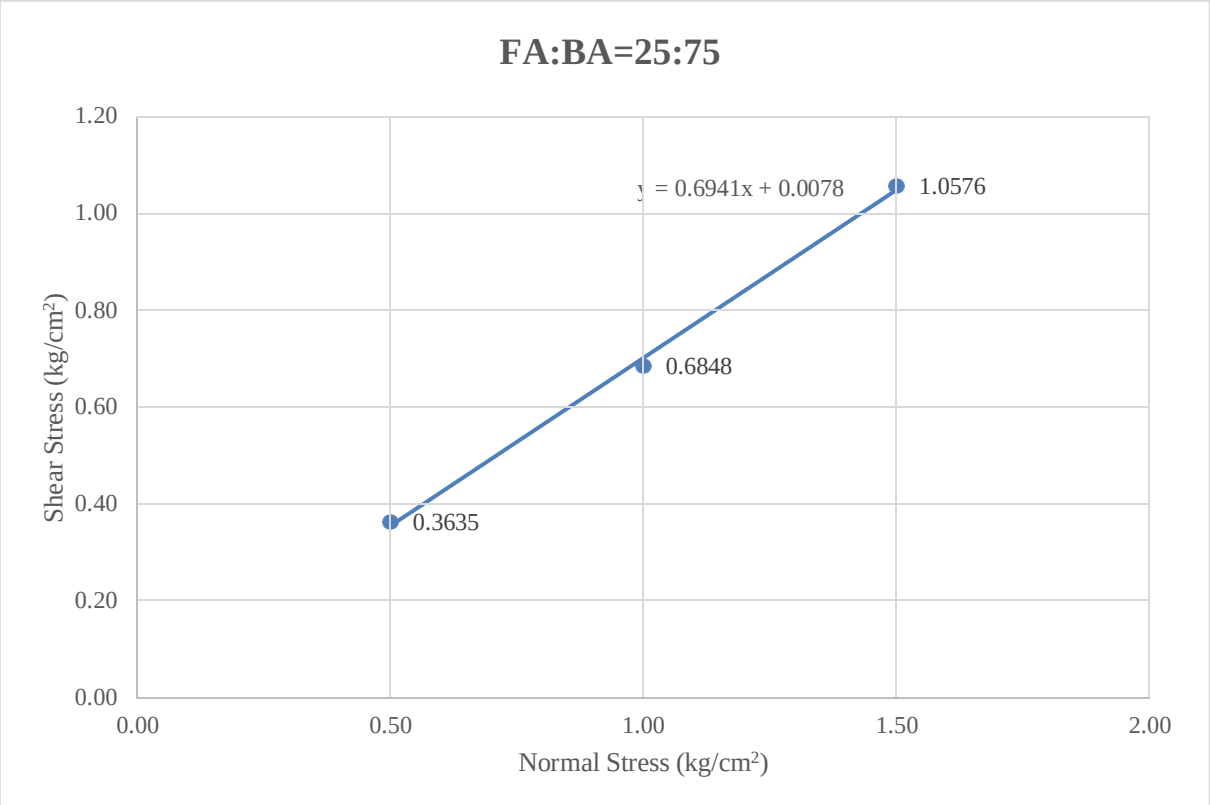

Graph 5.12: Mohr failure envelope for FA:BA=25:75 mix

Cohesion (kg/cm^2)	0.0078
Internal Friction Angle (˚)	34.76

5.1.5.5 FA:BA=0:100 mix

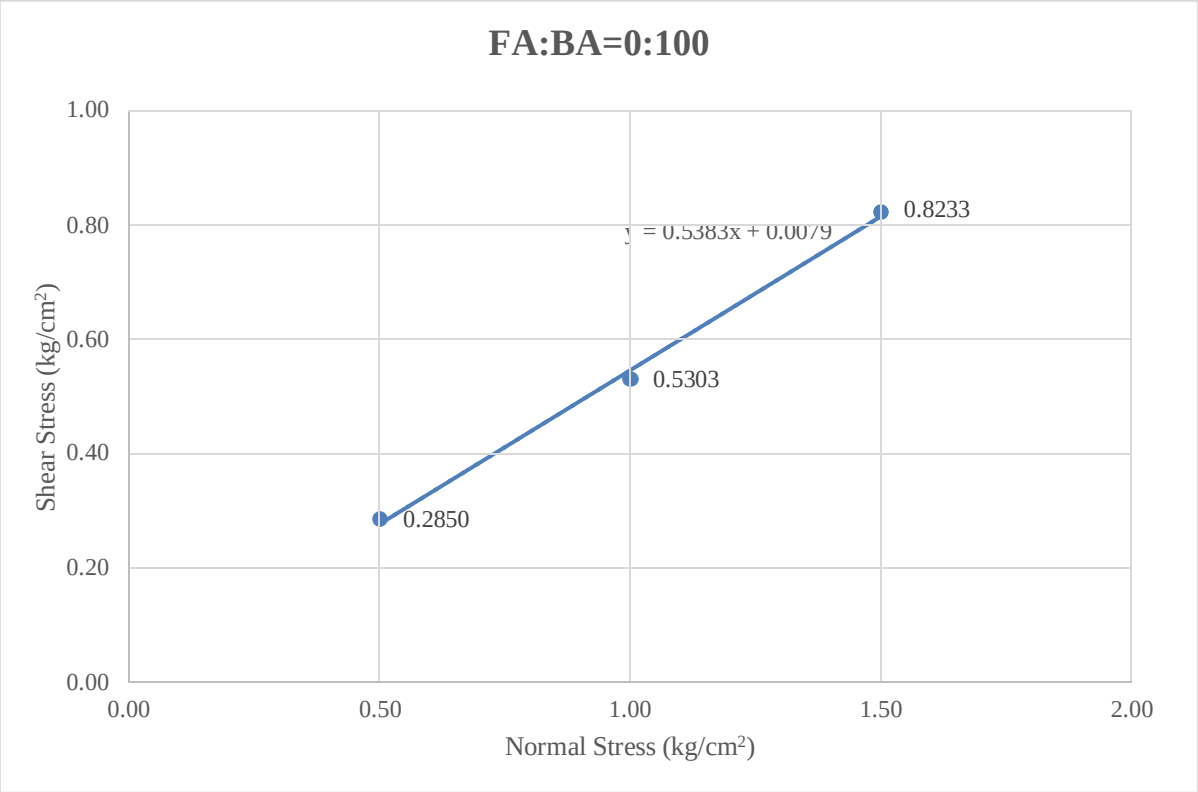

Graph 5.13: Mohr failure envelope for FA:BA=0:100 mix

Cohesion (kg/cm^2)	0.0079
Internal Friction Angle (˚)	28.30

5.1.5.6 Undisturbed DTU Soil

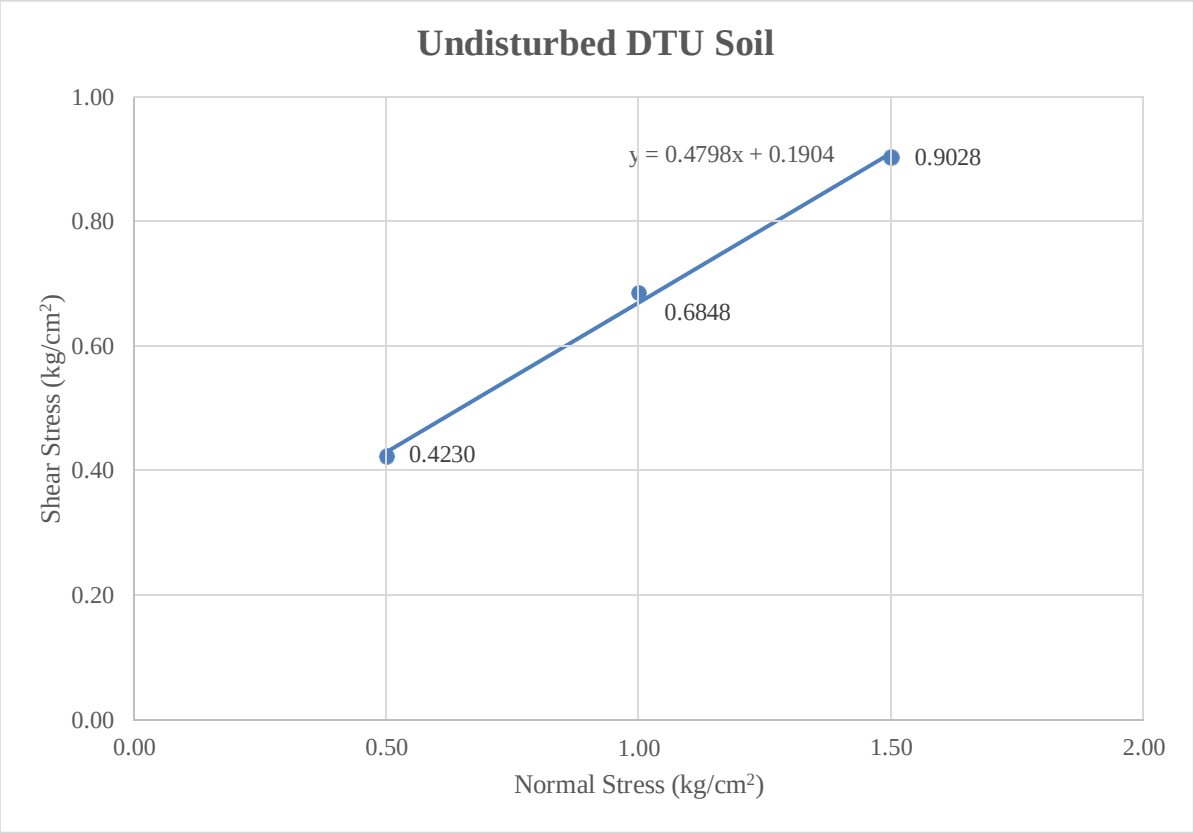

Graph 5.14: Mohr failure envelope for Undisturbed DTU soil

Cohesion (kg/cm^2)	0.1904
Internal Friction Angle (˚)	25.63

5.1.5.7 Compacted DTU Soil

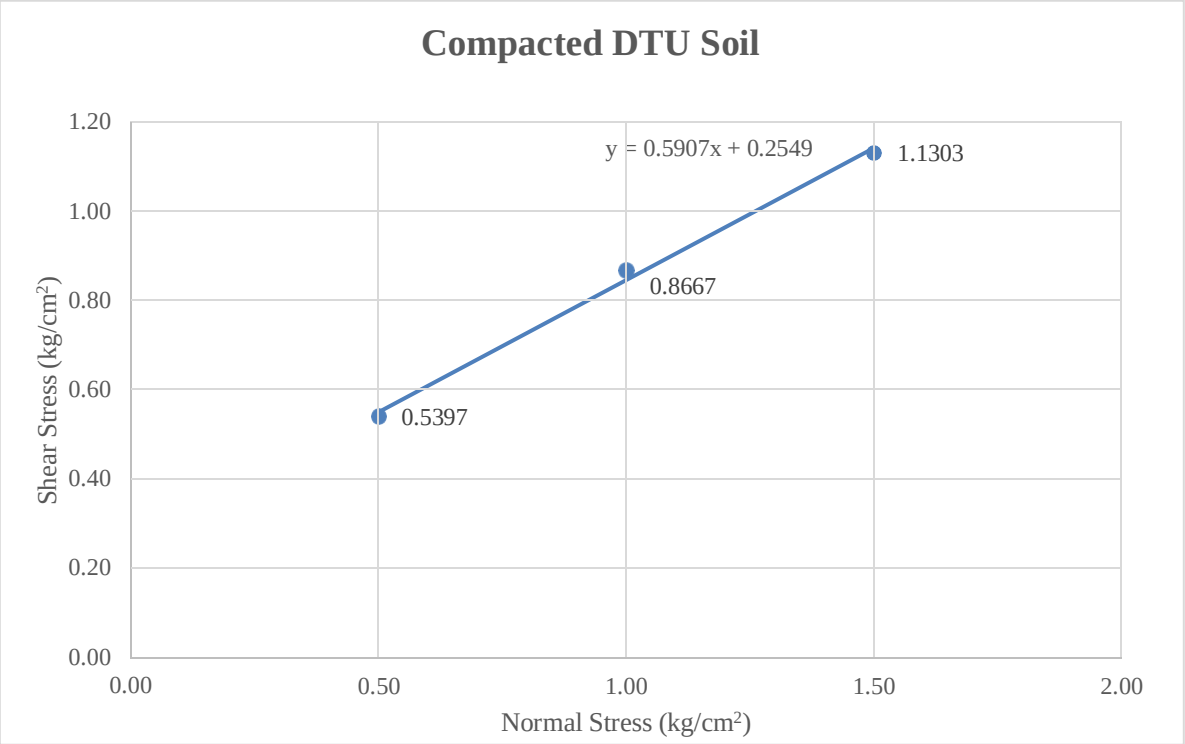

Graph 5.15: Mohr failure envelope for Compacted DTU soil

Cohesion (kg/cm^2)	0.2549
Internal Friction Angle (˚)	30.56

Table 5.14: Direct shear test results for all the tested samples

SAMPLE	**Cohesion (c)**		**Internal friction angle (φ)**
	(kg/cm^2)	**(kN/m^2)**	**(°)**
FA:BA=100:0	0.0088	0.863	29.94
FA:BA=75:25	0.0153	1.5	31.91
FA:BA=50:50	0.0109	1.069	32.48
FA:BA=25:75	0.0078	0.765	34.76
FA:BA=0:100	0.0079	0.775	28.30
DTU SOIL (UNDISTURBED)	0.1904	18.678	25.63
DTU SOIL (COMPACTED)	0.2549	25.005	30.56

Table 5.15: Direct shear and Compaction test results

Parameters	**FA:BA= 100:0**	**FA:BA= 75:25**	**FA:BA= 50:50**	**FA:BA= 25:75**	**FA:BA= 0:100**	**Compacted DTU soil**
MDD (kN/ m^3)	11.32	11.65	12.08	12.36	12.23	17.07
OMC (%)	23	22.2	21.6	19.2	17.6	13.1
C (kN/ m^2)	0.863	1.5	1.069	0.765	0.775	25.005
φ (°)	29.94	31.91	32.48	34.76	28.30	30.56

5.2 ANALYSIS AND INTERPRETATION OF SLOPE/W RESULTS

5.2.1 Model 1: Stability Analysis of FA:BA=100:0 mix embankment under the effect of its self-weight

Table 5.16: Properties of FA:BA=100:0 mix

Model	Mohr-Coulomb
Unit Weight	13.92 kN/m^3
Cohesion (c)	0.863 kN/m^2
Internal friction angle, φ	29.94°

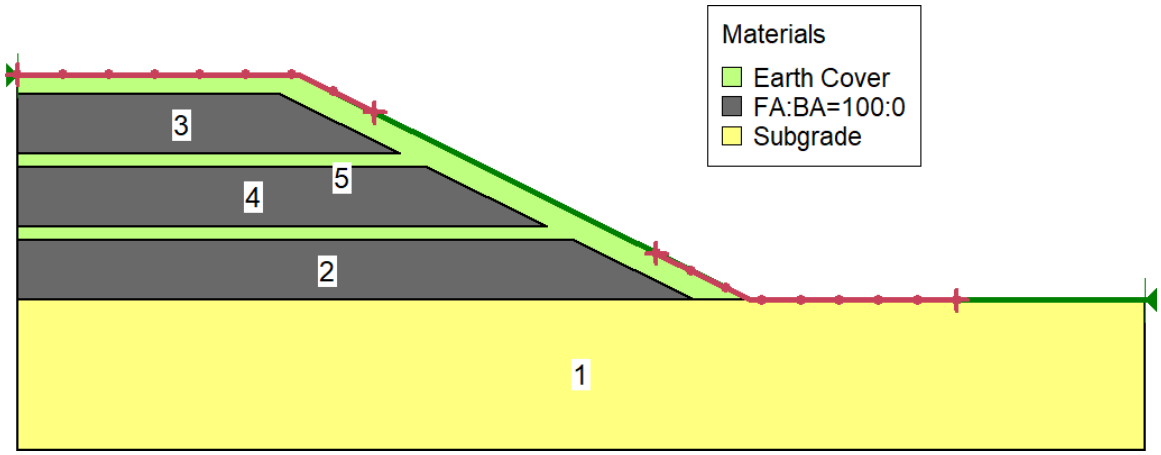

Figure 5.1: Geometry of Model 1 in SLOPE/W

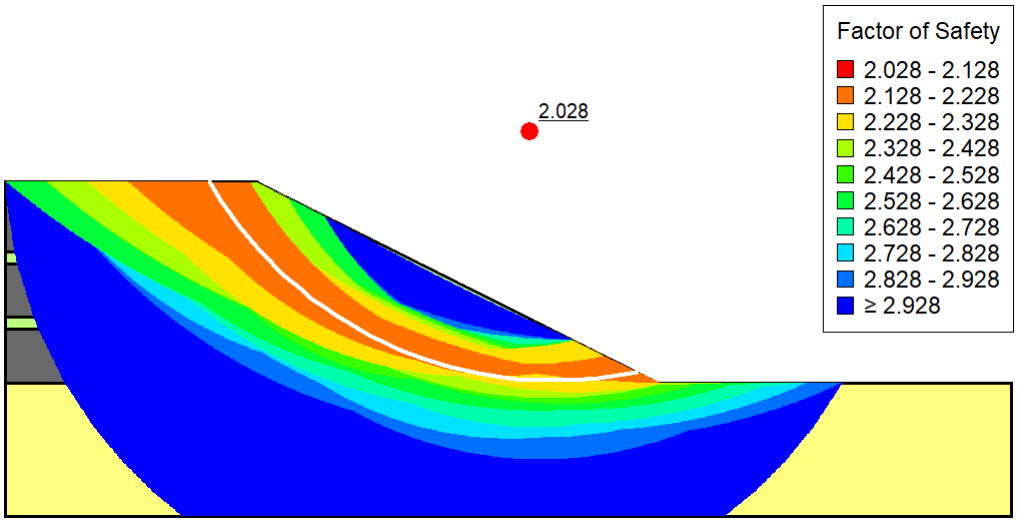

Figure 5.2: Contours showing various slip surfaces and critical FOS of Model 1

Table 5.17: Results obtained from Model 1

Method	Morgenstern-Price
Critical FOS	2.028
Radius of critical slip circle	11.888695 m

5.2.2 Model 2: Stability Analysis of FA:BA=100:0 mix embankment under the effect of its self-weight and surcharge load

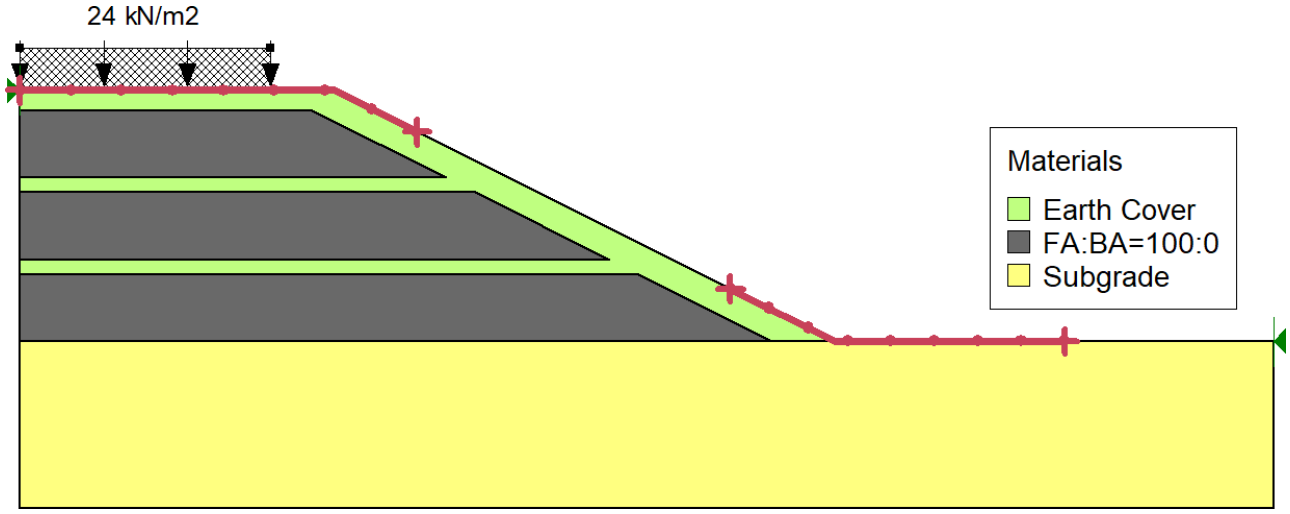

Figure 5.3: Geometry of Model 2 in SLOPE/W

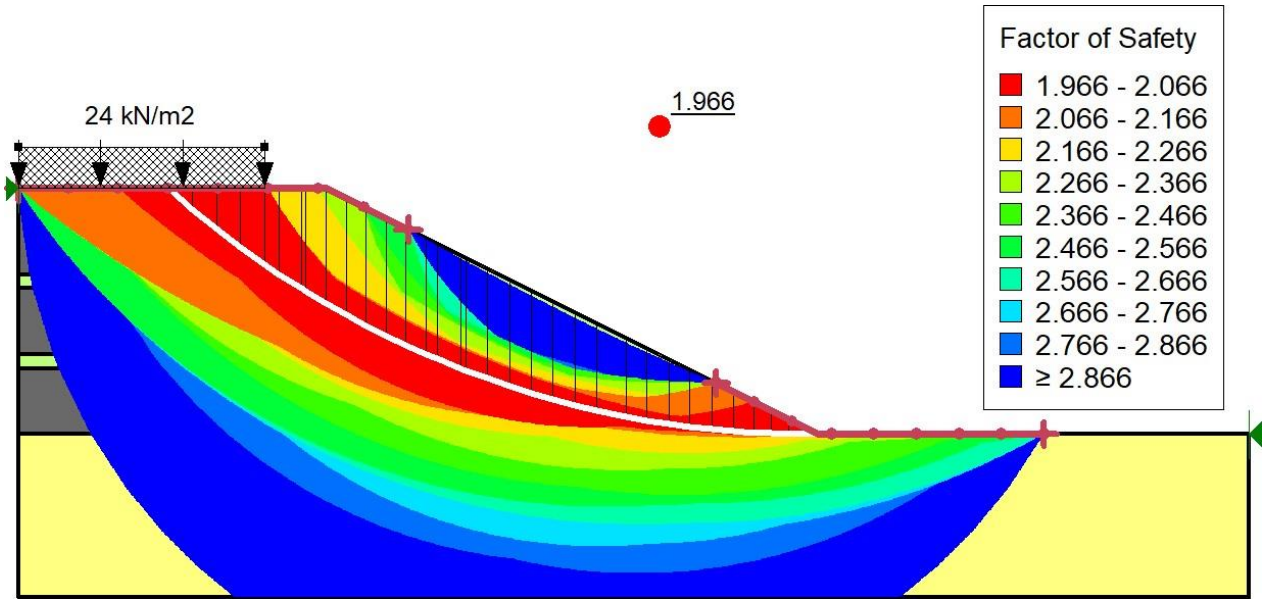

Figure 5.4: Contours showing various slip surfaces and critical FOS of Model 2

Table 5.18: Results obtained from Model 2

Method	Morgenstern-Price
Critical FOS	1.966
Surcharge load	24 kN/m^2
Radius of critical slip circle	23.36228 m

5.2.3 Model 3: Stability Analysis of FA:BA=100:0 mix embankment under the effect of its self-weight, water table at an elevation of 3 m from the top and surcharge load.

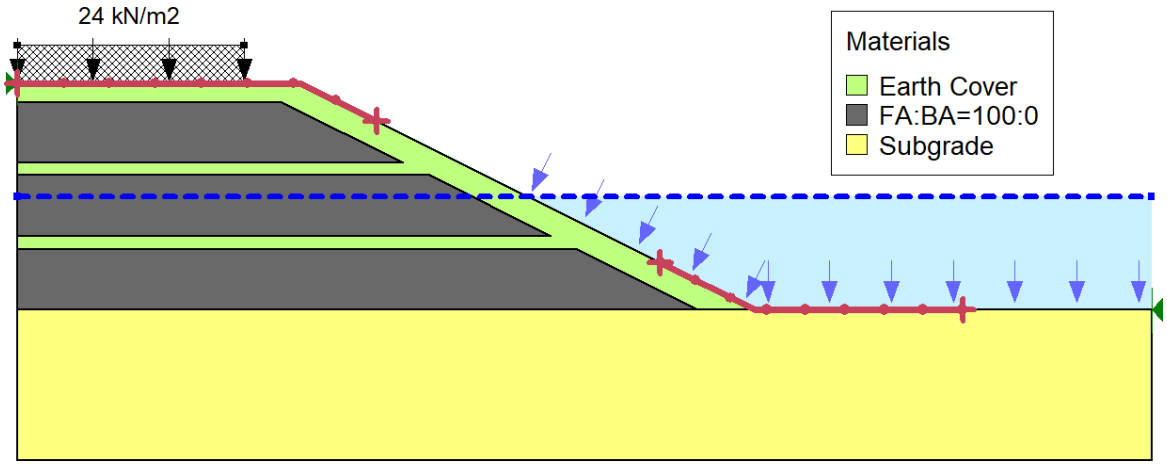

Figure 5.5: Geometry of Model 3 in SLOPE/W

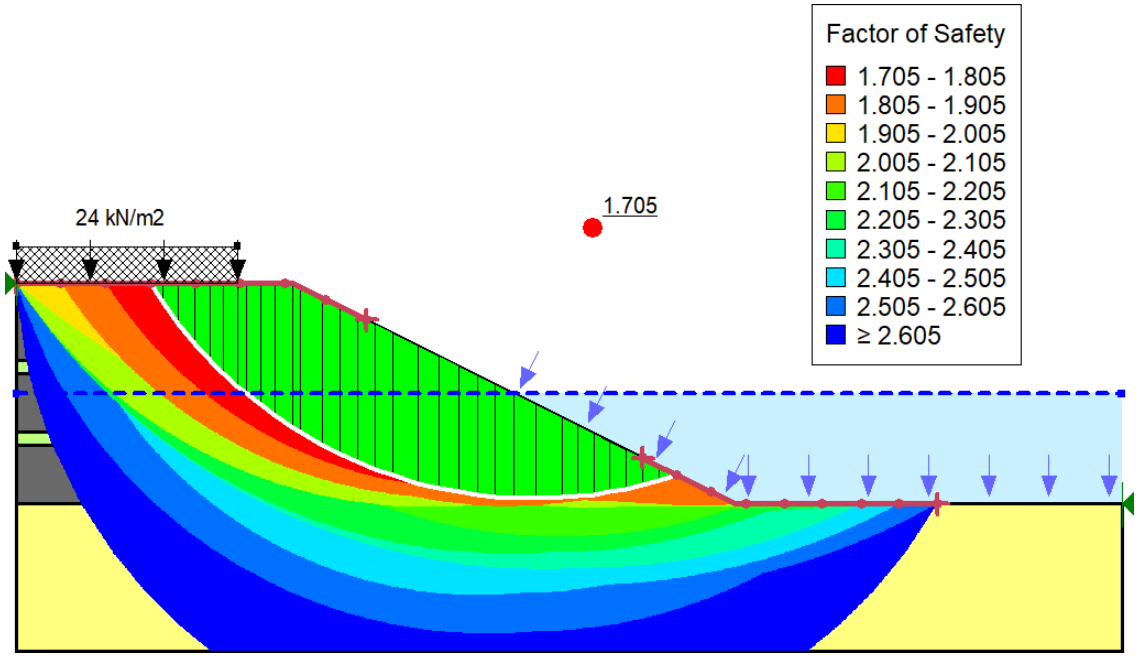

Figure 5.6: Contours showing various slip surfaces and critical FOS of Model 3

Table 5.19: Results obtained from Model 3

Method	Morgenstern-Price
Critical FOS	1.705
Surcharge load	24 kN/m^2
Radius of critical slip circle	12.194208 m

5.2.4 Model 4: Stability Analysis of FA:BA=100:0 mix embankment under the effect of its self-weight, water table, surcharge load and pseudo static load

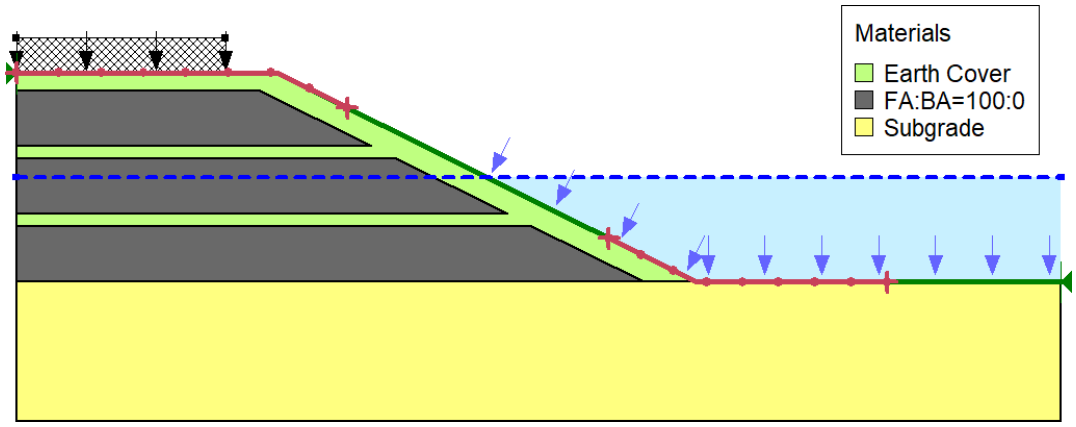

Figure 5.7: Geometry of Model 4 in SLOPE/W

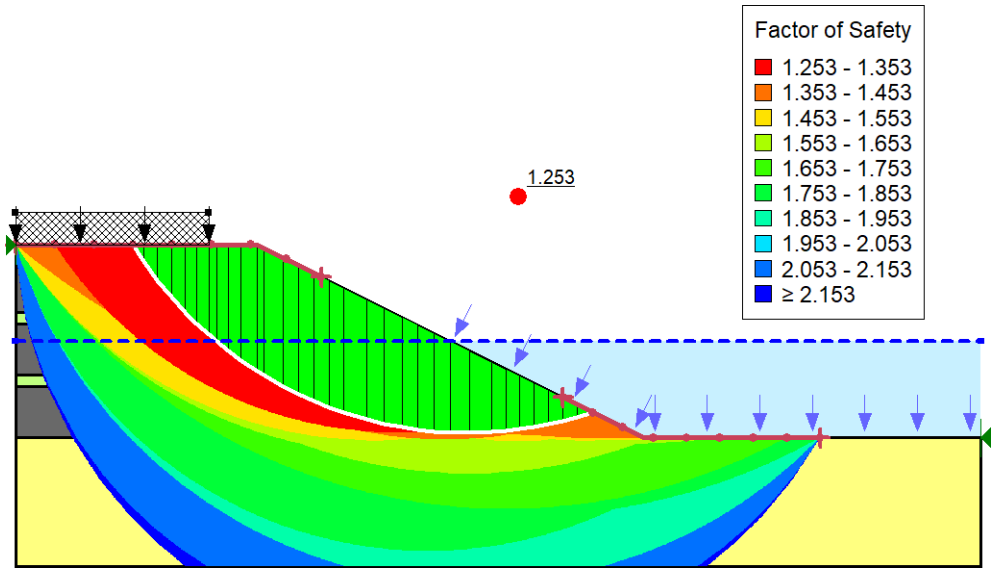

Figure 5.8: Contours showing various slip surfaces and critical FOS of Model 4

Table 5.20: Results obtained from Model 4

Method	Morgenstern-Price
Critical FOS	1.253
Surcharge load	24 kN/m^2
Horizontal seismic coefficient, K_h	0.12
Vertical seismic coefficient, K_v	-0.06 i.e., acting upward
Radius of critical slip circle	12.194208 m

5.2.5 Model 5: Stability Analysis of FA:BA=75:25 mix embankment under the effect of its self-weight

Table 5.21: Properties of FA:BA=75:25 mix

Model	Mohr-Coulomb
Unit Weight	14.23 kN/m^3
Cohesion, c	1.5 kN/m^2
Internal friction angle, φ	31.91°

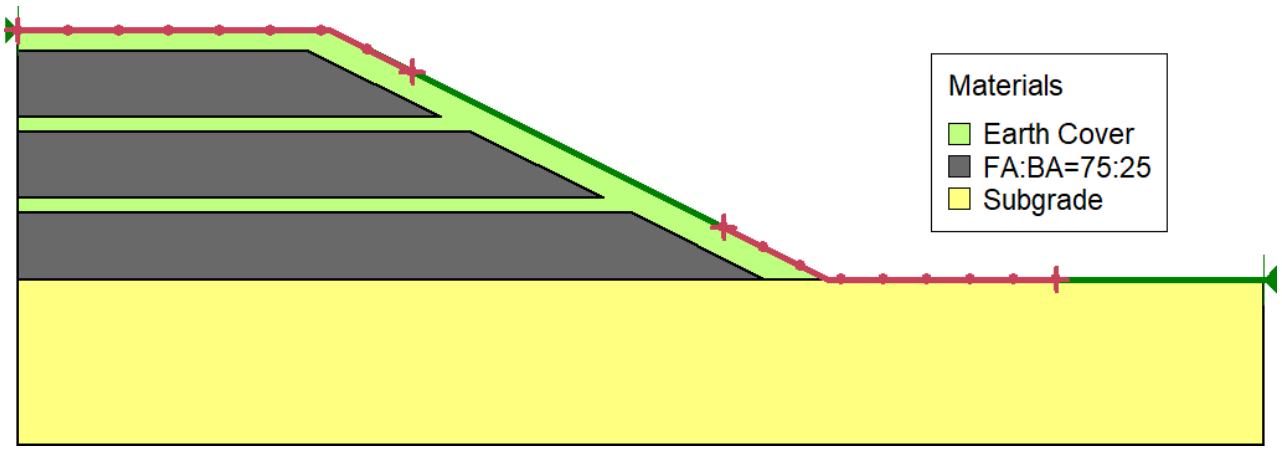

Figure 5.9: Geometry of Model 5 in SLOPE/W

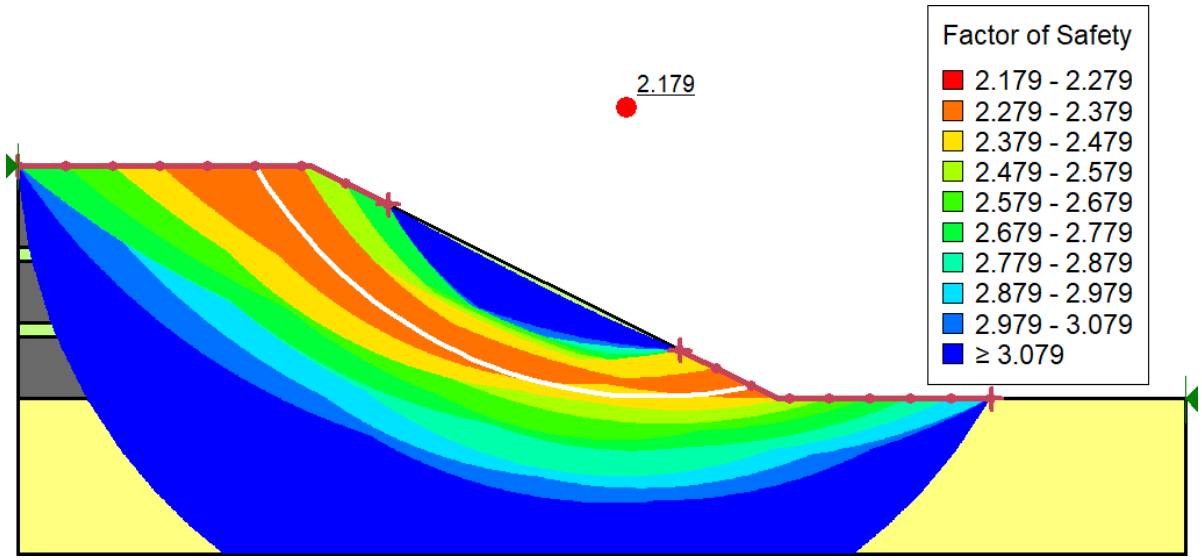

Figure 5.10: Contours showing various slip surfaces and critical FOS of Model 5

Table 5.22: Results obtained from Model 5

Method	Morgenstern-Price
Critical FOS	2.179
Radius of critical slip circle	11.888695 m

5.2.6 Model 6: Stability Analysis of FA:BA=75:25 mix embankment under the effect of its self-weight and surcharge load

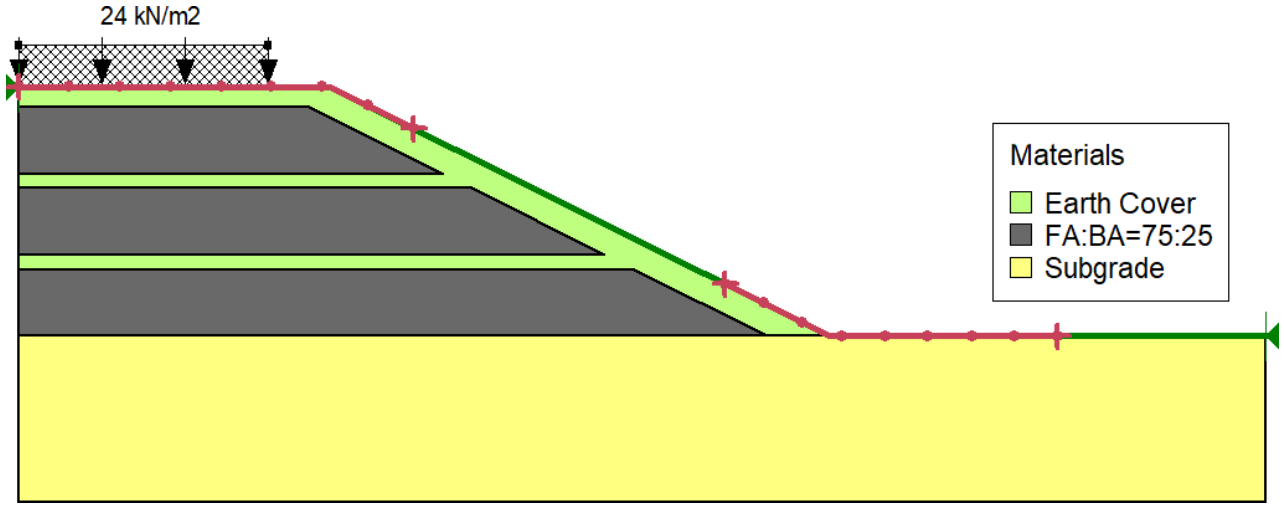

Figure 5.11: Geometry of Model 6 in SLOPE/W

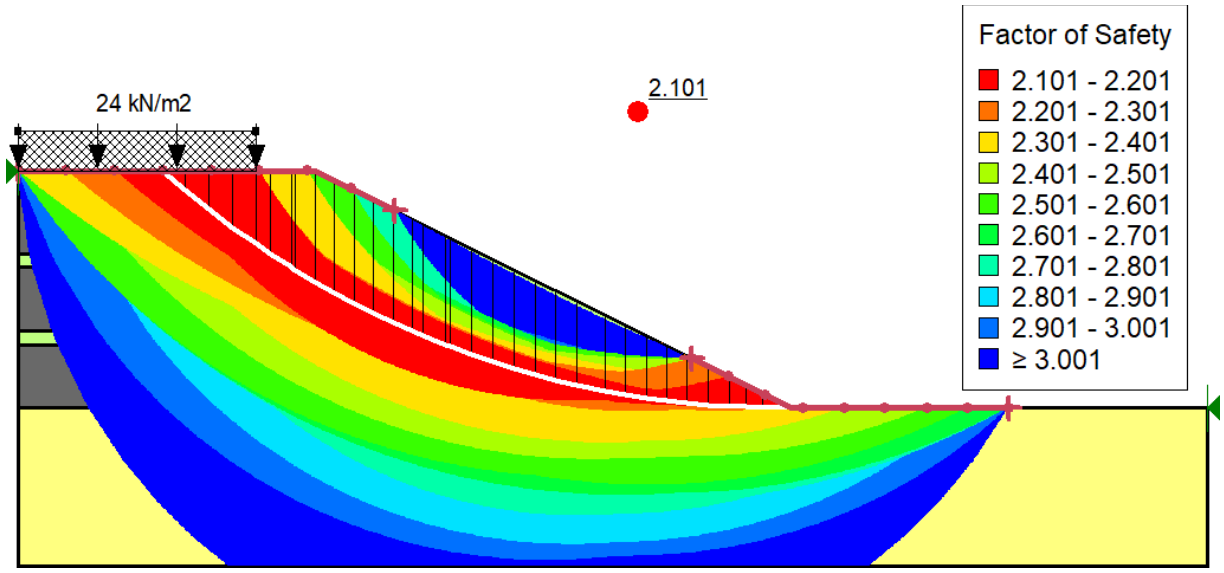

Figure 5.12: Contours showing various slip surfaces and critical FOS of Model 6

Table 5.23: Results obtained from Model 6

Method	Morgenstern-Price
Critical FOS	2.101
Surcharge load	24 kN/m^2
Radius of critical slip circle	23.36228 m

5.2.7 Model 7: Stability Analysis of FA:BA=75:25 mix embankment under the effect of its self-weight, water table and surcharge load

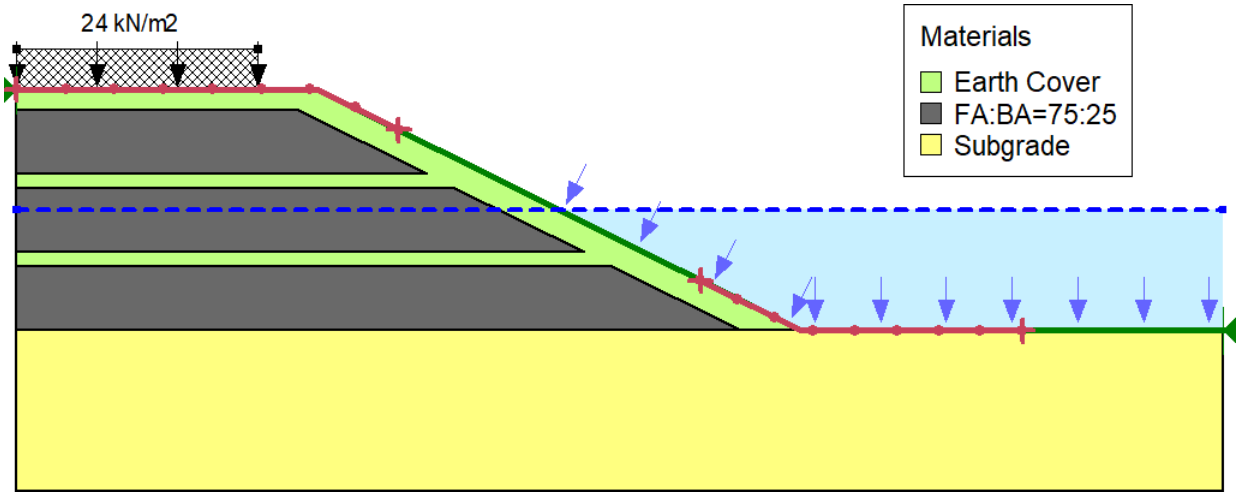

Figure 5.13: Geometry of Model 7 in SLOPE/W

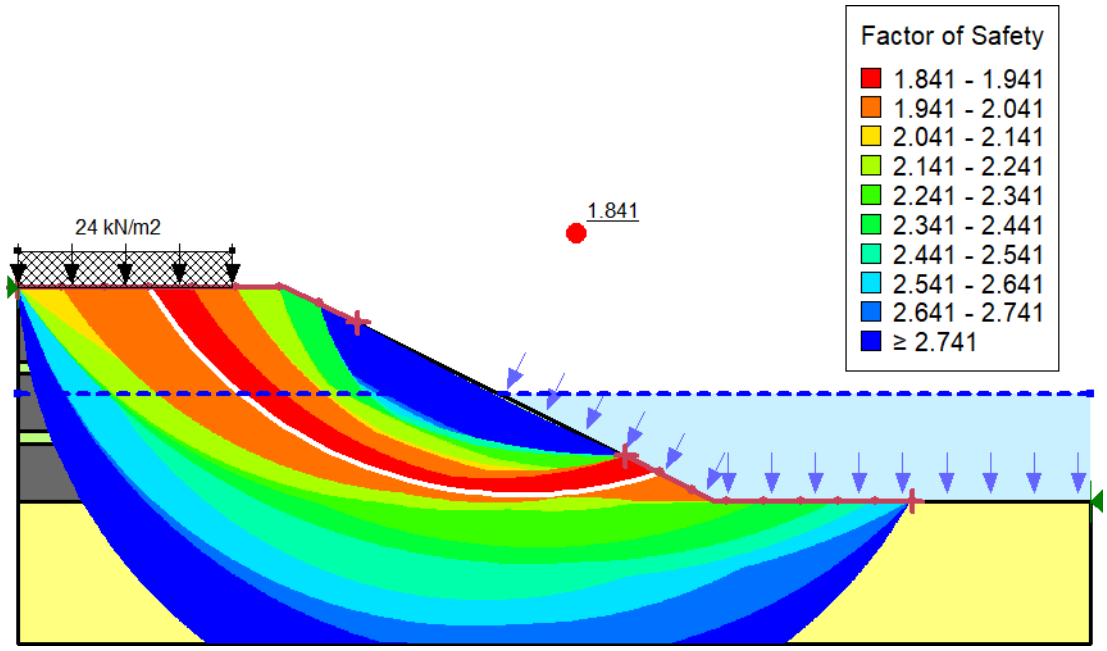

Figure 5.14: Contours showing various slip surfaces and critical FOS of Model 7

Table 5.24: Results obtained from Model 7

Method	Morgenstern-Price
Critical FOS	1.841
Surcharge load	24 kN/m^2
Radius of critical slip circle	12.194208 m

5.2.8 Model 8: Stability Analysis of FA:BA=75:25 mix embankment under the effect of its self-weight, water table, surcharge load and pseudo static load

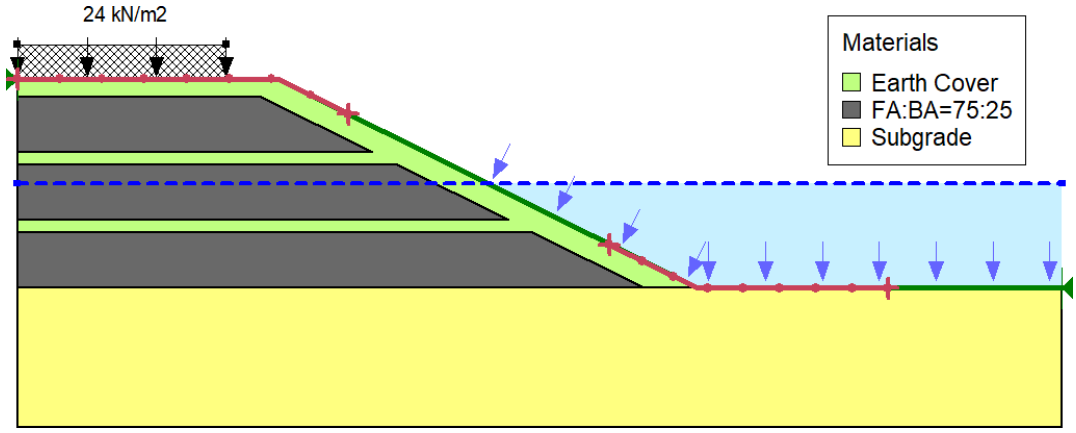

Figure 5.15: Geometry of Model 8 in SLOPE/W

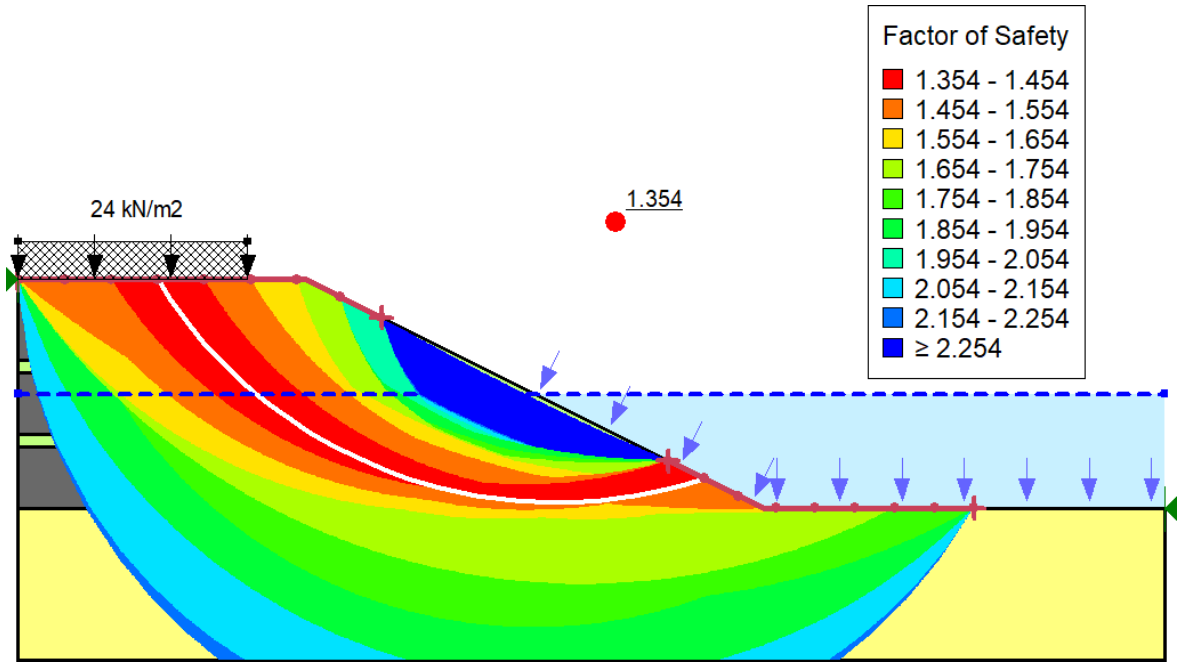

Figure 5.16: Contours showing various slip surfaces and critical FOS of Model 8

Table 5.25: Results obtained from Model 8

Method	Morgenstern-Price
Critical FOS	1.354
Surcharge load	24 kN/m^2
Horizontal seismic coefficient, K_h	0.12
Vertical seismic coefficient, K_v	-0.06 i.e., acting upward
Radius of critical slip circle	12.194208 m

5.2.9 **Model 9: Stability Analysis of FA:BA=50:50 mix embankment under the effect of its self-weight**

Table 5.26: Properties of FA:BA=50:50 mix

Model	Mohr-Coulomb
Unit Weight	14.69 kN/m^3
Cohesion, c	1.069 kN/m^2
Internal friction angle, φ	32.48°

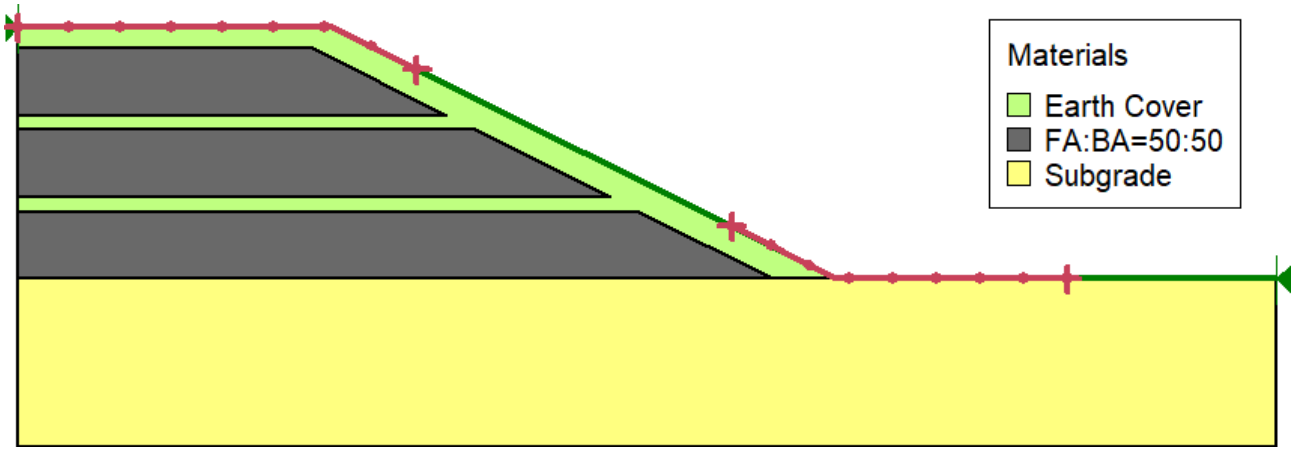

Figure 5.17: Geometry of Model 9 in SLOPE/W

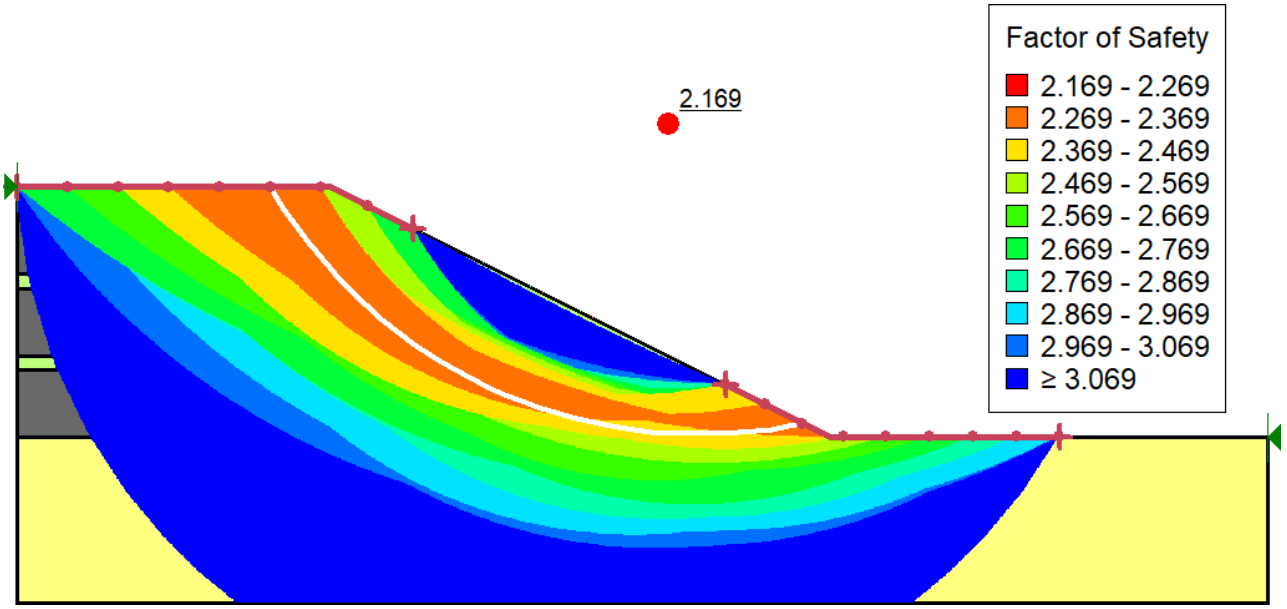

Figure 5.18: Contours showing various slip surfaces and critical FOS of Model 9

Table 5.27: Results obtained from Model 9

Method	Morgenstern-Price
Critical FOS	2.169
Radius of critical slip circle	11.888695 m

5.2.10 Model 10: Stability Analysis of FA:BA=50:50 mix embankment under the effect of its self-weight and surcharge load

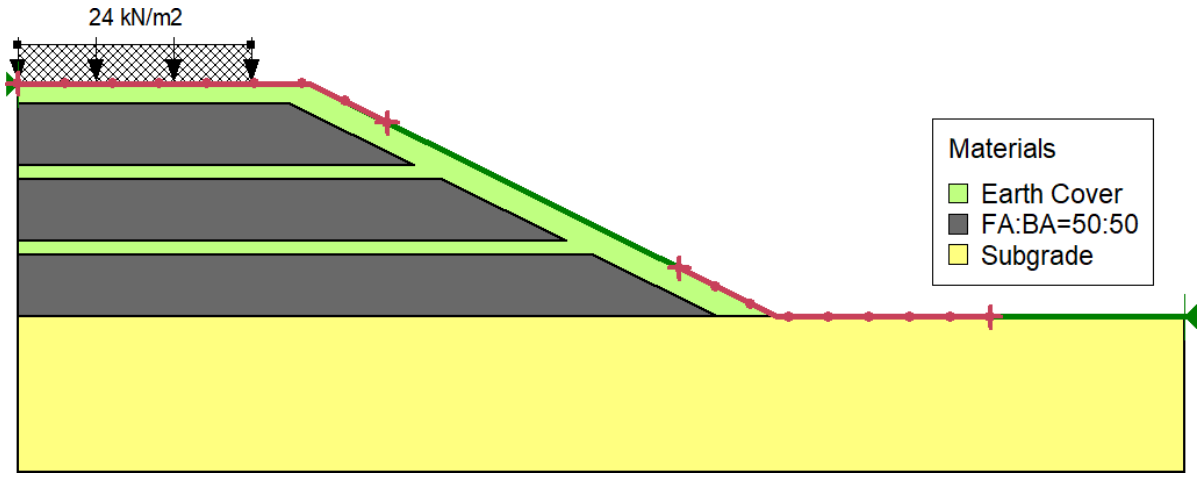

Figure 5.19: Geometry of Model 10 in SLOPE/W

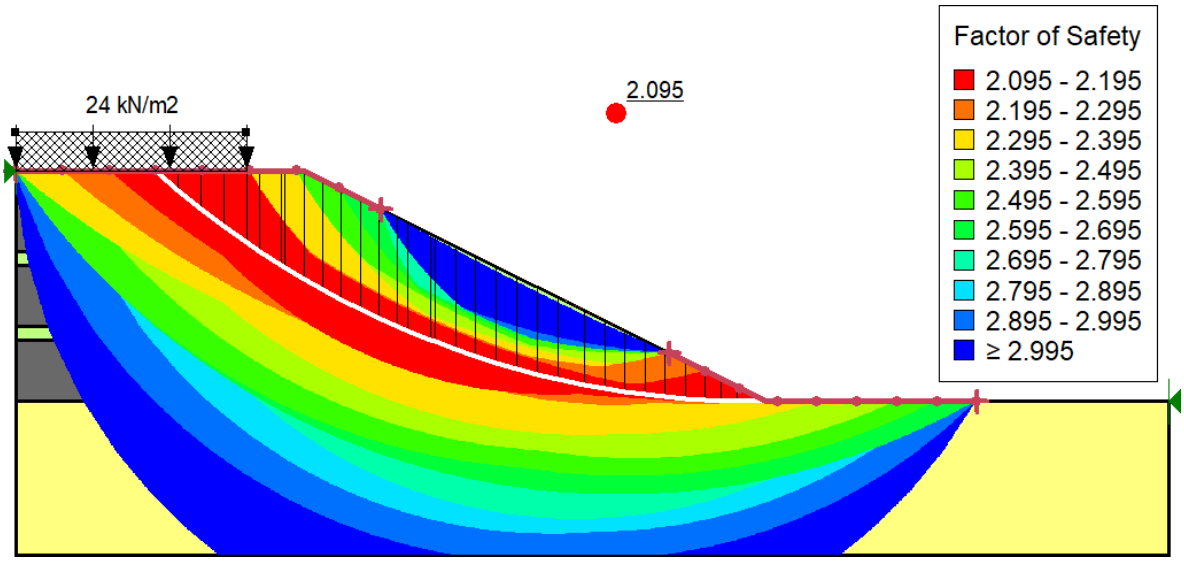

Figure 5.20: Contours showing various slip surfaces and critical FOS of Model 10

Table 5.28: Results obtained from Model 10

Method	Morgenstern-Price
Critical FOS	2.095
Surcharge load	24 kN/m^2
Radius of critical slip circle	23.36228 m

5.2.11 Model 11: Stability Analysis of FA:BA=50:50 mix embankment under the effect of its self-weight, water table and surcharge load

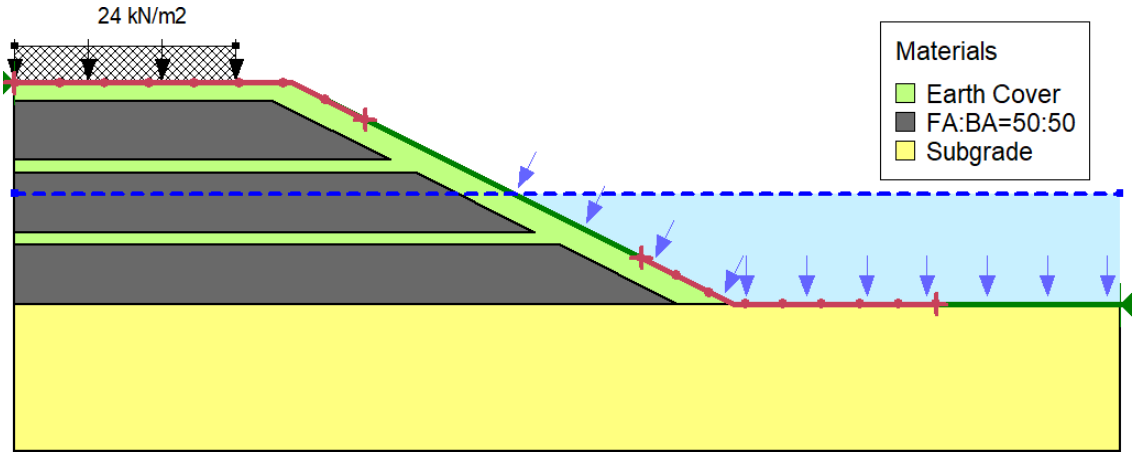

Figure 5.21: Geometry of Model 11 in SLOPE/W

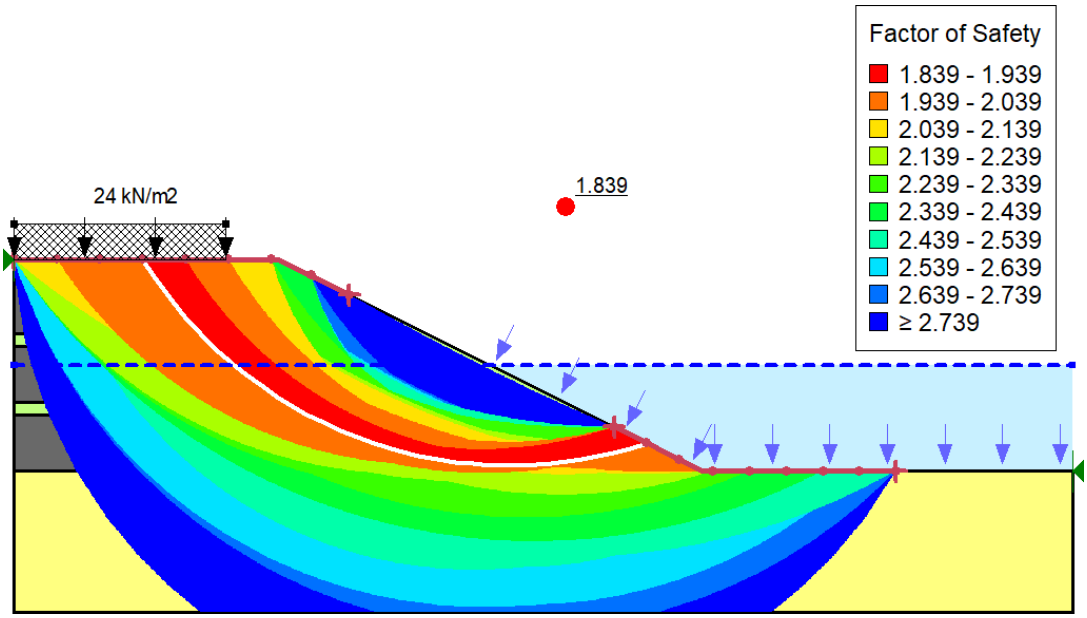

Figure 5.22: Contours showing various slip surfaces and critical FOS of Model 11

Table 5.29: Results obtained from Model 11

Method	Morgenstern-Price
Critical FOS	1.839
Surcharge load	24 kN/m^2
Radius of critical slip circle	12.194208 m

5.2.12 Model 12: Stability Analysis of FA:BA=50:50 mix embankment under the effect of its self-weight, water table, surcharge load and pseudo static load

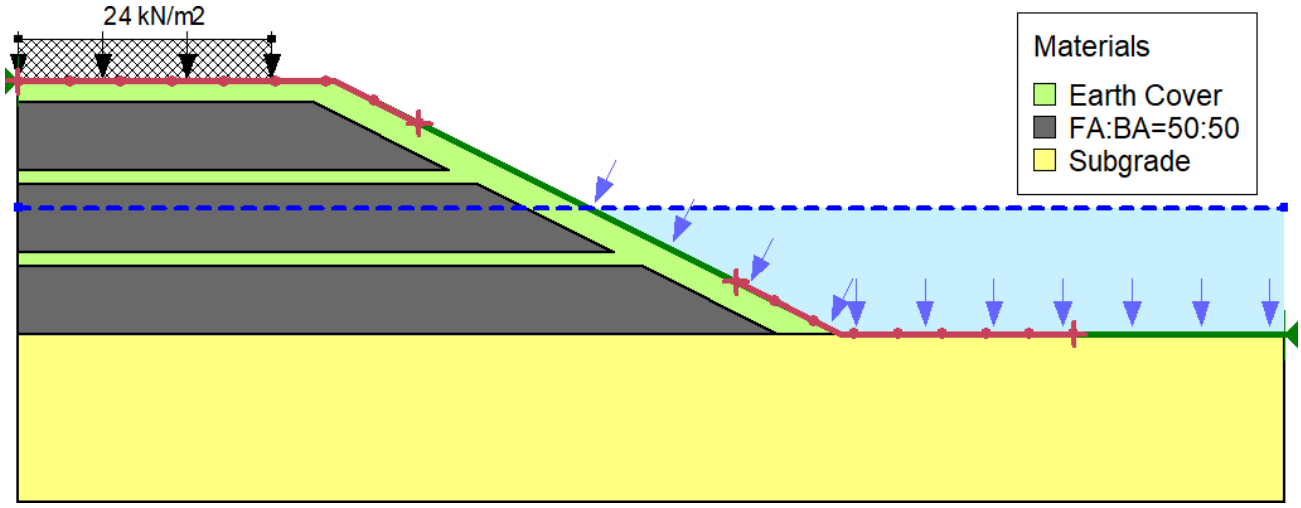

Figure 5.23: Geometry of Model 12 in SLOPE/W

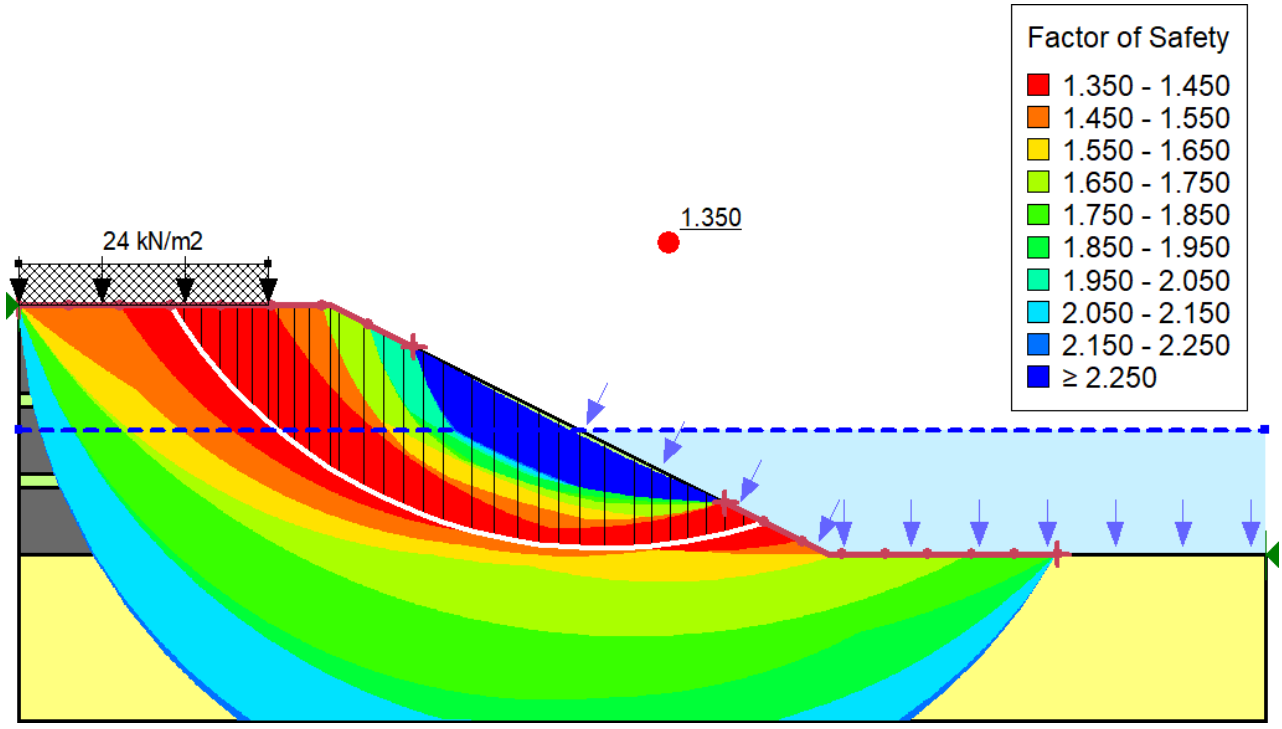

Figure 5.24: Contours showing various slip surfaces and critical FOS of Model 12

Table 5.30: Results obtained from Model 12

Method	Morgenstern-Price
Critical FOS	1.350
Surcharge load	24 kN/m^2
Horizontal seismic coefficient, K_h	0.12
Vertical seismic coefficient, K_v	-0.06 i.e., acting upward
Radius of critical slip circle	12.194208 m

5.2.13 Model 13: Stability Analysis of FA:BA=25:75 mix embankment under the effect of its self-weight

Table 5.31: Properties of FA:BA=25:75 mix

Model	Mohr-Coulomb
Unit Weight	14.72 kN/m^3
Cohesion, c	0.765 kN/m^2
Internal friction angle, φ	34.76°

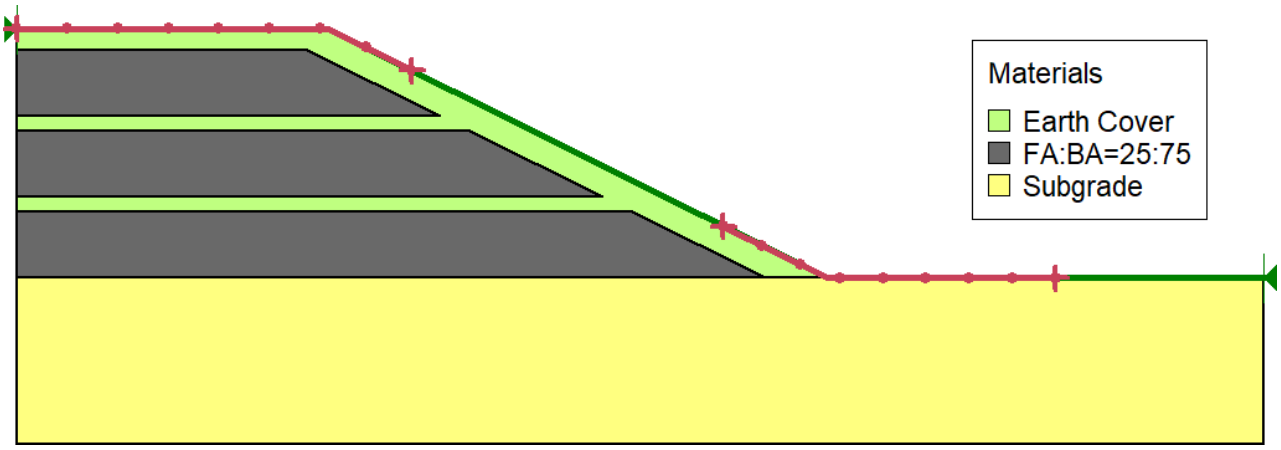

Figure 5.25: Geometry of Model 13 in SLOPE/W

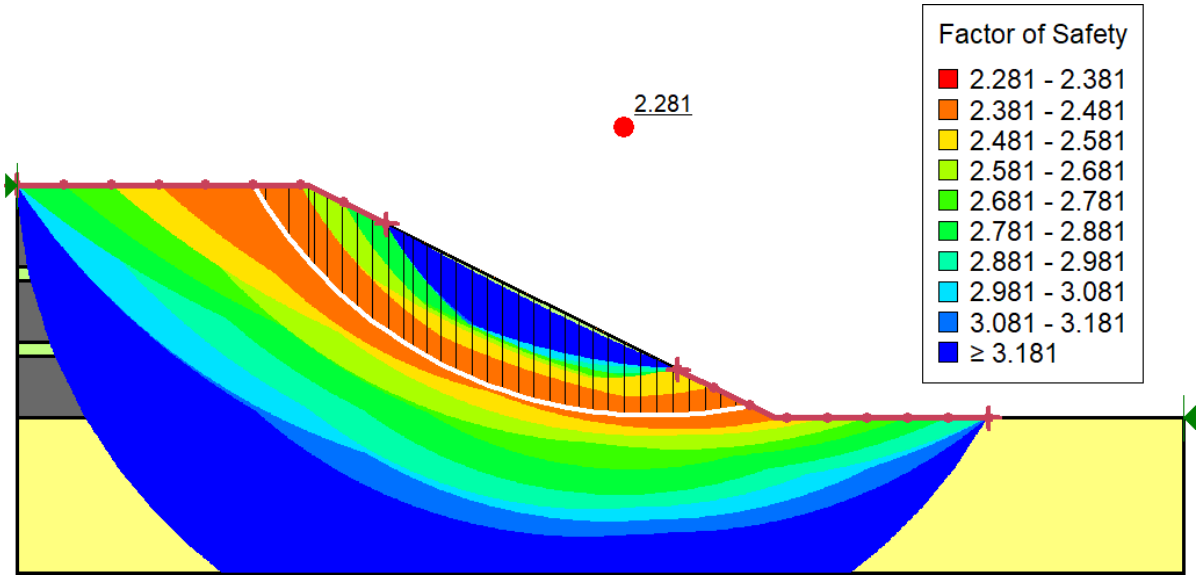

Figure 5.26: Contours showing various slip surfaces and critical FOS of Model 13

Table 5.32: Results obtained from Model 13

Method	Morgenstern-Price
Critical FOS	2.281
Radius of critical slip circle	11.888695 m

5.2.14 Model 14: Stability Analysis of FA:BA=25:75 mix embankment under the effect of its self-weight and surcharge load

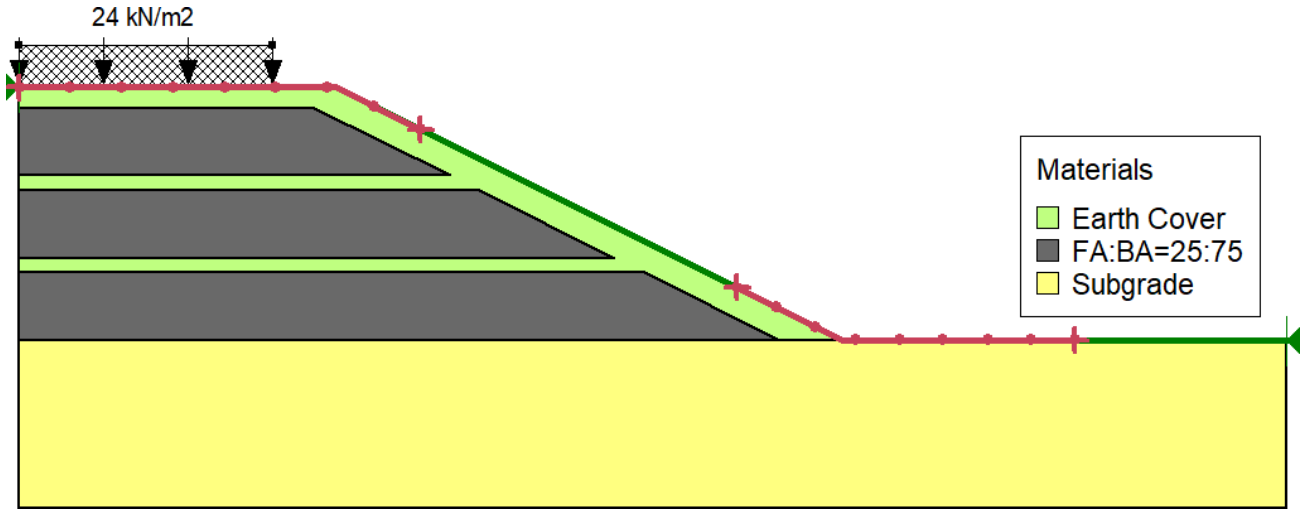

Figure 5.27: Geometry of Model 14 in SLOPE/W

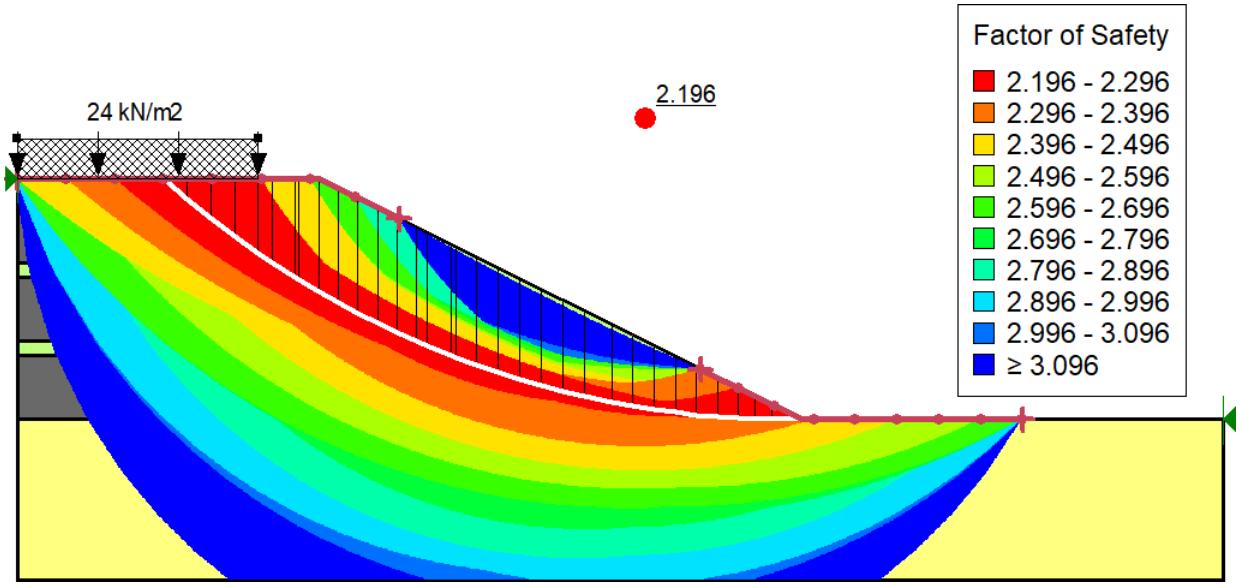

Figure 5.28: Contours showing various slip surfaces and critical FOS of Model 14

Table 5.33: Results obtained from Model 14

Method	Morgenstern-Price
Critical FOS	2.196
Surcharge load	24 kN/m^2
Radius of critical slip circle	23.36228 m

5.2.15 Model 15: Stability Analysis of FA:BA=25:75 mix embankment under the effect of its self-weight, water table and surcharge load

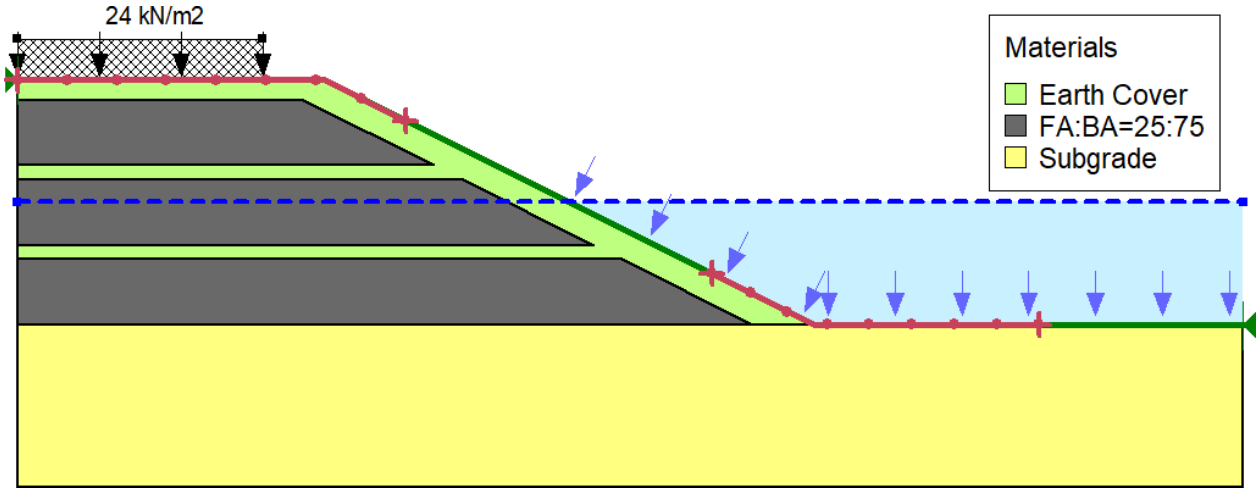

Figure 5.29: Geometry of Model 15 in SLOPE/W

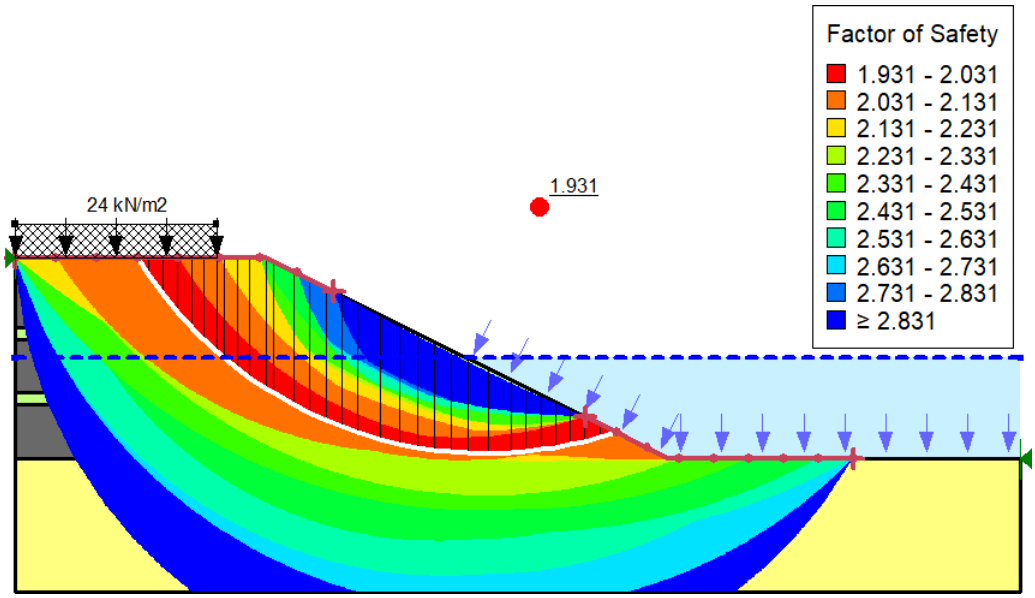

Figure 5.30: Contours showing various slip surfaces and critical FOS of Model 15

Table 5.34: Results obtained from Model 15

Method	Morgenstern-Price
Critical FOS	1.931
Surcharge load	24 kN/m^2
Radius of critical slip circle	12.194208 m

5.2.16 Model 16: Stability Analysis of FA:BA=25:75 mix embankment under the effect of its self-weight, water table, surcharge load and pseudo static load

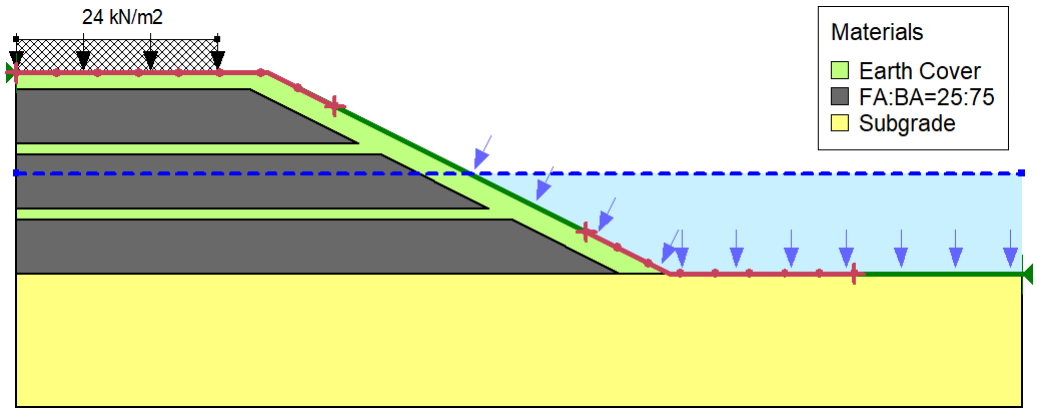

Figure 5.31: Geometry of Model 16 in SLOPE/W

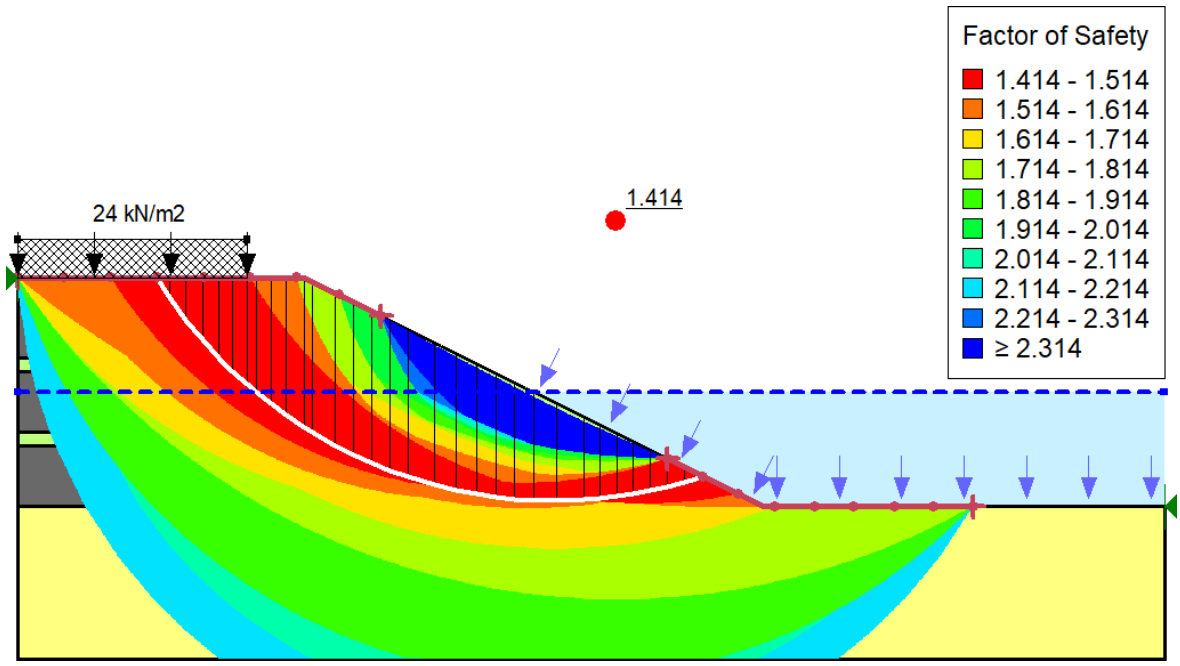

Figure 5.32: Contours showing various slip surfaces and critical FOS of Model 16

Table 5.35: Results obtained from Model 16

Method	Morgenstern-Price
Critical FOS	1.414
Surcharge load	24 kN/m^2
Horizontal seismic coefficient, K_h	0.12
Vertical seismic coefficient, K_v	-0.06 i.e., acting upward
Radius of critical slip circle	12.194208 m

5.2.17 **Model 17: Stability Analysis of FA:BA=0:100 mix embankment under the effect of its self-weight**

Table 5.36: Properties of FA:BA=0:100 mix

Model	Mohr-Coulomb
Unit Weight	14.38 kN/m^3
Cohesion, c	0.775 kN/m^2
Internal friction angle, φ	28.30°

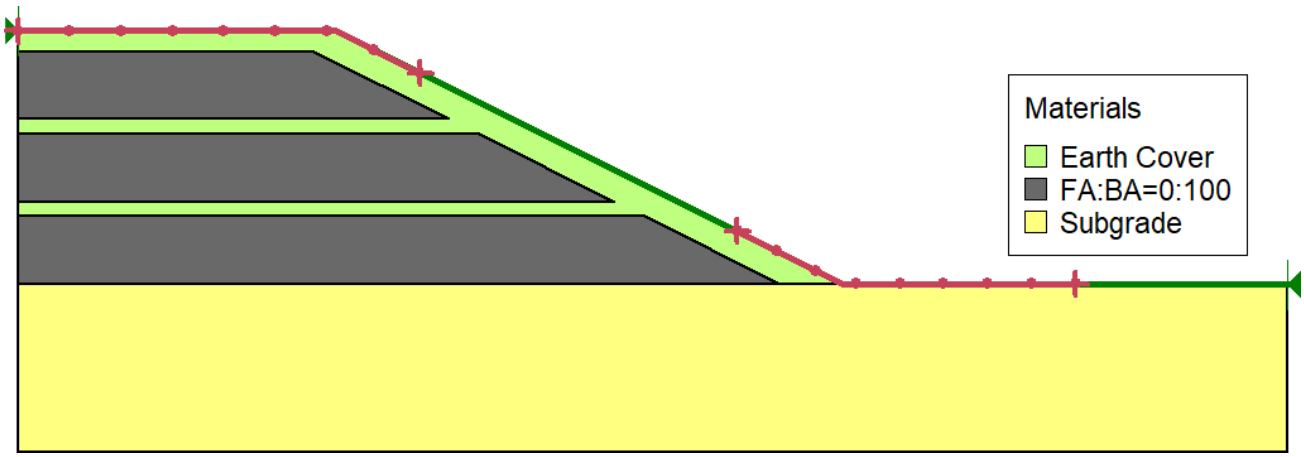

Figure 5.33: Geometry of Model 17 in SLOPE/W

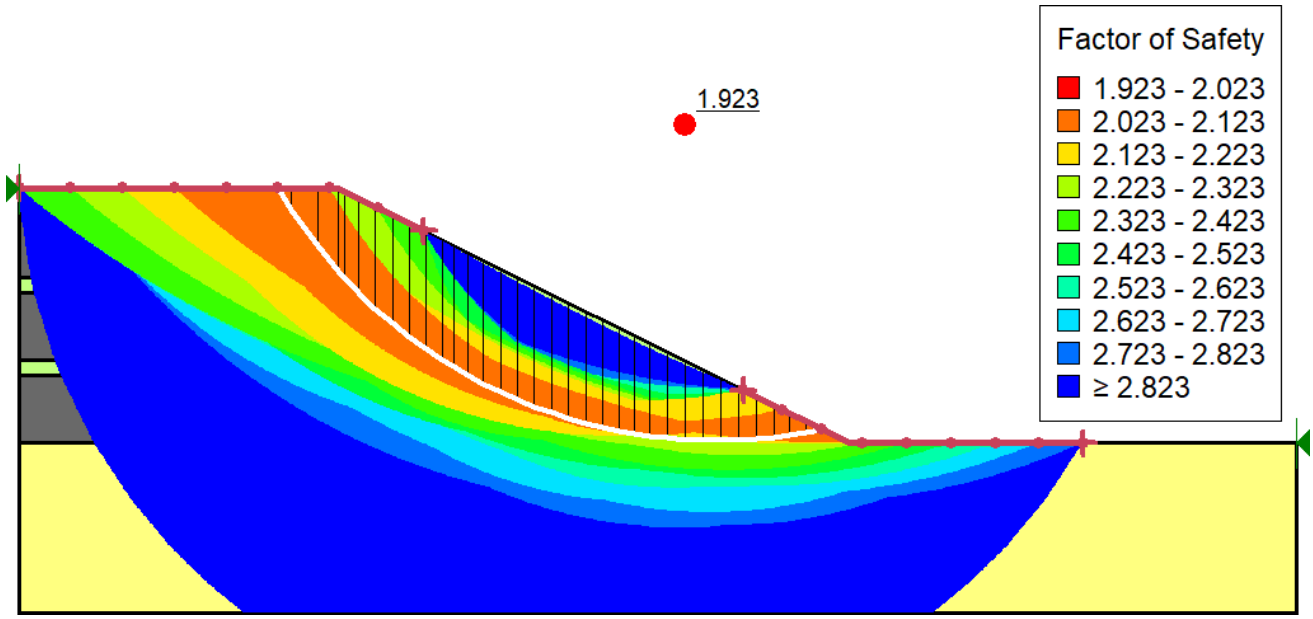

Figure 5.34: Contours showing various slip surfaces and critical FOS of Model 17

Table 5.37: Results obtained from Model 17

Method	Morgenstern-Price
Critical FOS	1.923
Radius of critical slip circle	11.888695 m

5.2.18 Model 18: Stability Analysis of FA:BA=0:100 mix embankment under the effect of its self-weight and surcharge load

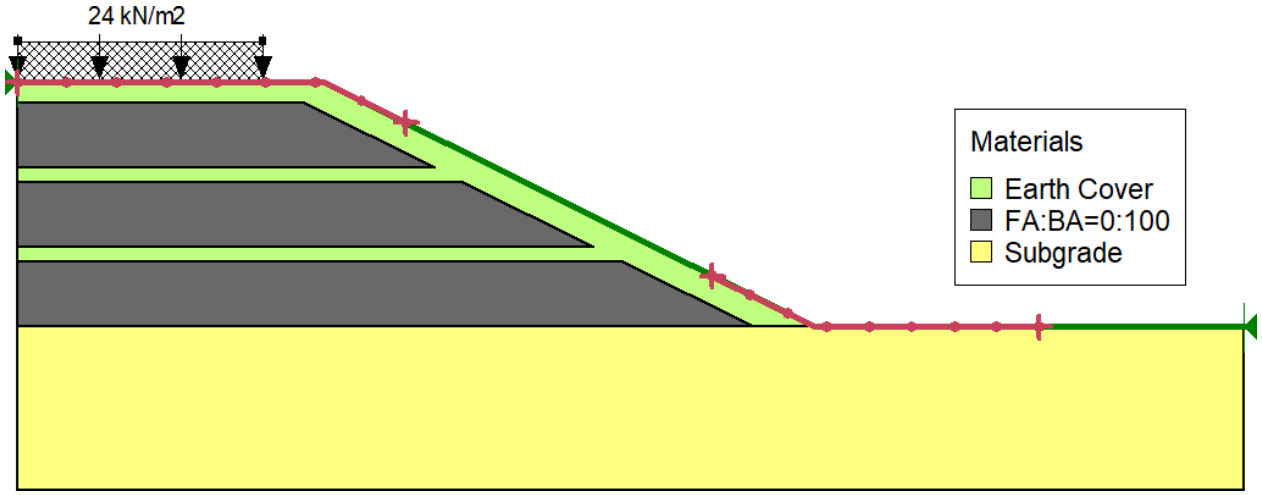

Figure 5.35: Geometry of Model 18 in SLOPE/W

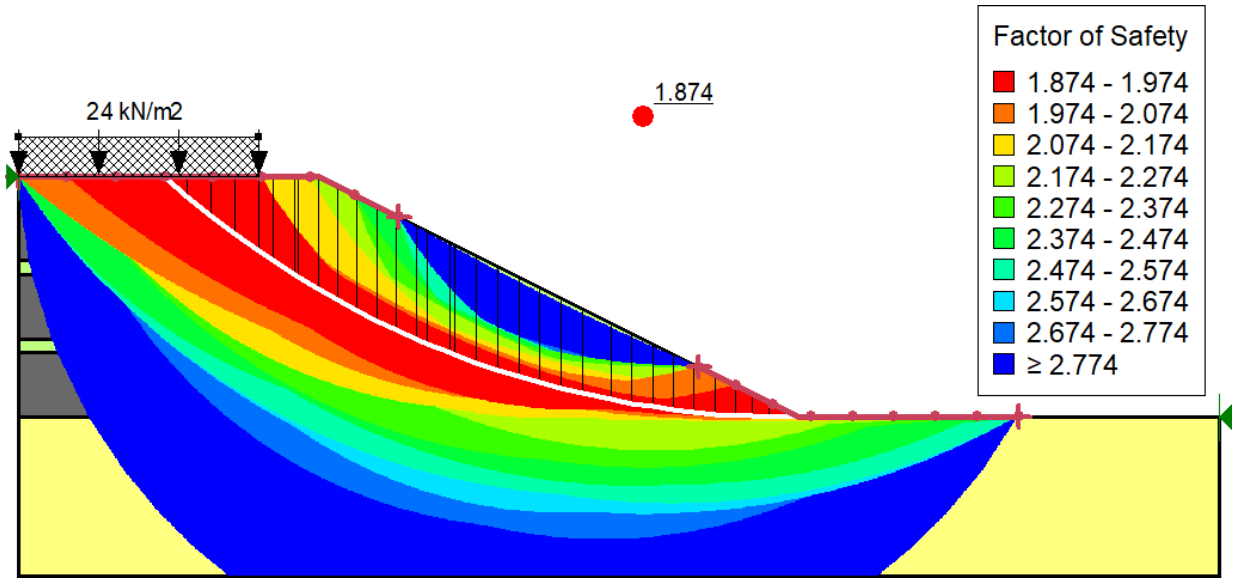

Figure 5.36: Contours showing various slip surfaces and critical FOS of Model 18

Table 5.38: Results obtained from Model 18

Method	Morgenstern-Price
Critical FOS	1.874
Surcharge load	24 kN/m^2
Radius of critical slip circle	23.36228 m

5.2.19 Model 19: Stability Analysis of FA:BA=0:100 mix embankment under the effect of its self-weight, water table and surcharge load

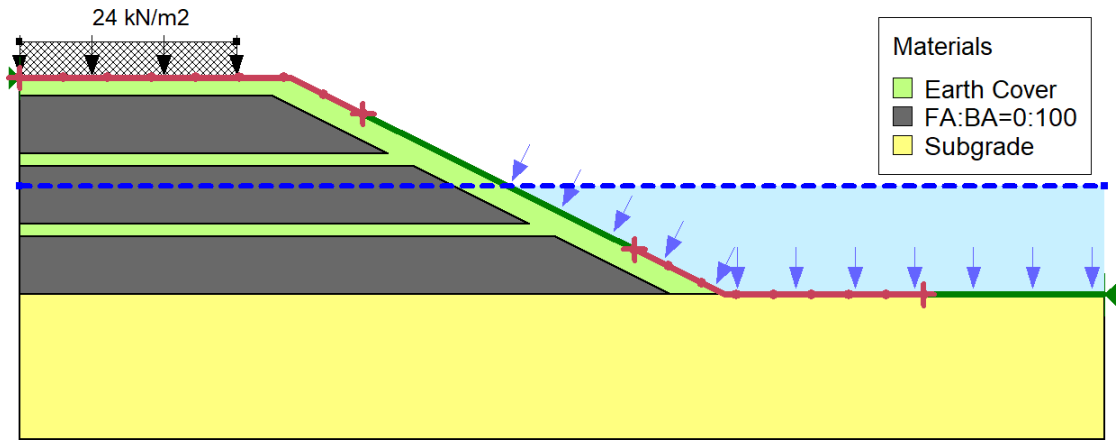

Figure 5.37: Geometry of Model 19 in SLOPE/W

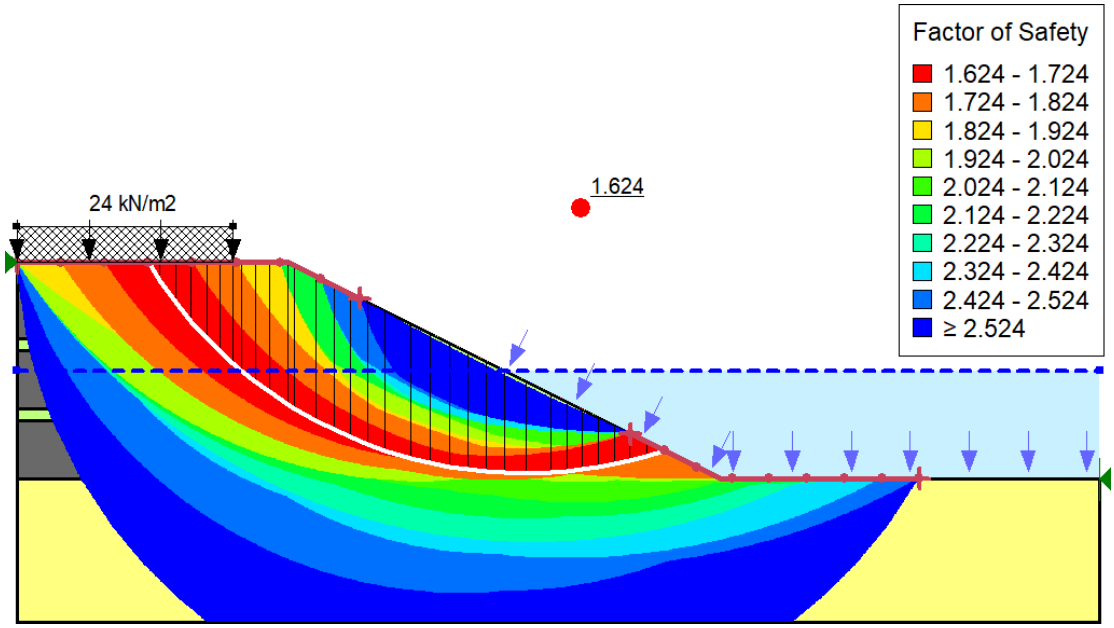

Figure 5.38: Contours showing various slip surfaces and critical FOS of Model 19

Table 5.39: Results obtained from Model 19

Method	Morgenstern-Price
Critical FOS	1.624
Surcharge load	24 kN/m^2
Radius of critical slip circle	12.194208 m

5.2.20 Model 20: Stability Analysis of FA:BA=0:100 mix embankment under the effect of its self-weight, water table, surcharge load and pseudo static load

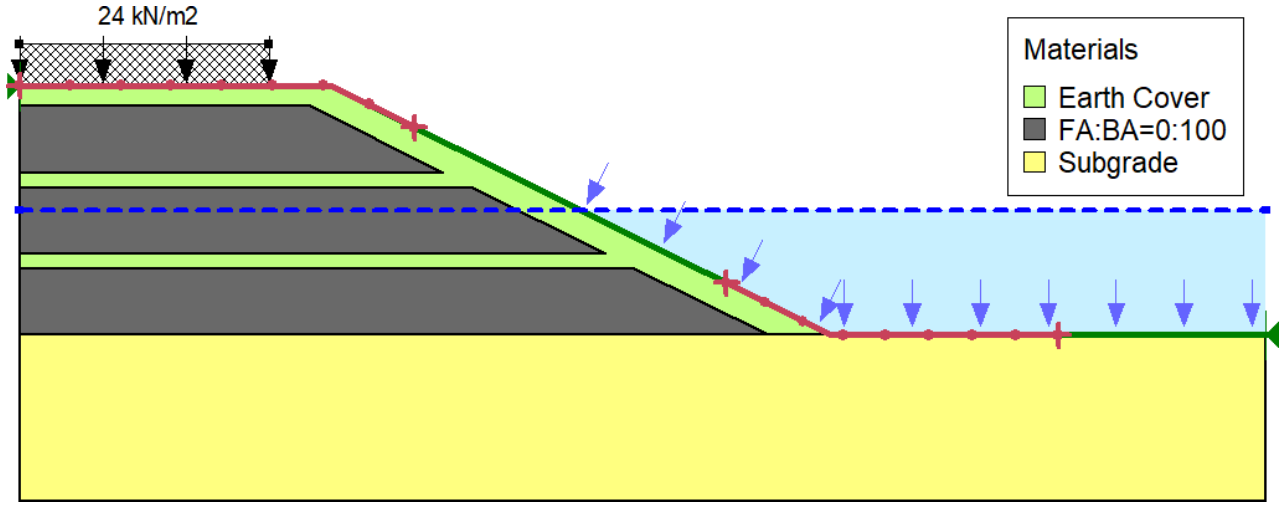

Figure 5.39: Geometry of Model 20 in SLOPE/W

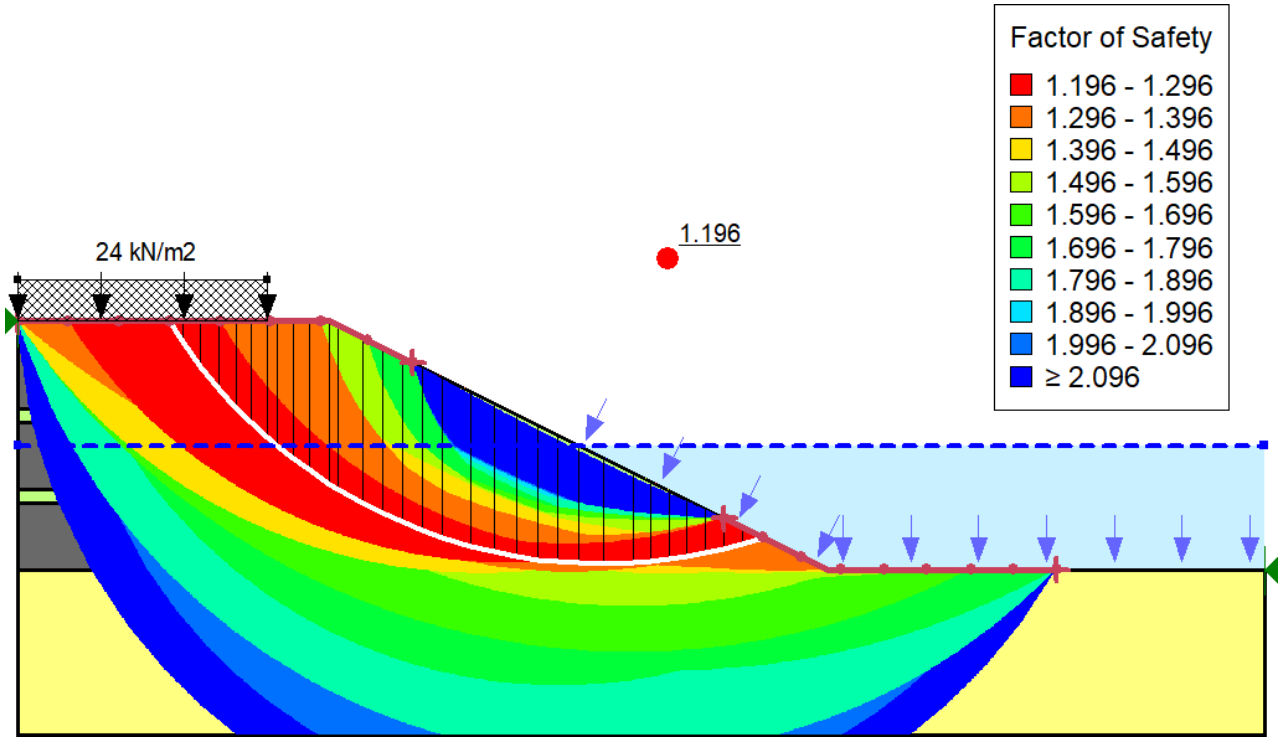

Figure 5.40: Contours showing various slip surfaces and critical FOS of Model 20

Table 5.40: Results obtained from Model 20

Method	Morgenstern-Price
Critical FOS	1.196
Surcharge load	24 kN/m^2
Horizontal seismic coefficient, K_h	0.12
Vertical seismic coefficient, K_v	-0.06 i.e., acting upward
Radius of critical slip circle	12.194208 m

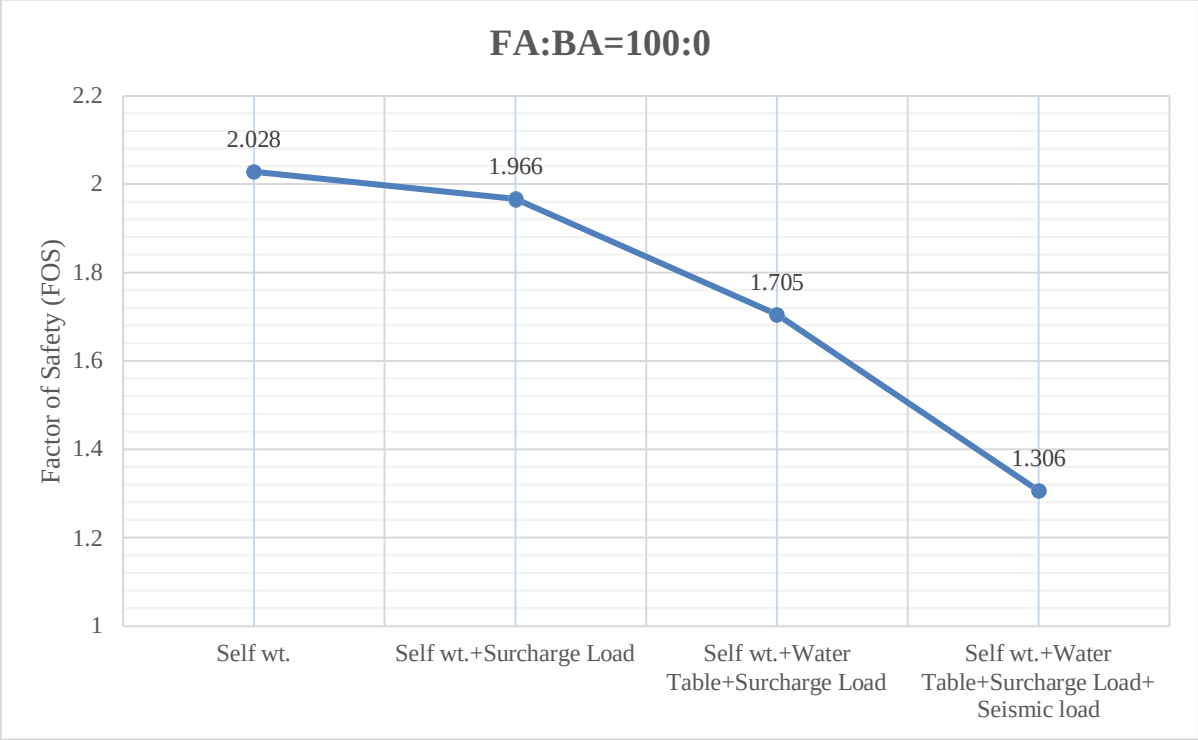

Graph 5.16: FOS for FA:BA=100:0 mix embankment under different loading conditions

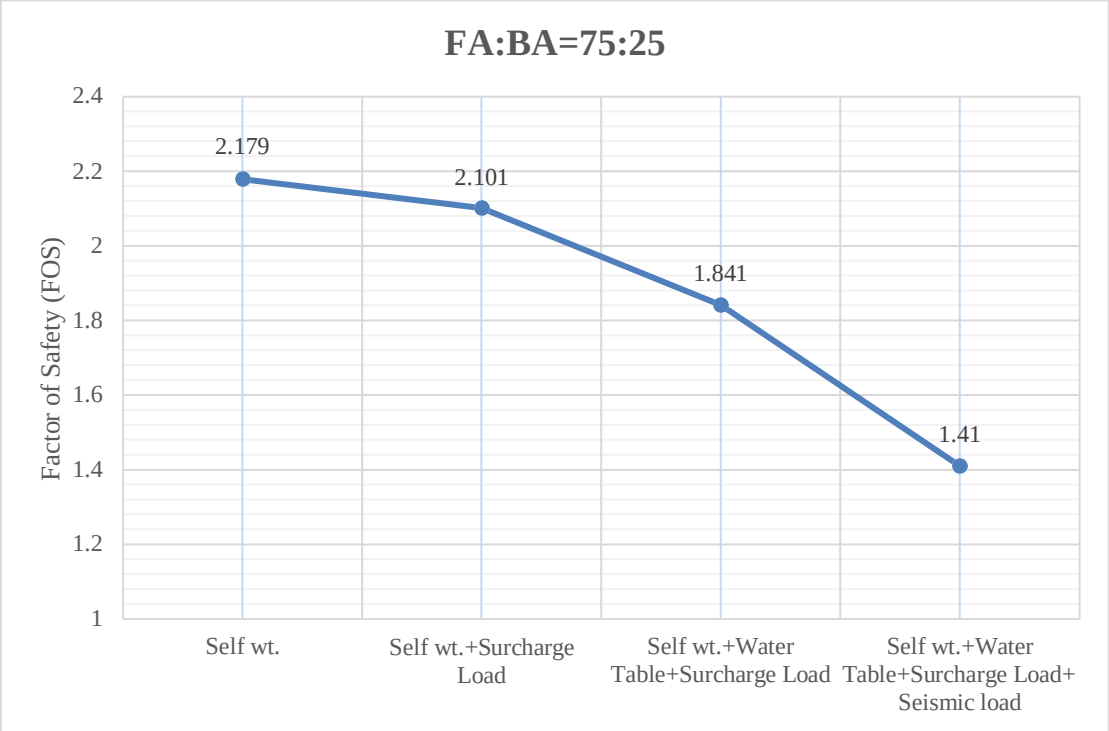

Graph 5.17: FOS for FA:BA=75:25 mix embankment under different loading conditions

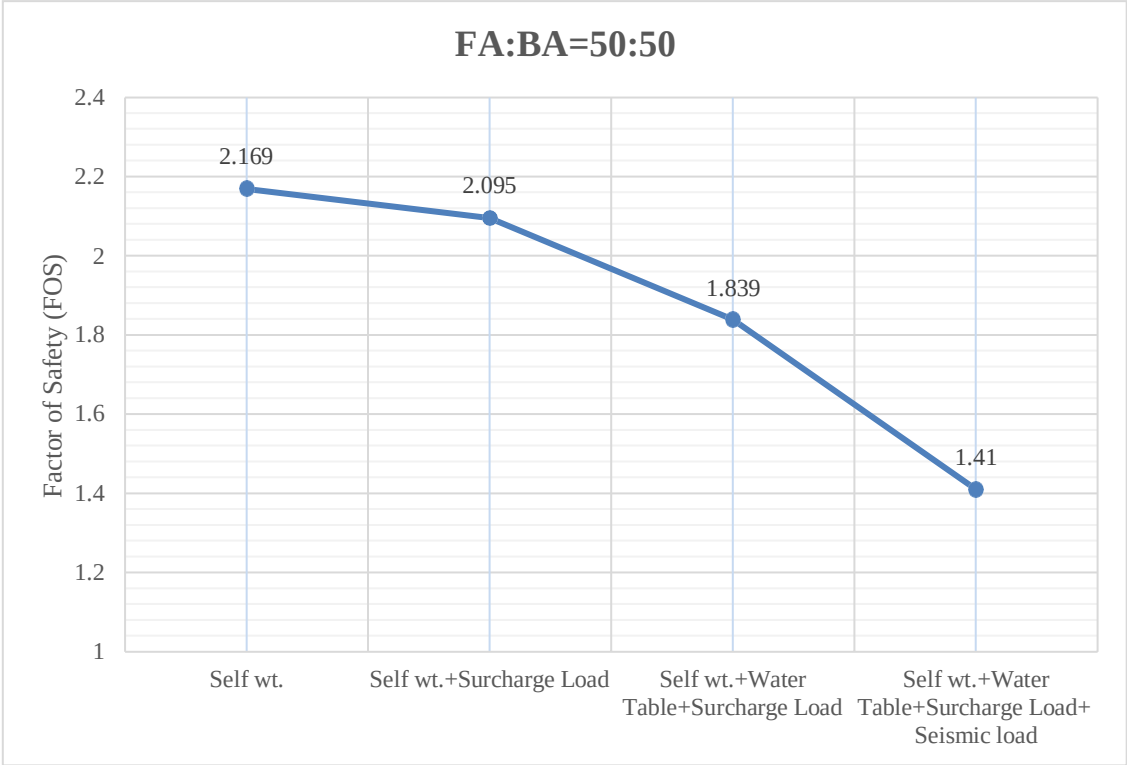

Graph 5.18: FOS for FA:BA=50:50 mix embankment under different loading conditions

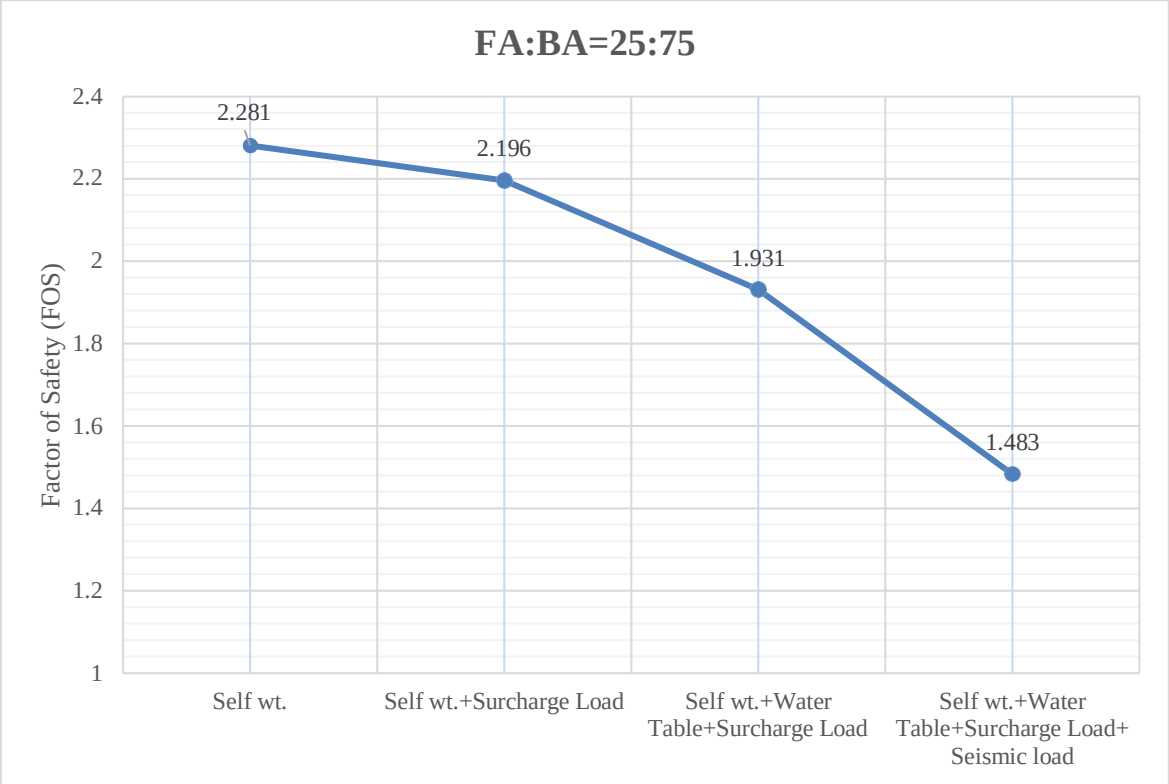

Graph 5.19: FOS for FA:BA=25:75 mix embankment under different loading conditions

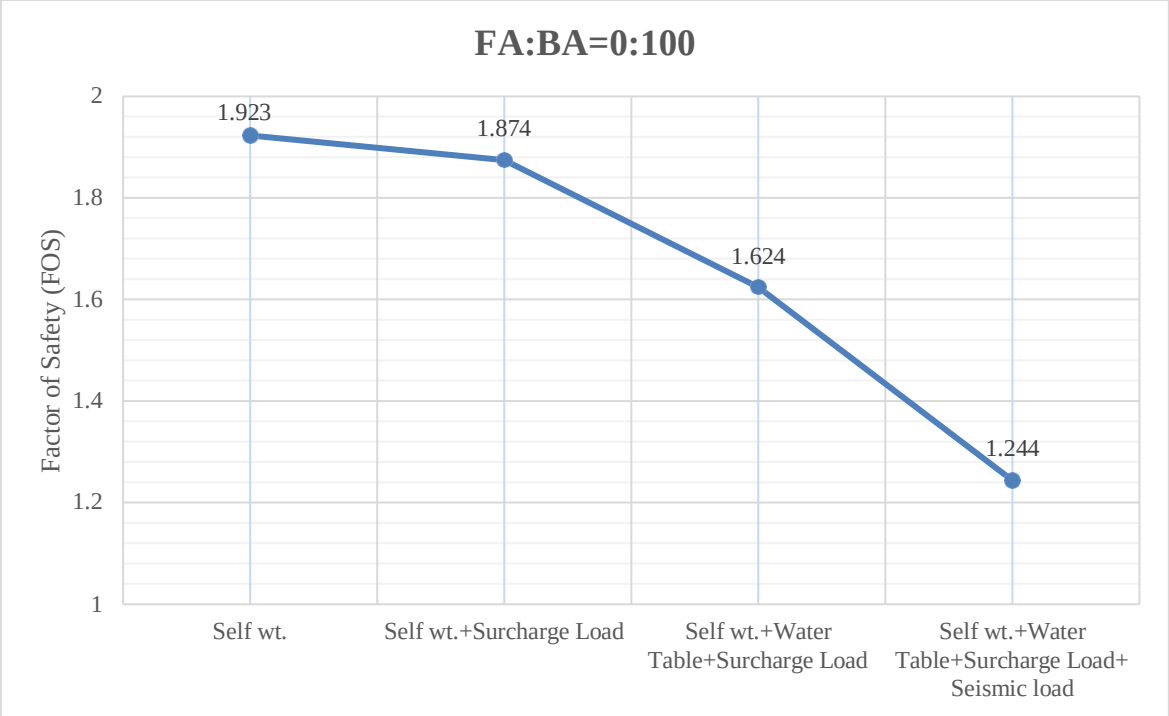

Graph 5.20: FOS for FA:BA=0:100 mix embankment under different loading conditions

CHAPTER 6 - CONCLUSION

6.1 CONCLUSION:

The present experimental study was carried out to determine the geotechnical characteristics of various mixes of fly ash and bottom ash and find their suitability as embankment materials. Following are the conclusions drawn from this work:

i. The fly ash and bottom ash obtained from Dadri plant are poorly graded. Most of the fly ash particles are of silt size whereas the bottom ash particles mostly lie in the range of fine sand.

ii. All the mixes of fly ash and bottom ash possess negligible cohesion value.

iii. The OMC of various mixes of fly ash and bottom ash ranges from 17.6 to 23 % and MDD ranges from 1.154 to 1.26 g/cm^3.

iv. All the mixes of fly ash and bottom ash shows lesser sensitivity to moisture as compared to the DTU campus soil.

v. The optimum moisture content (OMC) decreases with decrease in fly ash content in the fly ash-bottom ash mix. This is due to the reason that the particles of fly ash are finer in size than that of bottom ash, hence, more quantity of water is required by fly ash particles to reach their denser state.

vi. The maximum dry density and maximum value of angle of internal friction is achieved at FA:BA=25:75 mix (i.e., FA=25% and BA=75%). However, the value of MDD of FA:BA=25:75 mix is nearly 72 % than that of the compacted DTU soil. The lower unit weight of FA-BA mix is useful in reducing settlement due to self-weight of embankment. Hence FA-BA mixes can be defined as lightweight materials with comparable strength.

vii. The FOS obtained from SLOPE/W for all the FA-BA mix embankments was greater than 1 even under the worst conditions. However, the maximum FOS was obtained when FA-BA=25:75 mix.

viii. Hence the optimum fly ash-bottom ash mix obtained from Dadri plant is FA:BA=25:75 (i.e., FA=25% and BA=75%) for use as an embankment material.

Based on above findings, it can be concluded that the fly ash-bottom ash mix can be used as an embankment material. It is light weight material causing lesser settlement in embankment and having comparable strength to soil making it an efficient material in the construction of embankment and filling behind retaining walls. In the field of geotechnical engineering, bulk utilization of fly ash and bottom ash can be done, resulting in reduction in the amount of unutilized coal ash and, as a result, a reduction in the potential environmental hazard.

6.2 FUTURE SCOPE:

- Since the properties of coal ash obtained from different sources is different due to variation in their chemical, mineralogical composition and particle size distribution. Hence, there is a need of classification of various coal ashes. A better classification method should be developed that takes into account the chemical, mineralogical, and particle size characteristics of coal ash.

- This study employs Limit equilibrium method for the stability analysis which doesn't involve settlement analysis. Hence, settlement analysis should also be carried out to assess the settlement of embankment and subsoil.

- Also, there is a need to study the methods of stabilization of fly ash and bottom ash embankments such as soil nailing, geogrids etc. in order to achieve greater height and steeper slopes of embankments.

REFERENCES

- Sharma, Vishal, and Singh, Sandeep. 2020. "Modeling for the use of waste materials (Bottom ash and fly ash) in soil stabilization." Materials Today: Proceedings, 33(7), 1-7.
- Reddy, C.S., S. Mohanty, and R. Shaik. 2018. "Physical, chemical and geotechnical characterization of fly ash, bottom ash and municipal solid waste from Telangana State in India." International Journal of Geo-Engineering, 9(23), 1-23.
- Gimhan, P.G.S., J.B. Disanayaka, and M. Nasvi. 2018. "Geotechnical engineering properties of fly ash and bottom ash: Use as civil engineering construction material." Journal of the Institution of Engineers, Sri Lanka, 51(1), 49-57.
- Saravanan, S., S. Manikanta, C. Venkatsubramanian, and D. Muthu. 2017. "Effect of bottom ash on the soil." International Journal of Civil Engineering and Technology, 8(2), 117-127.
- Dungca, J. and J.A.L. Jao. 2017. "Strength and permeability characteristics of road base materials blended with fly ash and bottom ash." International Journal of GEOMATE, 12(31), 9-15.
- Dey, A., P. Talukdar, and R. Bora. 2016."Stability analysis of ash dykes in static pseudostatic and seismic conditions." 1st International Conference on Civil Engineering for Sustainable Development Opportunities and Challenges, Guwahati, India
- Yao, Z.T., P.K. Sarker, J.H. Tang, L.Q. Ge, M.S. Xia, and Y.Q. Xi. 2015. "A comprehensive review on the applications of coal fly ash." Earth-Science Reviews, 141, 105-121.
- Singh, R.R., N. Goyal, and N. Kaur. 2015. "Fly ash as an embankment material." SSRG International Journal of Civil Engineering, 2(3). 11-13.
- Saikia, R., P. Deka, and S.N. Kalita. 2015. "Pseudostatic seismic assessment of slopes and its remediation." Indian Geotechnical Conference, Pune, India.
- Latifi, N., A. Marto, A. Rashid, and J.L.J. Yii. 2015. "Strength and Physico-chemical Characteristics of Fly Ash–Bottom Ash Mixture." Arabian Journal for Science and Engineering, 40, 2447–2455.
- Shivamanth A., S.S. Athani, M.K. Desai, and G.R. Dodagoudar. 2015. "Stability analysis of dyke using limit equilibrium and finite element methods." International Conference on Water Resources, Coastal and Ocean Engineering. 4, 884-891.
- Kumar, D., N. Kumar, and A. Gupta. 2014. "Geotechnical properties of fly ash and bottom ash mixtures in different proportions." International Journal of Science and Research, 3(9), 1487-1494.
- Hasan, M., M.A. Khan, and J. Alam. 2014. "Morphological and geotechnical properties of dadri fly ash." Int. J. Struct. & Civil Engg. Res. 3(2), 7-15.
- Deb, T., and S.K. Pal. 2014. "Effect of fly ash on geotechnical properties of local soil-fly ash mixed samples." International Journal of Research in Engineering and Technology, 03(05), 507-516.

- Rai, A.K., B. Paul, and G. Singh. 2010. "A study on backfill properties and use of fly ash for highway embankment." Journal of Advanced Laboratory Research in Biology, 1(2), 110-114.
- Prakash, K., and A. Sridharan. 2009."Beneficial properties of coal ashes and effective solid waste management." Practice Periodical of Hazardous, Toxic, And Radioactive Waste Management, 13(4), 239-248.
- Yoon, S., U. Balunaini, I.Z. Yildirim, M. Prezzi, and N.Z. Siddiki. 2009."Construction of an embankment with a fly and bottom ash mixture: Field performance study." Journal of Materials in Civil Engineering, 21(6), 271-278.
- Kim, B., M. Prezzi, R. Salgado. 2005."Geotechnical properties of fly and bottom ash mixtures for use in highway embankments." 131(7), 914-924.
- Pandian, N.S. 2004. "Fly ash characterization with reference to geotechnical applications." J. Indian Inst. Sci. 84(6). 189-216.
- Benson, C.H., and T.B. Edil. 2004."Case study of subgrade stabilization using fly ash: State highway 32, Port Washington, Wisconsin." Recycled Materials in Geotechnics, ASCE. 123-136.
- Bhatt, A., S. Priyadarshini, A.A. Mohanakrishnan, A. Abri, M. Sattler, S. Techapaphawit. 2019."Physical, chemical, and geotechnical properties of coal fly ash: A global review." Case Studies in Construction Materials, 11, 1-11.
- Hynes-Griffin, M.E., A.G. Franklin. 1984."Rationalizing the seismic coefficient method." U.S. Army Corps of Engineers Waterways Experiment Station, Vicksburg, Mississippi.
- IS: 2720 (Part 3) (1980). Methods of Test for Soils: Determination of Specific Gravity, Bureau of Indian Standards, New Delhi, India
- IS: 2720 (Part 4) (1985). Methods of Test for Soils: Grain Size Analysis, Bureau of Indian Standards, New Delhi, India.
- IS: 2720 (Part 7) (1980). Methods of Test for Soils: Determination of Water Content-Dry Density Relation Using Light Compaction, Bureau of Indian Standards, New Delhi, India.
- IS: 2720 (Part 13) (1986). Methods of Test for Soils: Direct shear test, Bureau of Indian Standards, New Delhi, India.
- IS: 2720 (Part 29) (1975). Methods of Test for Soils: Determination of Dry Density of Soils In-place by the Core-cutter Method, Bureau of Indian Standards, New Delhi, India.
- IS: 1893 (Part 1) (2002). Criteria for Earthquake Resistant Design of Structures: General Provisions and Buildings, Bureau of Indian Standards, New Delhi, India.
- IRC: SP 58 (1999). Guidelines for use of fly ash in road embankments, Indian Road Congress, New Delhi, India.
- IRC: 75 (2015). Guidelines for the design of high embankments, Indian Road Congress, New Delhi, India.

- IRC: SP 73 (2018). Manual of specifications and standards for two laning of highways with paved shoulder, Indian Road Congress, New Delhi, India.
- Central Electricity Authority. (2021). Report on fly ash generation at coal / lignite based thermal power stations and its utilization in the country for the year 2020 – 21, New Delhi, India.
- Ministry of Road Transport and Highways. (2018). Use of fly ash in road/flyover embankments construction, New Delhi, India.

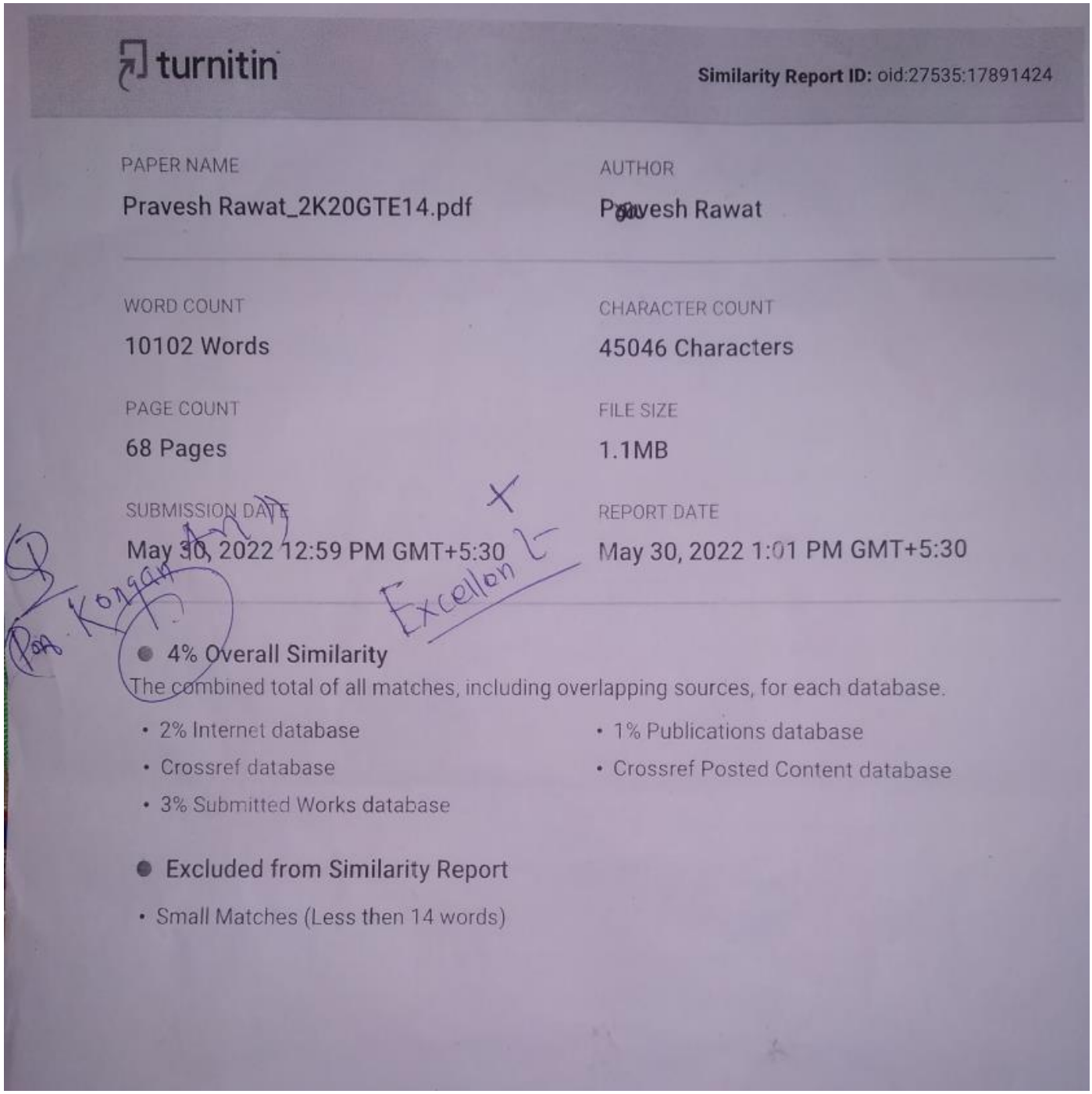

turnitin

Similarity Report ID: oid:27535:17891424

PAPER NAME
Pravesh Rawat_2K20GTE14.pdf

AUTHOR
Pravesh Rawat

WORD COUNT
10102 Words

CHARACTER COUNT
45046 Characters

PAGE COUNT
68 Pages

FILE SIZE
1.1MB

SUBMISSION DATE
May 30, 2022 12:59 PM GMT+5:30

REPORT DATE
May 30, 2022 1:01 PM GMT+5:30

Excellent

4% Overall Similarity
The combined total of all matches, including overlapping sources, for each database.

- 2% Internet database
- Crossref database
- 3% Submitted Works database
- 1% Publications database
- Crossref Posted Content database

Excluded from Similarity Report

- Small Matches (Less then 14 words)